APPLICATION OF DUAL RECIPROCITY BEM IN NONLINEAR TRANSIENT HEAT CONDUCTION

by

KRISHNA MOHAN SINGH

DEPARTMENT OF MECHANICAL ENGINEERING

INDIAN INSTITUTE OF TECHNOLOGY, KANPUR

JULY, 1988

APPLICATION OF DUAL RECIPROCITY BEM IN NONLINEAR TRANSIENT HEAT CONDUCTION

A Thesis Submitted
In Partial Fulfilment of the Requirements
for the Degree of

MASTER OF TECHNOLOGY

by

KRISHNA MOHAN SINGH

to the

DEPARTMENT OF MECHANICAL ENGINEERING
INDIAN INSTITUTE OF TECHNOLOGY, KANPUR

JULY, 1988

CERTIFICATE

This is to certify that this work entitled, "APPLICATION OF DUAL RECIPROCITY BEM IN NONLINEAR TRANSIENT HEAT CONDUCTION" has been carried out by Krishna Mohan Singh under my supervision and has not been submitted elsewhere for the award of a degree.

July, 1988.

MSKalra
(Manjeet S. Kalra)
Assistant Professor
Department of Mechanical Engineeri
Indian Institute of Technology
Kanpur, U.P. 208016, India

ACKNOWLEDGEMENTS

I wish to acknowledge my deep sense of gratitude to Dr. Manjeet S. Kalra for giving me this opportunity to work under his able guidance, for his unconditional approval, care, affection, constant encouragement and moral support. He initiated me in the Boundary Element Techniques, and he has been involved in this project at every level of details. Words are simply insufficient to express the indebtness which I owe to him. I gratefully acknowledge the encouragement and affection of Mrs. Kalra.

I am thankful to my teachers Prof. Madan M. Oberai, Drs. P.N. Kaul, Keshav Kant, T. Sundararajan and Prakash M. Dixit for their invaluable instructions, guidance and support. The advices of Drs. T. Sundararajan and Keshav Kant throughout the course of this study are greatly appreciated. I gratefully acknowledge the help and encouragement of Professors B.L. Dhoopar and R. Singh, and Drs.N.N. Kishore and M. Prasad. Advices of Professors P.C.Das and R.K.S. Rathore are gratefully acknowledged. Special thanks are due to Prof. P.C. Upadhyaya (I.T.-B.H.U.) who encouraged me to join in M.Tech. program.

I am particularly thankful to Mr. Prabhat Munshi for his guidance, encouragement, help and support throughout

the course of this study.

I sincerely thank my friends M/s. Manmohan Pandey, Sanjay Agrawal, Ajay Kumar, S. Pandimani, D. Prasad, Ramendra Mandal & Co. and Miss Richa Rastogi for their invaluable help on inumerable occassions and for providing me with a vivacious atmosphere throughout my stay here. Special thanks are due to M/s. D. Prasad and S. Pandimani for checking the final draft of the thesis.

I owe a deep sense of gratitude to my most beloved friend-trio of Richa, Manmohan and Sanjay for their unconditional acceptance, love, affection and help. Their friendship is my most prized possession.

I am thankful to office-staff of Department of Mechanical Engineering and Nuclear Engineering and Technology Program for their cooperation and help.

I greatly appreciate the excellent typing of Mr. U.S. Mishra, and neat tracings of Mr. B.N. Srivastava.

Finally, I wish to express my gratitude to my parents for their permission and encouragement to pursue graduate study against all odds. I am particularly grateful to my elder sisters Meera and Shail, and my brother-in-law Mr. Shyam Sundar Singh for their constant encouragements, affection, and support - moral and financial - without which I would have completed this program but in my dreams.

-Krishna Mohan Singh

CONTENTS

Page

LIST OF TABLES

LIST OF FIGURES

NOMENCLATURE

a	Thermal Diffusivity, $m^2 s^{-1}$ or dimensionless
A_e	Elemental Area, dimensionless
A(u)	Temperature Dependent Property, dimensionless
B	Global Matrix of Domain Integrals
Bi	Biot Number, dimensionless
c	Specific Heat, J $kg^{-1}K^{-1}$ or dimensionless
C	Global 'Damping' Matrix
Cb	Boundary Element Connectivity Matrix
Cc	Finite Element Connectivity Matrix
$c(\xi)$, c_i	Jump-Coefficient, dimensionless
d	Distance between two points, dimensionless
E	Thermal Energy, dimensionless
$f_c(x,t,u)$	Natural Boundary Condition
$f^j(x)$	Coordinate functions
G	Global Matrix of Boundary Integrals with Kernel $u^*(\xi,x$
Gr	Radiation Parameter, dimensionless
h	Convective Heat Transfer Coefficient, W $m^{-2}K^{-1}$
H	Global Matrix of Boundary Integrals with Kernel $q^*(\xi,x$
I^k, I^e	Integral over an Element
IFIX	Function defining Integer Part of a Real Number
J	Jacobian or Tangent Matrix
k	Thermal Conductivity, dimensionless
K	Thermal Conductivity, W $m^{-1}K^{-1}$
l	Length of a Boundary Element
L	Characteristic Length, m

n	Unit Outward Normal
n_G	Number of Gaussian Integration Points
N	Number of Freedom Nodes or Equations
N_b	Number of Boundary Nodes
N_c	Number of Finite Elements
N_e	Number of Boundary Elements
N_T	Total Number of Nodes (Boundary + Internal)
N^j	Time Interpolation or Shape Functions
q	Heat Flux, W m^{-2} or dimensionless
Q	Vector of Nodal Fluxes
$\dot{Q}_g$	Volumetric Heat Generation, W m^{-3}
$\dot{q}_g$	Volumetric Heat Generation, dimensionless
$q^*(\xi,x)$	Generalized Function
r	Euclidean Distance between Two Points, dimensionless
R	Energy Residual, dimensionless
$T(x,t)$	Temperature, K
T_a, T_b, T_c, T_r	Chosen or Specified Temperatures, K
$\bar{T}(x,t)$	Prescribed Surface Temperature, K
$T_o(x)$	Prescribed Initial Temperature, K
$T(u)$	Kirchhoff Transform, dimensionless
U	Vector of Nodal Temperatures
$u(x,t)$	Dimensionless Temperature
$\bar{u}(x,t)$	Dimensionless Prescribed Surface Temperature
$U(u)$	Kirchhoff Transform of u
$u^*(\xi,x)$	Generalized Function (Fundamental Solution to Laplace Equation)
w	Weighting Factors in Numerical Quadrature, dimensionle
W_j	Weighting Functions, dimensionless

x	Position Vector
X	Vector of Nodal Unknowns
x_1, x_2	Cartesian Coordinates
XNORM	Relative Norm of Increments of Vector of Unknowns
XTOL	Tolerance for Relative Norm of Increments of Unknowns
$(\hat{x}, \hat{y})$	Rectangular Coordinates
t	Time, s or dimensionless
$\dot{\alpha}(t)$	Time-dependent Approximation Functions
Γ	Boundary Surface
Γ_e	Boundary Element
δ	Dirac-delta Distribution
Δ	Increment or Difference
ε	Emissivity, dimensionless
$\zeta, \zeta_1, \zeta_2, \zeta_3$	Natural coordinates
η^j	Chosen Functions
Θ	Parameter for Time-Integration Schemes, dimensionless
λ	Dummy variable
ξ	Source point
$(\xi, \eta), (\xi_1, \eta_1)$	Rectangular Coordinates
Π	Least-Squares Functional
ρ	Mass Density, kg m^{-3} or dimensionless
Σ	Summation Sign
σ	Stefan-Boltzmann Constant, W $m^{-2}K^{-4}$
τ	Modified Time Variable
ϕ	Boundary Element Interpolation Functions

$\phi^e, \phi^{e'}$	Geometric Transformations
χ	Finite Element Interpolation Functions
ψ	Chosen Functions

Subscripts

a,b,c	Reference or specified values
e	Related to an element
g	Heat Generation
i,j,k,r,s	Matrix Elements
min	Minimum
n	Iteration Number
sub	Sub-divisions

Superscripts

e	Elemental
j	Related to j^{th} Node
k	k^{th} Element
m	m^{th} Time-instant
T	Transpose of a Matrix
.	Temporal Derivative

ABSTRACT

A computer program based on the dual reciprocity boundary element method has been developed for solution of nonlinear transient heat conduction problems in two-dimensional homogeneous isotropic regions. In the present work, nonlinear boundary conditions have also been incorporated. Further, the concept of the residual of input-output thermal energy balance has been used to assess the accuracy of computed solutions. This is particularly useful for nonlinear problems. Its application to boundary element solutions in the present work attests to the accuracy of the computed solutions. For problems solved here, the energy-residual was found to be of the order 0.5% or less.

A least-squares time integration scheme was introduced, and was found to be computationally more efficient and accurate than other schemes such as the fully implicit, the Crank-Nicholson and the Galerkin schemes. Numerical experiments on convergence indicate second order uniform convergence with spatial mesh-refinement for the fully implicit scheme. The rate of convergence for this scheme is of first order with respect to time increment. With the least-squares scheme, the convergence of the boundary solutions with spatial mesh-refinement is not uniform, whereas, quadratic (or higher) order convergence with respect to time increment is observed.

CHAPTER 1

INTRODUCTION

1.1 Motivation

Nature is inherently nonlinear. Hence, the occurrence of nonlinear processes is a rule rather than an exception. It is the nature of nonlinearities present in a process which dictates whether we can approximate it by a linear model or not. If the nonlinearities are weak, we can obtain significant insights into the process by analysing its linear model. Otherwise, we have no option except to model the process as it exists, with suitable approximations. Nonlinear heat conduction problems belong to this later class. These are encountered in a variety of processes of engineering interest such as thermal and nuclear power generation, space-applications, manufacturing processes etc.

Nonlinearities in a heat conduction process may arise from:

(i) Temperature dependent thermal diffusivity.

(ii) Nonlinear boundary conditions, e.g. due to heat radiation.

(iii) Nonlinear heat sources.

(iv) Moving interface, e.g. due to phase change.

The first two types of nonlinearities arise mostly in high-temperature applications, and these are addressed in the present work. The motivation has obviously come from a wide range of problems already indicated above.

1.2 Reasons for Interest in Boundary Element Techniques

Mathematical model of a transient heat conduction process gives us an initial-boundary value problem. This problem is, in general, not amenable to closed form analytical solutions. This is true for nonlinear problems in particular. Even for a linear problem which admits an analytical solution, the result is often in the form of integrals or infinite series. The above features have been the main reasons for interest in approximate numerical solution procedures.

The modern numerical techniques have been made possible by phenomenal advancements in digital computer-technology in the past three decades. The finite element and the finite difference methods have been the two most popular methods. The application of boundary element techniques to the transient heat-conduction problems has been a comparatively recent phenomenon.

The interest in the boundary element techniques stems from the fact that it requires, for the most part, the discretization of the boundary only, as compared to the finite element or finite difference methods which require the discretization of the entire domain. Even for the transient

problems which may require incorporation of initial conditions through domain integrals, the final system of equations is of the order of boundary unknowns only.

In the boundary element method, the governing differential equation is transformed into an equivalent integral equation using either an indirect formulation (i.e. by representing the unknown function as a single or double layer potential) or a direct formulation employing a weighted residual statement in conjunction with free space Green's functions. Owing to its conceptual simplicity and wide range of applicability the latter approach has been the most popular. The integral equation so obtained is solved in the same manner as in the finite element methods.

Various formulations proposed for the solution of transient heat conduction problems with the boundary element techniques include the use of Laplace transforms [1]*, finite-difference approximation of the time derivative [2], the time dependent fundamental solutions [3,4], and the dual reciprocity boundary element method [5-8]. The latter offers distinct advantages over the others as it involves only boundary integrals retaining the 'boundary-only' character of the method. It utilizes fundamental solution to Laplace equation which is only space dependent. This formulation has been extended to deal with nonlinear diffusion problems with linear boundary conditions [8]. We use this formulation in the present work.

Numbers in brackets denote References.

1.3 Objectives of the Present Work

Previous applications of the dual reciprocity boundary element method for linear as well as nonlinear conduction problems [5-8] have considered only linear boundary conditions. Time-integrations have been performed using only point-collocation schemes. Also, no systematic study has been reported concerning the convergence of numerical solutions with respect to mesh-refinement and decreasing time-increment except a tentative study presented in reference [8]. We take the above tasks in the present work. In order to achieve any of the above, our first task is to develop a comprehensive computer program based on the chosen formulation. We restrict ourselves to two-dimensional problems only. The program should be capable of dealing with linear as well as nonlinear conduction problems involving time-dependent or time-independent boundary conditions. We attempt to introduce the least-squares scheme in time for linear conduction problems and assess its viability in the boundary element techniques. We attempt a numerical study of convergence of the boundary solutions for the point-collocation, and the proposed least-squares time-integration scheme. As the final step, we propose to solve problems involving nonlinear boundary conditions. To assess the accuracy of numerical solutions, we propose to introduce the unbalance of input-output thermal energy as a measure of accuracy and physical acceptability of the computed solutions. Specific objectives of this work can be listed as:

i) Development of a comprehensive computer program for two dimensional transient conduction problems capable of dealing with material as well as boundary nonlinearities, time-dependent boundary conditions, and heat generation.

ii) Incorporation of the least-squares time integration scheme.

iii) Study of the convergence of the numerical solutions to the exact one with mesh-refinement and decreasing time-increment.

iv) Comparison of the least-squares scheme with point collocation schemes.

v) Some applications to problems involving nonlinear boundary conditions. Use of the energy residual to assess the accuracy of computed solutions.

CHAPTER 2

REVIEW OF LITERATURE

2.1 General Background

The modern theory of boundary integral equations finds its origin in Fredholm's work in 1903. The first numerical application was made in 1917 by Trefftz. Most of the early work with boundary integral equations has been concerned with applications in potential problems. However, actual numerical implementations for problems of engineering interest appear only in 1960s with availability of fast digital computers. Various applications in potential theory, elastostatics and electrostatics appeared in this decade. Detailed account of these developments with related references can be found in the references [9-11]. The first application of boundary element techniques to transient heat conduction problem appeared in 1970 [1]. We review some representative works related to the transient heat conduction in the following sections.

2.2 Boundary Element Methods in Transient Heat Conduction

In 1970, Rizzo and Shippy [1] proposed a boundary element formulation in conjunction with Laplace Transforms. Application of Laplace transform removes the time-dependence of the problem. The elliptic partial differential equation so obtained is used for boundary element formulation. The

problem is solved in Laplace transform space for sequence of real positive transform parameter, and numerical inversion is performed to compute the physical variables in the real space. Details of the method are available in references [1,10,12]. This method has found very limited application owing to its complexity.

Another approach based on time-dependent fundamental solutions in the context of the direct method was proposed by Chang et al. [3] and Shaw [13]. This approach has been the most popular one and has been extended to deal with axisymmetric and 3-D problems of practical interest, which we review later in this section.

A coupled boundary element-finite difference formulation was proposed by Brebbia and Walker [12] and Curran et al. [2] in 1980. This involves finite-difference approximation of time derivative obtaining an elliptic equation. This is solved at each time step using the boundary element method. Owing to finite-difference approximation involved, this method imposes severe restrictions on time-increment to obtain accurate results.

All the above mentioned approaches usually involve incorporation of the initial conditions through a domain integral which disturbs the 'boundary-only' character of the technique. In the context of the method employing time-dependent fundamental solution, a time-stepping algorithm in which initial conditions are accounted through the

boundary integrals was proposed by Wrobel and Brebbia [14]. This technique, though mathematically elegant, becomes computationally inefficient if the number of time-steps are large.

The latest approach in this series is the dual reciprocity boundary element method. This approach was proposed by Brebbia and Nardini [15] in context of elasto-dynamics, and has been applied to the transient conduction problems by Wrobel et al. [5-8]. This involves approximation of the temporal derivative by a specific type of product-approximation in conjunction with the fundamental solution of the Laplace's equation. By exploiting the special nature of space dependent functions chosen in above approximation in conjunction with the reciprocity principles, the domain integral is transformed into boundary integrals. We review this method in detail in next chapter. We refer to this method as DRBEM, and to the one employing time-dependent fundamental solutions as BEM in the following lines.

Wrobel and Brebbia [16] presented extension of BEM to deal with axisymmetric problems. They employed integral in θ-direction, of the three dimensional fundamental solution, over generating area and boundary contour of the axisymmetric body. This was referred to as axisymmetric fundamental solution. Reference [10] presents a detailed account of this method.

The BEM was applied to melting and solidification problems by Banerjee and Shaw [17] . They developed general boundary integral formulations for general one-, two- and three-dimensional problems of melting and solidification of metals as well as freezing and thawing of saturated soils, and presented their numerical solutions.

Problems involving phase change and solidification were also discussed by Hong et al. [18], and Wrobel [19].

Pina and Fernandes [20] presented solution of three-dimensional transient conduction problems with harmonic initial conditions. The assumption of harmonic initial conditions allows the conversion of corresponding domain integral into boundary integrals, thus, requiring discretization of boundary only. Examples of heat conduction in a cube and unit sphere with the Dirichlet boundary conditions and zero initial temperatures have been presented.

Kihara et al. [21] discussed the accuracy of boundary element solution for two-dimensional problems using the stability parameters $a\Delta t/(\Delta x)^2$ for constant boundary element discretization. They also discussed the effect of changes in mesh pattern, based on heat flux density, on the numerical solution.

Uniform convergence of boundary element solution of heat equations have been investigated by Onishi and Kuroki for pure Neumann conditions. Iso [22] extended the above investigation for problems with linear radiation boundary

conditions. Iso et al. [23] present mathematical theorems on uniform convergence of boundary solution and stability of the computing scheme for two-dimensional isotropic heat conduction problem involving non-isothermal boundary conditions. They also present numerical investigations of convergence of boundary solutions for mixed type problems. Problems involving singularities such as re-entrant corners, slit boundary and interzonal singularity, and infinite domains are also discussed.

2.3 Application in Nonlinear Problems involving Material Nonlinearities and Nonlinear Boundary Conditions

Koizumi et al. [24] discussed the application of the boundary element method to three-dimensional heat conduction problems with nonlinear boundary conditions. Onishi and Kuroki [25] discussed the nonlinear problems of heat conduction subject to radiation boundary conditions, and the unsteady problems subject to forced and natural convection using stream function and vorticity formulation.

For problems involving material nonlinearities, Brebbia and Skerget [26] introduced Kirchoff's transform as the new dependent variable in conjunction with constant diffusivity approximation and closed form variation of thermal conductivity. The resulting system was solved in Kirchoff's transform space, and analytical inversion was done to obtain temperature in real space.

Kikuta et al. [27,28] assumed linear variation of thermal conductivity. Using Kirchoff's transform they obtain a pseudo-linear integral equation in transform space with nonlinearities being shifted to a domain integral term having time derivative of transform variable in its kernel. The use of constant element in time, in conjunction with usual BEM procedure, made the evaluation of domain integrals corresponding to nonlinearities unnecessary. Several examples were presented.

Finally, in the context of the dual reciprocity boundary element formulation, Wrobel and Brebbia [8] extended this method to deal with nonlinear material problems by introducing the integral of conductivity (Kirchoff's Transform) as a new variable, together with a modified time variable. They obtained a pseudo-linear equation in transform space which was solved using a Newton-Raphson iteration procedure. Examples of problems with linear boundary conditions were presented. We start our work with this formulation which is reviewed in detail in the next chapter.

CHAPTER 3

DUAL RECIPROCITY BOUNDARY ELEMENT FORMULATION

3.1 Mathematical Model of Heat Conduction Problem

Let Ω be a homogeneous isotropic heat conducting domain with a piecewise smooth boundary Γ. Let n be the external normal to boundary Γ, and, x denote the spatial coordinates of a field point. The transient heat conduction in finite time interval $t_o < t \leq t_F$ is governed by the well known equation

$$\rho c \frac{\partial T}{\partial t} = \nabla . (K \nabla T) + \dot{Q}_g \quad \text{in } \Omega \times (t_o, t_F] . \qquad (3.1)$$

Here, ρ is the mass-density, c, the specific heat, K the thermal conductivity, $T(x, t)$ the temperature at field point x at time t, $\dot{Q}_g$ the rate of heat generation (per unit volume), and ∇ denotes the gradient operator.

The initial condition for Eq. (3.1) is given by

$$T(x, t_o) = T_o(x) \quad \text{on } \Omega \qquad (3.2)$$

where $T_o(x)$ is a known function.

The boundary conditions for Eq. (3.1) can, in general, be written as:

$$T(x,t) = \bar{T}(x,t) \quad \text{on} \quad \Gamma_T \times (t_o, t_F] \qquad (3.3)(a)$$

$$q(x,t) = \bar{f}_c(T,x,t) \quad \text{on} \quad \Gamma_q \times (t_o, t_F] \qquad (3.3)(b)$$

with $\Gamma_T \cup \Gamma_q = \Gamma$. In the above expressions $\bar{T}$ and $\bar{f}_c$ are given functions.

3.2 Non-dimensionalization of Governing Equations

We define following dimensionless quantities:

Temperature	:	$u = (T-T_a)/(T_b-T_a)$
Spatial coordinates	:	$x^* = x/L$
Time (the Fourier Number)	:	$t^* = (K_r/\rho_r c_r).(t/L^2)$
Thermal conductivity	:	$k^* = K/K_r$
Mass density	:	$\rho^* = \rho/\rho_r$
Specific Heat	:	$c^* = c/c_r$
Volumetric heat generation	:	$\dot{q}_g = (\dot{Q}_g L^2)/(K_r(T_b - T_a))$

(3.4)

In the above definitions, T_a and T_b are suitably chosen reference temperatures. Subscript r with property values K, ρ and c indicates value of these at the chosen reference temperature T_r. L is the characteristic dimension of the problem.

Introduction of definitions (3.4) in governing equations (3.1) - (3.3) gives us following set of non-dimensional equations in which we have dropped superscript '*' for sake of convenience:

-Field Equation:

$$\rho c \frac{\partial u}{\partial t} = \nabla . (k \nabla u) + \dot{q}_g \text{ in } \Omega \times (t_o, t_F] \qquad (3.5)$$

-Initial Condition:

$$u(x,0) = u_o(x) \quad \text{on} \quad \Omega \qquad (3.6)$$

-Boundary Conditions:

$$u(x,t) = \bar{u}(x,t) \text{ on } \Gamma_u \times (t_o, t_F] \qquad (3.7)$$

$$q(x,t) = f_c(x,t,u) \text{ on } \Gamma_q \times (t_o, t_F] \qquad (3.8)$$

with $\Gamma_u \cup \Gamma_q = \Gamma$.

We may note here that for linear heat conduction problems, parameters, ρ , c and k in Eq. (3.5) become unity as per definitions (3.4).

3.3 Dual Reciprocity Boundary Element Formulation for Linear Heat Conduction [5- 8]

3.3.1 Boundary Integral Equations [5-8]

From section 3.2, we have governing field equation for linear heat conduction given by:

$$\frac{\partial u}{\partial t} = \nabla^2 u + \dot{q}_g \quad \text{in} \quad \Omega \times (t_o, t_F] \qquad (3.9)$$

As the first step in formulation of integral equations, we construct a relationship based on so-called

reciprocity principles using the fundamental solution to the Laplace's equation, i.e. the generalized function u^* satisfying the equation

$$- \nabla^2 u^* (\xi, x) = \delta(\xi, x), \tag{3.10}$$

where $\delta(\xi, x)$ is the Dirac delta function, and Green's second identity

$$\int_\Omega (v \nabla^2 w - w \nabla^2 v) \, d\Omega = \int_\Gamma (v \frac{\partial w}{\partial n} - w \frac{\partial v}{\partial n}) \, d\Gamma, \tag{3.11}$$

where ∇^2 is the Laplacian operator. We have from Eq.(3.11):

$$\int_\Omega (u^* \nabla^2 u - u \nabla^2 u^*) d\Omega = \int_\Gamma (u^* q - q^* u) \, d\Gamma \tag{3.12}$$

with

$$q = \frac{\partial u}{\partial n} \quad \text{and} \quad q^*(\xi, x) = \frac{\partial u^*(\xi, x)}{\partial n}$$

Substitution of Eq. (3.10) into Eq. (3.12) gives:

$$\int_\Omega u^* \nabla^2 u \, d\Omega = -c(\xi) \, u(\xi) + \int_\Gamma (u^* q - q^* u) d\Gamma \tag{3.13}$$

where

$$c(\xi) = \int_\Omega \delta(\xi, x) \, d\Omega \tag{3.14}$$

Eq. (3.13) is the relation we shall be using in the formulation. We may note here from Eq. (3.14) and well known properties of the Dirac-delta distribution that if the

source point lies in the interior of Ω , $c(\xi) = 1$. Further, if ξ is on the boundary Γ of Ω, then $c(\xi)$ equals the fraction of internal angle subtended by the boundary Γ at ξ , relative to the solid angle of the sphere in R^d, where d denotes the dimension of the problem [29] . For smooth points on Γ , $c(\xi) = 1/2$.

We now construct the following weighted-residual statement for approximate solution of Eq. (3.9):

$$\int_{\Omega} \left(\frac{\partial u}{\partial t} - \dot{q}_g - \nabla^2 u\right) u^* \, d\Omega = 0 \qquad (3.15)$$

Use of Eq. (3.13) in Eq. (3.15) yields:

$$\int_{\Omega} \dot{u}\, u^* \, d\Omega - \int_{\Omega} \dot{q}_g \, u^* \, d\Omega = -c(\xi)\, u(\xi) + \int_{\Gamma} (u^* q - q^* u) \, d\Gamma \, . \qquad (3.16)$$

in which dot stands for temporal derivative.

For evaluation of the first domain integral in Eq. (3.16), we approximate $\dot{u}$ at any point in the domain Ω by

$$\dot{u}(x,t) = \sum_{j=1}^{N} f^j(x)\, \dot{\alpha}^j(t) \qquad (3.17)$$

where $f^j(x)$ are chosen such that there exist functions $\psi^j(x)$ satisfying the relation,

$$\nabla^2 \psi^j = f^j \, . \qquad (3.18)$$

In the above N refers to the number of functions f^j chosen. With approximation (3.17), we have

$$\int_\Omega \dot{u} u^* \, d\Omega = \sum_{j=1}^{N} \dot{\alpha}^j \int_\Omega f^j u^* \, d\Omega \tag{3.19}$$

In the light of condition given by Eq.(3.18), Eq. (3.19) becomes:

$$\int_\Omega \dot{u} u^* \, d\Omega = \sum_{j=1}^{N} \dot{\alpha}^j \int_\Omega \nabla^2 \psi^j u^* \, d\Omega \tag{3.20}$$

We now appeal to the transformation expressed by Eq.(3.13) obtaining

$$\int_\Omega \dot{u} u^* d\Omega = \sum_{j=1}^{N} \left[-c(\xi) \psi^j(\xi) + \int_\Gamma (u^* \eta^j - q^* \psi^j) d\Gamma \right] \dot{\alpha}^j \tag{3.21}$$

with

$$\eta^j = \frac{\partial \psi^j}{\partial n} .$$

Substituting Eq. (3.21) into Eq. (3.16) we finally arrive at the expression

$$c_i u_i + \int_\Gamma (q^* u - u^* q) d\Gamma = \sum_{j=1}^{N} \left[c_i \psi_i^j + \int_\Gamma (q^* \psi^j - u^* \eta^j) d\Gamma \right] \dot{\alpha}^j + \int_\Omega \dot{q}_g u^* \, d\Omega \tag{3.22}$$

where subscript i refers to the source point ξ. We may note that the above integral equation involves only boundary integrals in the absence of the heat generation term. Since

the above expression has been obtained by a double application of reciprocity principles through transformation (3.13), the technique based on it is called the dual reciprocity boundary element method [5].

3.3.2 Spatial Discretization

To model the geometry of the domain surface, we discretize the boundary into a series of segments Γ_e which are either straight or curved lines for a 2-D problem. These segments are called boundary elements. Geometry of a boundary element is defined by the coordinates of a number of points inside it (called geometric nodes) and associated shape functions. The variations of field variables and other functions in a boundary element are modelled using interpolation functions associated with chosen points (called freedom nodes) in it. In this work, we have restricted our choice to straight line elements with constant or linear interpolation functions.

While using continuous elements, the freedom nodes are located at the element edge. Modelling difficulties arise when the element edge coincides with a singularity in problem definition such as an abrupt change in boundary condition or a corner etc. At a corner, normal to the boundary is not defined. At an interface where the type of boundary conditions changes, at the same freedom node two different conditions are known corresponding to respective

boundary elements on the two sides. To overcome these modelling difficulties, two approaches have been used in practice. The first of these employs two freedom nodes close together on either side of problem singularity ignoring the corner region. The second consists in locating the freedom nodes in the interior of the element instead of at the element edge. The first approach with double nodes at the corners, introduces strong linear dependence in the algebraic system as functions $u^*(\xi, x)$ and $f^j(x)$ are virtually the same at both nodes. Thus, this approach is inapplicable in the context of the dual reciprocity boundary element method, and we opt for the second approach. Partially discontinuous elements with freedom nodes at the usual locations where continuity is required, and, moved into the element where a discontinuous interpolation is needed, have been found to be the best choice [30], and we opt for these. Figure 3.1 illustrates constant, continuous linear, and two variants of partially discontinuous linear elements.

Furthermore, we divide the domain Ω into N_c finite element cells $\{ \Omega_m \}_{m = 1, N_c'}$ with Ω_m as a linear triangle. This division is done in such a way that the nodal points of the cells adjacent to the boundary coincide with the geometric nodes of boundary elements taken on Γ. Figure 3.2 shows a sketch of discretization of the boundary and the domain using linear elements.

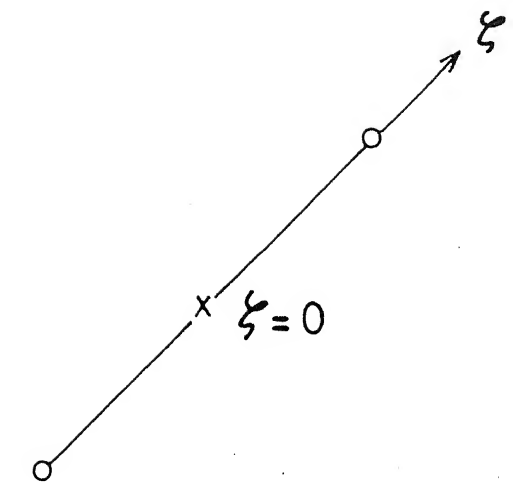

(a)

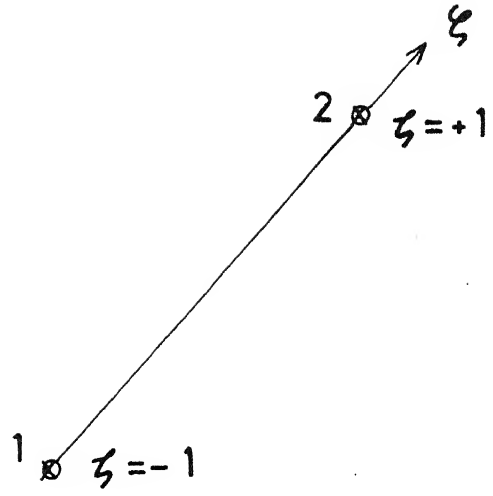

(b)

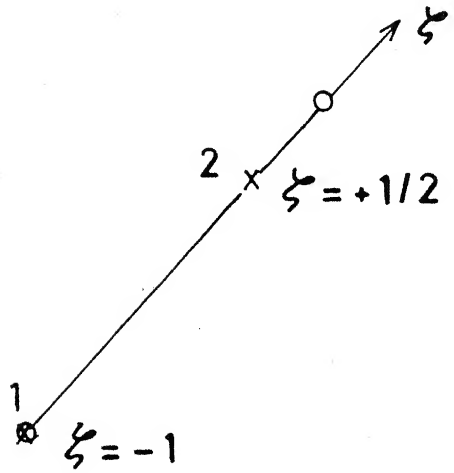

Type 1

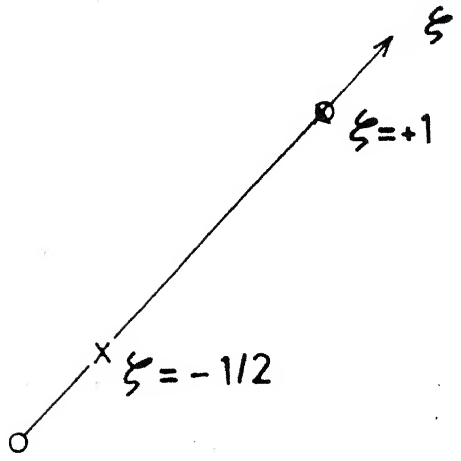

Type 2

(c)

o Geometric nodes

x Freedom nodes

Fig. 3.1 Straight line elements
(a) Constant element
(b) Continuous linear element
(c) Partially discontinuous linear elements.

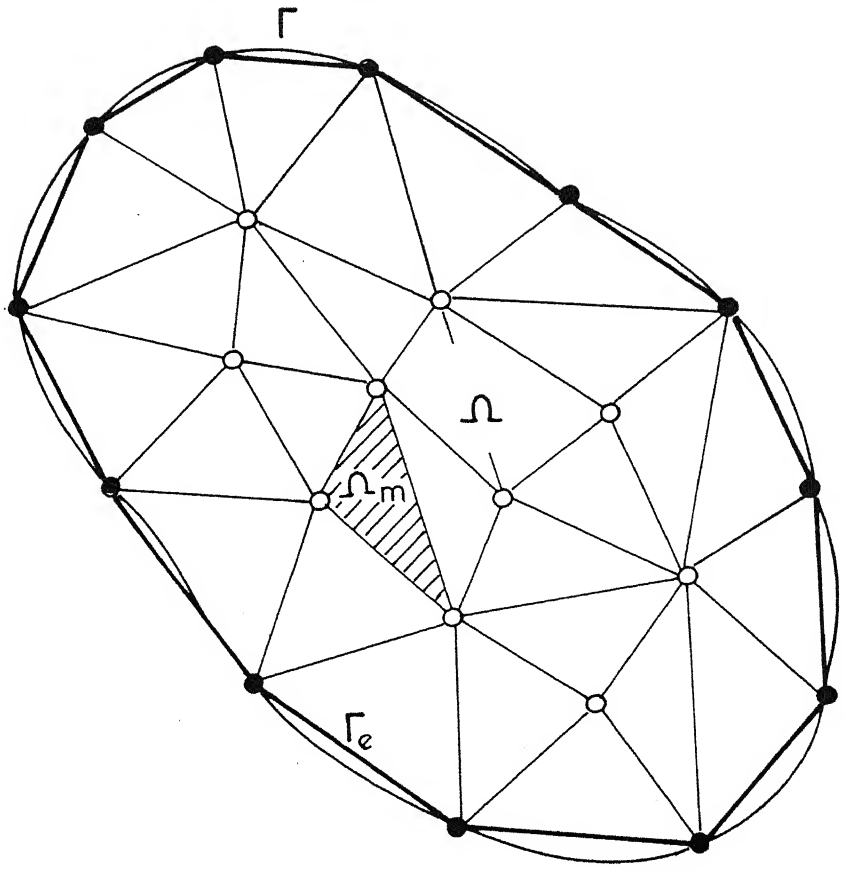

- ● Boundary nodes
- o Internal nodes
- Γ_e Boundary element
- Ω_m Finie element cell

Fig. 3.2 Spatial discretization.

3.3.3 Interpolation of Functions

We can approximate the variation of functions u, q, ψ, and η within each boundary element using a unique set of interpolation functions, denoted by a column vector ϕ [8]. We may note here that it is not necessary to approximate ψ and η using interpolation functions as these are known functions. However, this type of approximation brings significant reduction is necessary boundary integrations with some sacrifice in accuracy [8]. Thus,

$$u|_{\Gamma_e} = \phi^T u_e, \quad \psi^j|_{\Gamma_e} = \phi^T \psi_e^j$$
$$q|_{\Gamma_e} = \phi^T q_e, \quad \eta^j|_{\Gamma_e} = \phi^T \eta_e^j \qquad (3.23)$$

where u_e, q_e, ψ_e^j and η_e^j denote (column) vectors of nodal values of respective functions.

For constant elements: $\phi = 1$. The freedom node is usually taken at the midpoint of the element [Fig.3.1(a)].

For linear elements, with two freedom nodes:

$$\phi = [\phi_1 \quad \phi_2]^T \qquad (3.24)$$

We have, for continuous linear elements [Fig.3.1(b)], the interpolation functions given by [10,30]

$$\phi_1 = \frac{1}{2}(1-\zeta) \; ; \quad \phi_2 = \frac{1}{2}(1+\zeta) \qquad (3.25)$$

Interpolation functions for partially discontinuous elements [Fig.3.1(c)] are [30]:

Type 1 (Discontinuity at $\zeta = +1$	Type 2 (Discontinuity at $\zeta =$
$\phi_1 = 2/3\ (1/2 - \zeta)$	$\phi_1 = 2/3\ (1 - \zeta)$
$\phi_2 = 2/3\ (1 + \zeta)$	$\phi_2 = 2/3\ (1/2 + \zeta)$

(3.26)

Furthermore, we interpolate function $\dot{q}_g$ on Ω using conventional finite element approximation. Let χ be the set of finite element linear interpolation functions on the triangle Ω_m, then

$$\dot{q}_g|_{\Omega_m} = \chi^T \dot{q}_g^m \tag{3.27}$$

with

$$\chi = [\chi_1 \quad \chi_2 \quad \chi_3]^T, \text{ and } \dot{q}_g^m = [\dot{q}_g^1 \quad \dot{q}_g^2 \quad \dot{q}_g^3]_m^T$$

Expressions for interpolation function χ in terms of natural coordinates for a triangular element [Fig.3.3] are:

$$\chi_1 = \zeta_1 \ ; \ \chi_2 = \zeta_2 \ ; \ \chi_3 = \zeta_3 \tag{3.28}$$

where

$$\zeta_3 = 1 - (\zeta_1 + \zeta_2).$$

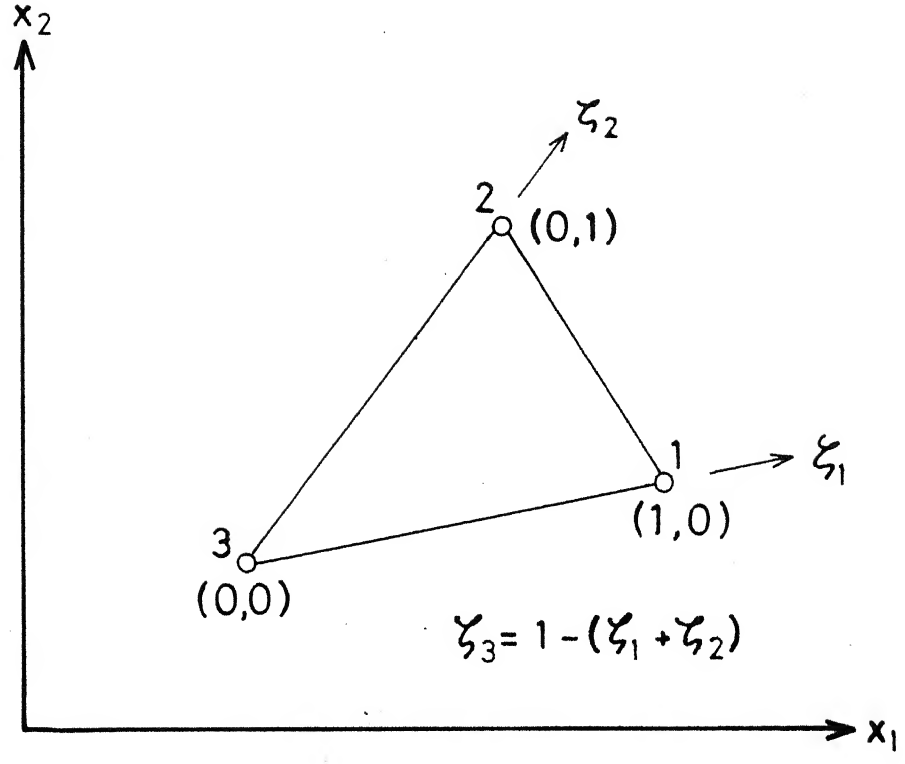

Fig. 3.3 Natural coordinates (ζ_1 , ζ_2) for a triangular element

3.3.4 Selection of Functions f^j, ψ^j and η^j

A number of possibilities, such as polynomials, trigonometric series, and concentrated nodal functions related to fixed points in space, have been suggested by Nardini and Brebbia [31]. Wrobel et al. 8 used the set of concentrated nodal functions, referring to the fixed points in space as poles. We employ this set of functions, and in following lines we present expressions for these functions from reference [8].

For two- and three-dimensional problems,

$$f^j(x) = r(x, x_j) \tag{3.29}$$

where r denotes the Euclidean distance between two points in space, x a field point, and x_j denotes the position of j^{th} pole. Expressions for the corresponding ψ and η are:

$$\psi^j(x) = \frac{1}{a} r^3(x, x_j) \tag{3.30}$$

$$\eta^j(x) = \frac{3}{a} r^2(x, x_j) d(x, x_j) \tag{3.31}$$

with $a = 9$ (or 12) for 2-D (or 3-D) problems, and

$$d(x, x_j) = (x - x_j) \cdot n(x) \tag{3.32}$$

n being the unit outward normal.

Expressions for ψ and η corresponding to a constant function

$$f^j(x) = c \tag{3.33}$$

associated to an internal pole, chosen to better simulate the heating of the whole body by a constant value, are:

$$\psi^j(x) = \frac{1}{b} r^2 (x, x_j) \cdot c \qquad (3.34)$$

$$\eta^j(x) = \frac{2}{b} r (x, x_j) d(x, x_j) \cdot c \qquad (3.35)$$

with $b = 4$ for 2-D, and $b = 6$ for 3-D problems. The constant c is taken as maximum distance between any pair of boundary nodes.

It may be noted that in order to satisfy the requirement of linear independence of coordinate functions $f^j(x)$, coincident poles (as will the case if modelling with continuous elements with double nodes at corners) must be avoided.

3.3.5 The Discretized Boundary Element Equations

Introduction of boundary element approximations (3.23) in conjunction with the spatial discretization and domain approximations (3.27) into integral equation (3.22) yields:

$$c_i u_i + \sum_{e=1}^{N_e} \left[\left(\int_{\Gamma_e} \phi^T q^* d\Gamma \right) u_e - \left(\int_{\Gamma_e} \phi^T u^* d\Gamma \right) q_e \right]$$

$$= \sum_{j=1}^{N} \left[c_i \psi_i^j + \sum_{e=1}^{N_e} \left\{ \left(\int_{\Gamma_e} \phi^T q^* d\Gamma \right) \psi_e^j - \left(\int_{\Gamma_e} \phi^T u^* d\Gamma \right) \eta_e^j \right\} \right] \dot{\alpha}^j$$

$$+ \sum_{m=1}^{N_c} \left(\int_{\Omega_m} \chi^T u^* d\Omega \right) \dot{q}_g^m \qquad (3.36)$$

where N, N_e and N_c denote the number of poles, the number of boundary elements, and the number of internal finite element cells respectively.

To obtain a discrete system of boundary element equations for nodal boundary unknowns, we employ the collocation procedure. By establishing the fulfilment of Eq. (3.36) at the N poles (which include all boundary freedom nodes plus atleast one internal pole), and utilizing boundary element and internal cell connectivities, we obtain following system of equations:

$$H\,U - G\,Q = (H\Psi - G\eta)\,\dot{\alpha} + B\,\dot{Q}_g \qquad (3.37)$$

in which U, Q, $\dot{\alpha}$ and $\dot{Q}_g$ represent nodal vectors corresponding to functions u, q, $\dot{\alpha}$ and q_g respectively. The elements of matrices H, G, Ψ, η and B are constituted from the terms of the form:

$$H_{ij} = \hat{H}_{ij} + c_i\,\delta_{ij}$$

with

$$\hat{H}^k_{ir} = \int_{\Gamma_j} \phi_k\, q^*(x_i,x)\, d\Gamma(x)$$

$$G^k_{ir} = \int_{\Gamma_j} \phi_k\, u^*(x_i,x)\, d\Gamma(x)$$

$$\Psi_{ij} = \psi^j(x_i);\quad \eta_{ij} = \eta^j(x_i) \qquad (3.38)$$

$$B^k_{is} = \int_{\Omega_m} \chi_k\, u^*(x_i,x)\, d\Omega(x)$$

where r = Cb(j,k) and s = Cc(m,k). Cb and Cc denote global boundary element connectivity matrix and finite element connectivity matrix respectively.

Evaluation of expression (3.17) at all poles obtains:

$$\dot{U} = F \dot{\alpha} \tag{3.39}$$

which is used in the form

$$\dot{\alpha} = F^{-1} \dot{U} \tag{3.40}$$

Substituting Eq. (3.40) into Eq. (3.37), we get

$$C\dot{U} + HU - GQ - B\dot{Q}_g = 0 \tag{3.41}$$

with

$$C = (G\eta - H\Psi) F^{-1} . \tag{3.42}$$

System of equations (3.41) is similar in form to the one obtained using the finite element method with the difference that the presence of vector Q renders it into a 'mixed-type' system as compared to 'displacement-only' type finite-element system of equations. We can utilize any time integration scheme for solution of this system.

3 .3.6 Time-Integration Schemes

For solving the system of equations (3.41), we shall use a finite element discretization applied to time-domain. In view of infinite extent of time domain, we concentrate on finite domains of time, and repeat the computation for subsequent domains with new initial conditions [32] . In following lines, we assume that full domain of investigation corresponds with that of one element and, derive recurrence relations between two successive values - two point recurrence relations - using the weighted residual and the least squares formulations.

Following standard finite element approximation procedure, we can write

$$A(t) = \sum_j N^j(t)\, A^j \tag{3.43}$$

where A^j denotes vector A at time t_j, and $N^j(t)$ are scalar shape functions.

Compatibility and completeness conditions require the N^j to be at least of first order, as only the first order derivatives are involved in Eq. (3.41). For a typical linear time element shown in Fig. (3.3), interpolation and shape functions, and their first derivatives in terms of local variable

$$\zeta = (t - t_m)/\Delta t \,, \quad 0 \leq \zeta \leq 1 \tag{3.44}$$

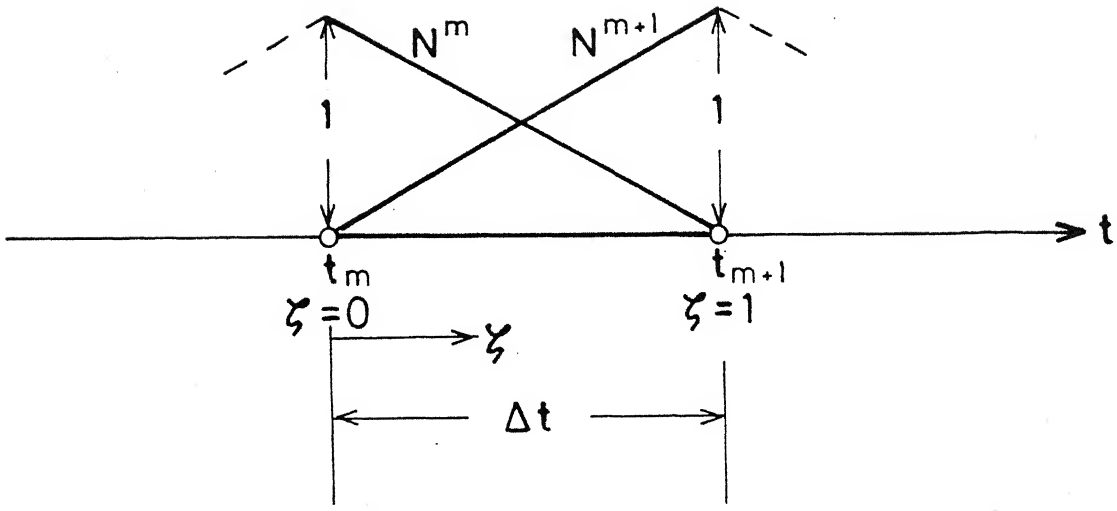

$$\zeta = \frac{t - t_m}{\Delta t}$$

Fig. 3.4 Shape functions for linear time' element '

are:

$$N^m = 1 - \zeta \quad , \quad \dot{N}^m = -\frac{1}{\Delta t}$$
$$N^{m+1} = \zeta \quad , \quad \dot{N}^{m+1} = \frac{1}{\Delta t} \qquad (3.45)$$

with Δt as length of the element.

Using the same set of interpolation functions for all functions viz., U, Q, and $\dot{Q}_g$, in Eq. (3.41) we get:

$$C(\dot{N}^m U^m + \dot{N}^{m+1} U^{m+1}) + H(N^m U^m + N^{m+1} U^{m+1}) - G(N^m Q^m + N^{m+1} Q^{m+1})$$
$$- B(N^m \dot{Q}_g^m + N^{m+1} \dot{Q}_g^{m+1}) = 0 \qquad (3.46)$$

A. Weighted Residual Formulation 32

Under the assumption of one element representing the full domain of investigation in time, we can write a weighted residual statement, corresponding to Eq. (3.46), given by:

$$\int_0^1 W_j \left[C(\dot{N}^m U^m + \dot{N}^{m+1} U^{m+1}) + H(N^m U^m + N^{m+1} U^{m+1}) \right.$$
$$\left. - G(N^m Q^m + N^{m+1} + Q^{m+1}) - B(N^m \dot{Q}_g^m + N^{m+1} \dot{Q}_g^{m+1}) \right] d\zeta = 0 \quad (j=1) \qquad (3.47)$$

where W_j represents a weighting function.

Inserting Eq. (3.45) into Eq. (3.47), we obtain a recurrence relation:

$$(C/\Delta t + \Theta H) U^{m+1} - \Theta G\, Q^{m+1} = [C/\Delta t - (1-\Theta) H] U^m + (1-\Theta) G\, Q^m$$
$$+ B\left[(1-\Theta)\, \dot{Q}_g^m + \Theta \dot{Q}_g^{m+1} \right] \qquad (3.48)$$

where

$$\Theta = \int_0^1 W_j \, \zeta \, d\zeta \; / \; \int_0^1 W_j \, d\zeta$$

Values of Θ for a series of weighting functions are:

$$\begin{aligned}
W_j &= \delta(\zeta) &&: \quad \Theta = 0 \\
W_j &= \delta\left(\zeta - \tfrac{1}{2}\right) &&: \quad \Theta = 1/2 \\
W_j &= \delta(1 - \zeta) &&: \quad \Theta = 1 \\
W_j &= 1 &&: \quad \Theta = 1/2 \\
W_j &= 1 - \zeta &&: \quad \Theta = 1/3 \\
W_j &= \zeta &&: \quad \Theta = 2/3
\end{aligned} \tag{3.49}$$

From stability considerations, $\Theta \geq 1/2$ for unconditionally stable scheme. The fully implicit scheme corresponding to $\Theta = 1$ is mostly used in present work as it gives stable and oscillation free solution.

B. Least Squares Formulation

In context of finite element methods in space and time, Zienkiewicz [32] has given a least-square scheme in time-domain, and shown that this scheme is the most accurate amongst various two-point integration scheme, though at a greater associated cost. In the following lines, we construct a similar scheme. Motivation for ensuing formulation is expected high accuracy.

In the context of one element representing the whole domain and linear interpolation functions, we write a functional Π given by integral of square of error over the element, i.e.

$$\Pi = \int_0^1 [\, C(\dot{N}^m U^m + \dot{N}^{m+1} U^{m+1}) + H(N^m U^m + N^{m+1} U^{m+1})$$

$$- G(N^m Q^m + N^{m+1} Q^{m+1}) - B(N^m \dot{Q}_g^m + \dot{N}^{m+1} \dot{Q}_g^{m+1})\,]^T$$

$$[\, C(\dot{N}^m U^m + \ldots.]\; d\zeta \qquad (3.50)$$

We minimize functional Π with respect to variables U^{m+1}, and Q^{m+1} subject to prescribed constraints in form of boundary conditions. We can adopt two approaches. The first consists in introduction of a set of Lagrange multipliers, whereas the second involves a direct substitution process eliminating some of variables (equal to number of constraints) using constraint conditions. The first approach, though very general, would entail the solution of an algebraic system of order 3N as compared to the one obtained using second approach having order N, N being the number of freedom nodes. Simple form of boundary (constraint) conditions offers further incentive for choice of second approach, and we opt for it.

Introducing boundary conditions (3.7) and (3.8) and Eq. (3.45) into Eq. (3.50), and minimizing the functional with respect to vector of unknowns X defined as

$X_j = Q_j^{m+1}$, if boundary condition (3.7) specified at node j.

$= U_j^{m+1}$, if boundary condition (3.8) specified at node j or it is an internal point.

We obtain following set of recurrence relations:

-- If $X_i = U_i^{m+1}$, then, i^{th} equation has the form:

$$\sum_j \Big[\Big\{ \frac{C^T C}{(\Delta t)^2} + \frac{(C^T H + H^T C)}{2\Delta t} + \frac{H^T H}{3} - A^T \Big(\frac{G^T C}{2\Delta t} + \frac{G^T H}{3}\Big) \Big\}_{ij} U_j^{m+1}$$

$$- \Big\{\frac{C^T G}{2\Delta t} + \frac{H^T G}{3} - A^T \frac{G^T G}{3}\Big\}_{ij} Q_j^{m+1} - \Big\{\frac{C^T G}{2\Delta t} + \frac{H^T G}{6} - A^T \frac{G^T G}{6}\Big\}_{ij} Q_j^m$$

$$+ \Big\{ - \frac{C^T C}{(\Delta t)^2} + \frac{(C^T H - H^T C)}{2\Delta t} + \frac{H^T H}{6} - A^T \Big(\frac{G^T C}{2\Delta t} - \frac{G^T H}{6}\Big) \Big\}_{ij} U_j^m$$

$$- \Big\{ \frac{C_{ij}^T}{2\Delta t} (S_j^m + S_j^{m+1}) + \frac{H_{ij}^T}{3} \Big(\frac{S_i^m}{2} + S_j^{m+1}\Big) - \frac{(A^T G)^T_{ij}}{3}$$

$$\Big(\frac{S_i^m}{2} + S_j^{m+1}\Big) \Big\} \Big] = 0 \qquad (3.51)\,(a)$$

-- If $X_i = Q_i^{m+1}$, then, i^{th} equation has the form:

$$\sum_j \Big[\Big\{ - \Big(\frac{G^T C}{2\Delta t} + \frac{G^T H}{3}\Big) \Big\}_{ij} U_j^{m+1} + \frac{(G^T G)_{ij}}{3} Q_j^{m+1}$$

$$- \Big\{\frac{G^T H}{6} - \frac{G^T C}{2\Delta t}\Big\}_{ij} U_j^m + \frac{(G^T G)_{ij}}{6} Q_j^m$$

$$+ \frac{(G^T)_{ij}}{3} \Big(\frac{S_j^m}{2} + S_j^{m+1}\Big) \Big] = 0 \qquad (3.51)\,(b)$$

In the above equation, A is a diagonal matrix, and S is a column vector. These are defined as:

$$A_{ij} = \frac{\partial Q_i}{\partial U_j}$$

$$S_j^m = \sum_k B_{jk} \left(\dot{Q}_g^m\right)_k \qquad (3.52)$$

Equations (3.51) represent the recurrence relation obtained from least squares formulation. Obviously this scheme involves more computations as compared to the scheme given by Eq. (3.48).

System of equations (3.48) or (3.51) can be solved by using either a direct elimination procedure such as Gauss elimination, if the system is linear, or, a Newton-Raphson procedure, if it is nonlinear.

3.3.7 Solution at Internal Points

After we have obtained boundary unknowns and temperature(s) at internal pole(s), we appeal to Eq. (3.36) to compute value of temperature at any specified internal point . Noting that for an internal point i, $c_i = 1$, we can rewrite Eq. (3.36) as:

$$u_i = \sum_{e=1}^{N_e} \left[\left(\int_{\Gamma_e} \phi^T u^* d\Gamma \right) q_e - \left(\int_{\Gamma_e} \phi^T q^* d\Gamma \right) u^e \right]$$

$$+ \sum_{m=1}^{N_c} \left(\int_{\Omega_m} \chi^T u^* \, d\Omega \right) \dot{q}_g^m$$

$$+ \sum_{j=1}^{N} \left[\psi_i^j + \sum_{e=1}^{N_e} \left\{ \left(\int_{\Gamma_e} \phi^T q^* d\Gamma \right) \psi_e^j - \left(\int_{\Gamma_e} \phi^T u^* d\Gamma \right) \eta_e^j \right\} \right] \dot{\alpha}^j \qquad (3.53)$$

which after application of element connectivities takes the form:

$$u_i = \sum_{i=1}^{N_b} (G_{ij} Q_j - H_{ij} U_j) + \sum_{j=1}^{N} \left[\psi_{ij} + \sum_{k=1}^{N_b} (H_{ik} \psi_{kj} - G_{ik} \eta_{kj}) \right] \dot{\alpha}$$

$$+ \sum_{k=1}^{N_T} B_{ik} \dot{Q}_{gk} \qquad (3.54)$$

where N_b, N and N_T denote the number of boundary nodes, the number of poles, and the number of total nodes (boundary + internal) respectively. Values of $\dot{\alpha}_j$ can be calculated using Eq. (3.40), and interpolation given by Eq. (3.45), i.e.,

$$\dot{\alpha}_j = \sum_{k=1}^{N} (F^{-1})_{jk} \dot{U}_k \qquad (3.55)$$

and

$$\dot{U}_k = \frac{1}{\Delta t} (U_k^{m+1} - U_k^m) \, .$$

Fluxes at internal points can be computed by taking derivative of Eq. (3.53) with respect to coordinates of the internal point.

3.4 DRBEM Formulation for Nonlinear Conduction [8]

The general heat conduction equation can be written as:

$$\rho c \frac{\partial u}{\partial t} = \nabla . (k \nabla u) + \dot{q}_g \qquad (3.5)$$

with associated initial and boundary conditions given by Eqs. (3.6) - (3.8). In order to obtain a boundary element formulation corresponding to the above problem, Wrobel and Brebbia [8] introduced the integral of conductivity as new dependent variable in conjunction with a modified time variable obtaining a linear conduction equation in Kirchhoff transform space. In following lines, we review the above mentioned formulation and the solution procedure based on it.

3.4.1 Transformation of Governing Equations

We introduce a new dependent variable defined as:

$$U = \int_{u_r}^{u} k(u)\, du \qquad (3.56)$$

where u_r denotes an arbitrary reference value. The above

relation represents the so-called Kirchhoff's transformation. We denote this transformation rule by T, i.e.

$$U = T(u) \tag{3.57}$$

From equation (3.56), we have

$$\nabla U = k \nabla u \tag{3.68}$$

$$\frac{\partial U}{\partial t} = k \frac{\partial u}{\partial t} \tag{3.59}$$

Introducing Eqs. (3.58) and (3.59) into (3.5) obtains:

$$\frac{1}{a} \frac{\partial U}{\partial t} = \nabla^2 U + \dot{q}_g \tag{3 .60}$$

with $a = a(u) = k/\rho c$, the non-dimensional thermal diffusivity. Since u is a continuous function of x and t, we can write $a = a(x,t)$. We now define a modified time variable τ by the relation:

$$\tau = \int_{t_o}^{t} a(x,t)\, dt \tag{3.61}$$

From Eq. (3.61), we get

$$\frac{\partial \tau}{\partial t} = a \tag{3.62}$$

Substituting Eq. (3.62) into Eq. (3.60), we obtain

$$\frac{\partial U}{\partial \tau} = \nabla^2 U + \dot{q}_g \quad \text{in} \quad \Omega \times (t_o, t_F] \tag{3.63}$$

Initial and boundary conditions in the Kirchhoff Transform space are given by:

$$U(x,0) = T(u_o(x)) \quad \text{on} \quad \Omega \tag{3.64}$$

$$U(x,t) = \bar{U}(x,t) = T(\bar{u}(x,t)) \quad \text{on } \Gamma_u \times (t_o, t_F]$$

$$Q(x,t) = \frac{\partial U}{\partial n} = q(x,t) = f_c(x,t,T^{-1}(U)) \tag{3.65}$$

$$\text{on } \Gamma_q \times (t_o, t_F]$$

We note that the Eq. (3.63) has the same form as the linear conduction equation (3.9) with the exception that the modified time variable in it is itself a function of x. This necessiates the employment of an iterative solution process, which is outlined in next sub-section.

3.4.2 Solution Process

The application of the dual reciprocity boundary element method to Eq. (3.63) obtains a system of equations similar to Eq. (3.48) with the weighted residual formulation. The recurrence relation can be written as:

$$(\bar{C} + \theta H)\ U^{m+1} - \theta G\ Q^{m+1} = [\bar{C} - (1-\theta) H\ ]\ U^{m} + (1-\theta) G\ Q^{m} + B[\ (1-\theta)\dot{Q}_g^{m} + \theta\ \dot{Q}_g^{m+1}\ ] \qquad (3.66)$$

with $\bar{C}_{ij} = C_{ij}/\Delta\tau_j$. In above equation U and Q represent nodal vectors in the Kirchhoff Transform space, and $\Delta\tau_j$ denotes the step value of the modified time variable τ at node j, i.e.,

$$\Delta\tau_j = a_j\ \Delta t \qquad (3.67)$$

For the special case of constant diffusivity, i.e., a = 1, $\Delta\tau_j = \Delta t$ for all points j. In this case, we can employ a standard equation solver to obtain the solution in transform space. For general case, we employ following iterative procedure [8] based on the Newton-Raphson method:

Step 1 : Obtain a linear solution of Eq. (3.66) for a constant $\Delta\tau = \Delta t$, and using only the linear part of flux boundary conditions with assumption u = U.

Step 2 : With values of U at all nodes, find u, material property values, and time step $\Delta\tau$ at all nodes. Also compute derivatives of material properties required in evaluation of coefficients of the Jacobian matrix.

Step 3 : Update the Jacobian matrix and the residual vector, and find a new solution.

Step 4 : Check if specified tolerance(s) is (are) achieved. If yes, then go to next step. Otherwise, go to step 2.

Step 5 : With converged solution at current time-step, update initial conditions, and carry out steps (1) - (4) for solution at next step, if desired.

In the above, the residual vector refers to $f(x^*)$ where x^* is an approximate solution for nonlinear equations

$$f(x) = 0 \tag{3.68}$$

The Jacobian or tangent matrix (J) is defined as:

$$J_{ij} = \frac{\partial f_i}{\partial x_j} \tag{3.69}$$

We present a Newton-Raphson algorithm in next chapter.

3.5 Energy Residual - A Physical Error Estimate

In this work, we do not make any attempt to present numerical error estimates which we consider to be outside its purview. In the following lines, we present a physical error estimate based on conservation of thermal energy. We check the input-output balance of thermal energy. The unbalance, herein referred to as the energy residual, can provide us with a fair estimate of accuracy and physical

acceptability of the computed approximate solution [25].

The total thermal energy of the heat conducting system under consideration can be calculated at any time t^m from:

$$E^m = \int_\Omega \rho c\, u^m(x)\, d\Omega\,(x) \tag{3.70}$$

where ρ, c, and u^m denote the mass density, the specific heat, and the temperature at point x at time t^m. Net inflow of energy across the boundary Γ during the time period $t^{m-1} < t < t^m$ is given by

$$E^m_{in} = \int_{t^{m-1}}^{t^m} dt \left(\int_\Gamma q\, d\Gamma\right) \tag{3.71}$$

q being the heat-influx, $k(\partial u/\partial n)$.
If rate of volumetric heat generation be $\dot{q}_g$, then total energy generation in time-period $t^{m-1} < t < t^m$ is:

$$E_g = \int_{t^{m-1}}^{t^m} dt \left(\int_\Omega \dot{q}_g\, d\Omega\right) \tag{3.72}$$

Assuming that all other forms of energy contained in the system remain constant during the interval $t^{m-1} < t < t^m$, conservation of energy requires:

$$E^m - (E^{m-1} + E^m_{in} + E_g) = 0 \tag{3.73}$$

where E^{m-1} represents the thermal energy of the system at time t^{m-1}.

Relation (3.73) is satisfied if solutions obtained were exact. With approximate solution the above relation is not satisfied exactly. We define the residual of the input-output balance by

$$R^m = E^m - (E^{m-1} + E^m_{in} + E^m_g) \tag{3.74}$$

We call R^m as the energy residual. We can clearly see that if $R^m = 0$, then we have exact conservation of thermal energy. Furthermore, smaller the magnitude of R^m, closer is the satisfaction of energy conservation, and this in turn, implies the accuracy of approximate solution.

We may note that the above approach can be used in case of linear as well as nonlinear conduction problems. For evaluation of integrals in Eqs. (3.70) - (3.72) we employ finite-element approximations.

We now proceed to the next chapter in which we discuss some important computational aspects related to numerical integration, solution of system of equations, approximations of variations of physical properties in case of nonlinear problems etc. We also present a macro-structure of the computer program developed.

CHAPTER 4

COMPUTATIONAL ASPECTS

4.1 Evaluation of Boundary Integrals

The integrals of following form need to be evaluated during the actual computations:

$$I^e(q, u^*, \xi) = \int_{\Gamma_e} \phi^e(x)\, u^*(\xi, x)\, d\Gamma(x) \tag{4.1}$$

$$I^e(u, q^*, \xi) = \int_{\Gamma_e} \phi^e(x)\, q^*(\xi, x)\, d\Gamma(x) \tag{4.2}$$

where Kernel functions $u^*(\xi, x)$ and $q^*(\xi, x)$ for two-dimensional problems are given by

$$\begin{aligned} u^*(\xi, x) &= \frac{1}{2\pi} \ln\left(\frac{1}{r}\right) \\ q^*(\xi, x) &= \frac{d}{2\pi r^2} \end{aligned} \tag{4.3}$$

with $d = (\xi - x).n$, n being the unit outward normal, and $r = |\xi - x|$. ξ denotes the collocation point, x, the field point, and $\phi^e(x)$ represents the interpolation function. We note from Eq. (4.3) that Kernels $u^*(\xi, x)$ and $q^*(\xi, x)$ remain regular as long as the collocation point ξ and the integration element Γ_e do not coincide. Also that farther the integration element from the collocation point,

flatter is the variation of integration Kernels over it. This nature of functions u^* and q^* suggests the use of selective numerical integration scheme. When the integration element contains the collocation point or is very close to it, a standard numerical scheme fails to give accurate results. This situation warrants special attention.

Approaches which have been suggested and used in the literature can be classified into four broad categories [33]. The first approach consists in the use of analytical integration over the elements which contain the collocation point or lie within a minimum distance from it, and, standard numerical quadrature over the rest of the elements. The analytical integration is, however, possible only for very simple elements.

The second approach advocates the use of a special scheme - analytic, semi-analytic or numerical - for "the singular elements" (i.e. those elements to which the collocation point belongs), and the use of a standard numerical scheme for the rest. This scheme has some problems when the collocation point is very close to the integration element.

The third approach is to use special numerical integration schemes for the singular elements and also for the closest of the rest according to some specific criterion such as ratio of the distance between the collocation point and the integration element to the size

of this element, limitation of the truncation error of the integration etc.

The fourth approach employs a standard numerical integration scheme with varying number of integration points over different elements (with increasing number of points of integration over the closest elements to the collocation point) according to one of the previous criteria. This is referred to as adaptive numerical integration.

In present work, we use the analytic approach for evaluation of singular integrals, and a form of the fourth approach for the rest. In following lines we briefly outline the methods used.

4.1.1 Regular Boundary Integrals

The integrals over the elements not containing the collocation point are regular. We employ standard Gaussian quadrature with varying number of integration points such that farther the integration element lies from the collocation point, the fewer the number of integration points:

$$\int_{-1}^{1} f(y)\, dy = \sum_{k=1}^{n_G} f(y_k) w_k \qquad (4.4)(a)$$

where y_k, w_k and n_G denote the point of integration, the weight corresponding to integration point y_k, and total number of points of integration. We use the following

heuristic criterion suggested in references 10,34,35 based on the ratio (s) of distance of the integration element from the collocation point to length of the integration element for selection of number of integration points (n_G) for linear elements:

$$\begin{aligned} s &\leq 1.5 &&: \quad n_G = 6 \\ 1.5 < s &\leq 2.5 &&: \quad n_G = 4 \\ s &\geq 5.5 &&: \quad n_G = 2 \end{aligned} \qquad (4.4)(b)$$

with $$s = \frac{|\xi - x_c|}{l}$$

where x_c is centroid of the integration element and l its length.

For integration over elements very close to the collocation point such that the minimum distance of the integration element from the collocation point is less than the length of the element, we can divide the element into number of sub-elements, do the integration over each sub-element using above method, and add the contributions of all sub-elements [33]. Division could be either uniform or graded. A criterion for uniform sub-division given in Reference [33] is :

$$N_{sub} = IFIX\,[l/d_{min}] + 1 \qquad (4.5)$$

where d denotes the distance of collocation point from integration element, IFIX denotes the integer part of the quotient, and N_{sub} the number of sub-divisions. A more sophisticated adaptive numerical integration scheme and related references can be found in Reference [33].

4.1.2 Singular Boundary Integrals

Over the element containing the collocation point, the integral Kernels u^* and q^* become singular. The integral containing u^* as its Kernel has integrable (logarithmic) singularity, whereas the one having q^* as its Kernel can be evaluated only in Cauchy principal value sense. In what follows, we present a brief review of methods available, and results obtained with the one used in our present work.

A. Boundary Integrals with Integrable Singularity

For evaluation of integral

$$I_e(q,u^*,\xi) = \int_{\Gamma_e} \phi^e(x)\, u^*(\xi,x)\, d\Gamma(x) \qquad (4.1)$$

over singular element, we can use adaptive numerical integration, semi-analytic, or analytic integration, or special numerical integration schemes. Adaptive numerical integration schemes use a large number of integration points near the singularity. Semi-analytic methods make use of analytical integration over a short segment of integration element, and standard numerical quadrature over the rest. For singularity at hand, i.e. $\ln(\frac{1}{r})$, we can make use of logarithmic weighting functions [36] in conjunction with Gaussian quadrature. For very simple elements, such as constant or linear elements, we can evaluate this integral analytically [10,34,35].

To utilize Logarithmic Gaussian quadratures, we need to make some changes in integral (4.1), as these quadrature formulas apply to interval $[0,1]$ with singularity at zero. Following Pina [37], we put

$$\ln(1/r) = \ln(\hat{x}/r) + \ln(1/\hat{x}) \tag{4.6}$$

Now, we can write:

$$I_e(q,u^*,\xi) = I_{er}(q,u^*,\xi) + I_{es}(q,u^*,\xi) \tag{4.7}$$

with $$I_{er} = \int_0^1 \frac{1}{2\pi} \ln(\hat{x}/r)\, \phi^e(x)\, J_e(\hat{x}')\, d\hat{x}' \tag{4.8}$$

$$I_{es} = \int_0^1 \frac{1}{2\pi} \ln(1/\hat{x})\, \phi^e(x)\, J_e(\hat{x}')\, d\hat{x}' \tag{4.9}$$

In the above $J_e(\hat{x}')$ denotes Jacobian of transformation mapping Γ_e onto interval $[0,1]$. Since $\hat{x}/r(\hat{x})$ remains bounded as $x \to \xi$, the integral in (4.8) is regular, and standard Gaussian quadrature can be used for its evaluation. Singular integral in Eq. (4.9) has the proper form required by Logarithmic quadrature.

The above approach is useful for any choice of boundary elements. However, for constant and linear elements, we can easily use analytical integration procedure. For these elements, results of analytical integrations are :

A.1 Constant Elements [10] [Fig. 3.1(a)]

$$I_e(u^*, \xi) = \frac{1}{2\pi}[1 - \ln(1/2)] \tag{4.10}$$

A.2 Continuous Linear Elements [10, 34] [Fig. 3.1(b)]

When collocation point is node 1 of the integration element:

$$I_e^1(u^*, \xi) = \frac{1}{4\pi}[\frac{3}{2} - \ln(1)] \tag{4.11}$$

$$I_e^2(u^*, \xi) = \frac{1}{4\pi}[\frac{1}{2} - \ln(1)] \tag{4.12}$$

Similarly, when collocation point coincides with local node 2 of the element, we have:

$$I_e^1(u^*, \xi) = \frac{1}{4\pi}[\frac{1}{2} - \ln(1)] \tag{4.13}$$

$$I_e^2(u^*, \xi) = \frac{1}{4\pi}[\frac{3}{2} - \ln(1)] \tag{4.14}$$

A.3 Partially Continuous Linear Elements [Fig. 3.1(c)]

Elements of Type 1:

Case 1: When collocation point coincides with freedom node 1 of the element:

$$I_e^1(u^*, \xi) = \frac{1}{4\pi}[\frac{4}{3} - \frac{2}{3}\ln(1)] \tag{4.15}$$

$$I_e^2(u^*, \xi) = \frac{1}{4\pi}[\frac{2}{3} - \frac{4}{3}\ln(1)] \tag{4.16}$$

Case 2 : Collocation point is local node 2 of the element:

$$I_e^1 (u^*, \xi) = \frac{1}{4\pi} \left[\left(\frac{1}{3} - \frac{3}{4} \ln 3\right) - \frac{2}{3} \ln (1/4) \right]$$

$$I_e^2 (u^*, \xi) = \frac{1}{4\pi} \left[\left(\frac{5}{3} - \frac{3}{4} \ln 3\right) - \frac{4}{3} \ln (1/4) \right] \quad (4.17)$$

Elements of Type 2:

Case 1: Collocation point is local node 1 of the element:

$$I_e^1 (u^*, \xi) = \frac{1}{4\pi} \left[\left(\frac{5}{3} - \frac{3}{4} \ln 3\right) - \frac{4}{3} \ln (1/4) \right]$$

$$I_e^2 (u^*, \xi) = \frac{1}{4\pi} \left[\left(\frac{1}{3} - \frac{3}{4} \ln 3\right) - \frac{2}{3} \ln (1/4) \right] \quad (4.18)$$

Case 3: Collocation point is local node 2 of the element:

$$I_e^1 (u^*, \xi) = \frac{1}{4\pi} \left[\frac{2}{3} - \frac{4}{3} \ln (1) \right]$$

$$I_e^2 (u^*, \xi) = \frac{1}{4\pi} \left[\frac{4}{3} - \frac{2}{3} \ln (1) \right] \quad (4.19)$$

In all the above expressions, l denotes the length of the element.

B. Cauchy Principal Value Integrals

Integrals defined by (4.2),

$$I_e\ (u,q^*,\xi) \quad = \int_{\Gamma_e} \phi^e\ (x)\ q^*(\xi,\ x)\ d\Gamma(x) \qquad (4.2)$$

exist only in Cauchy principal value sense when collocation point lies on integration element. These integrals can be computed by using the finite parts of the integrals involved. Numerical integration formulas for finite part integrations are given in References [10,38] . For our present work, in which we use either constant or linear isoparametric elements, over the singular element, $q^*(\xi,x)$ is identically zero owing to orthogonality of vectors r and n. Thus, for constant and linear element:

$$I_e\ (u,\ q^*,\xi) \quad \equiv\ 0 \qquad (4.20)$$

whenever the collocation point and integration element coincide.

4.2 Evaluation of Domain Integrals

Presence of heat generation (source/sink) inside the domain necessiates evaluation of domain integrals. When we use finite element type approximation for source term as discussed in Chapter 3, we are required to evaluate

integrals of the form:

$$I^k = \int_{\Omega_e} \chi^k u^* \, d\Omega \tag{4.21}$$

we again observe that this integral becomes singular when collocation point belongs to the domain element Ω_e, as u^* contains a $\ln(1/r)$ factor. In the following lines, we discuss the numerical methods used to evaluate these integrals. We restrict ourselves to linear triangular finite elements.

4.2.1 Regular Domain Integrals

If collocation point ξ does not belong to the integration domain element Ω_e, integral in (4.21) is regular. For triangular domain elements, we use quadrature scheme due to Hammer et al. given in Reference [10]:

$$\int_0^1 \left(\int_0^{1-\zeta_2} f(\zeta_1, \zeta_2, \zeta_3) \, d\zeta_1 \right) d\zeta_2 = \frac{1}{2} \sum_{i=1}^{n} f(\zeta_1^i, \zeta_2^i, \zeta_3^i) w_i \tag{4.22}$$

where ζ_i's are triangular coordinates defined in Fig. (3.3), and w_i are weighting factors.

Using (4.22), we can write:

$$I^k = A_e \sum_{i=1}^{n} f(\zeta_1^i, \zeta_2^i, \zeta_3^i) \, w_i \tag{4.23}$$

with $f = \chi^k u^*$.

We adopt the following criterion for the number of integration point on the basis of ratio of distance of collocation point from centroid of the element to the characteristic length of element:

$$\begin{aligned} &\text{If } s \leq 3, \quad : \quad n = 7 \text{ (Quintic scheme)} \\ &\text{If } s > 3 \quad : \quad n = 4 \text{ (Cubic scheme)}, \end{aligned} \tag{4.24}$$

with $s = \dfrac{|x_c - \xi|}{l_e}$, and $l_e = \sqrt{2A_e}$. x_c is the centroid of the element, l_e is its characteristic length, and A_e is the area.

4.2.2 Singular Domain Integrals

When collocation point ξ belongs to the domain element Ω_e, the integral

$$I^k = \int_{\Omega_e} \chi^k \, u^* \, d\Omega(x) \tag{4.21}$$

becomes singular. To evaluate it, we follow the method proposed by Pina [37]. Let singular point coincides with the origin under isoparametric transformation. Letting $\hat{r}$ to denote the distance of the field point $\hat{x}$ from origin in isoparametric reference element, we can write:

$$\begin{aligned} I^k &= \int_{\Omega_e} \chi^k u^* \, d\Omega = \int_{\Omega_e} \chi^k \, \frac{1}{2\pi} \ln(1/r) \, J_e(\hat{x}) \, d(\hat{x}) \\ &= \int_{\Omega_e} \chi^k \, \frac{1}{2\pi} \ln(\hat{r}/r) \, J_e(\hat{x}) \, d\Omega(\hat{x}) \\ &\quad + \int_{\hat{\Omega}_e} \chi^k \, \frac{1}{2\pi} \ln(1/\hat{r}) \, J_e(\hat{x}) \, d\hat{\Omega} \\ &= I_{et} + I_{es} \end{aligned} \tag{4.25}$$

where $\hat{\Omega}$ denotes isoparametric reference element Fig.4.1 .

We choose a special reference element shown in Fig. 4.1(c). Jacobian of transformation in 2 A_e. $\hat{r}$ in (4.25) is defined by (with reference to Fig. 4.1 (c))

$$\hat{r} = \sqrt{\hat{x}^2 + \hat{y}^2} \tag{4.26}$$

We observe that first integral in right hand side of Eq. (4.25) is regular, and hence, method discussed in the previous section can be used for its evaluation. To perform integration using Hammer's quadrature scheme, we transform the integration domain $\hat{\Omega}_e$ into $\hat{\Omega}_e'$ in natural triangular coordinates. Jacobian of transformation is unity, and $(\hat{x},\hat{y})$ and (ζ_1,ζ_2) are related by:

$$\hat{x} = \zeta_1 + \zeta_2 , \quad \hat{y} = \zeta_2 \tag{4.27}$$

Therefore,

$$\begin{aligned} I_{er} &= \int_{\hat{\Omega}_e} \chi^k \frac{1}{2\pi} \ln (\hat{r}/r)\, J_e(\hat{x})\, d\Omega(\hat{x}) \\ &= A_e \sum_{i=1}^{n} f(\zeta_1^i, \zeta_2^i, \zeta_3^i)\, w_i \end{aligned} \tag{4.28}$$

where

$$f = \frac{1}{2\pi} \ln (\hat{r}/r), \quad \hat{r} = \sqrt{\hat{x}^2+\hat{y}^2} = \sqrt{(\zeta_1+\zeta_2)^2 + \zeta_2^2}$$

$\Phi^{e'}$: Isoparametric transformation

Φ^{e} : Special transformation

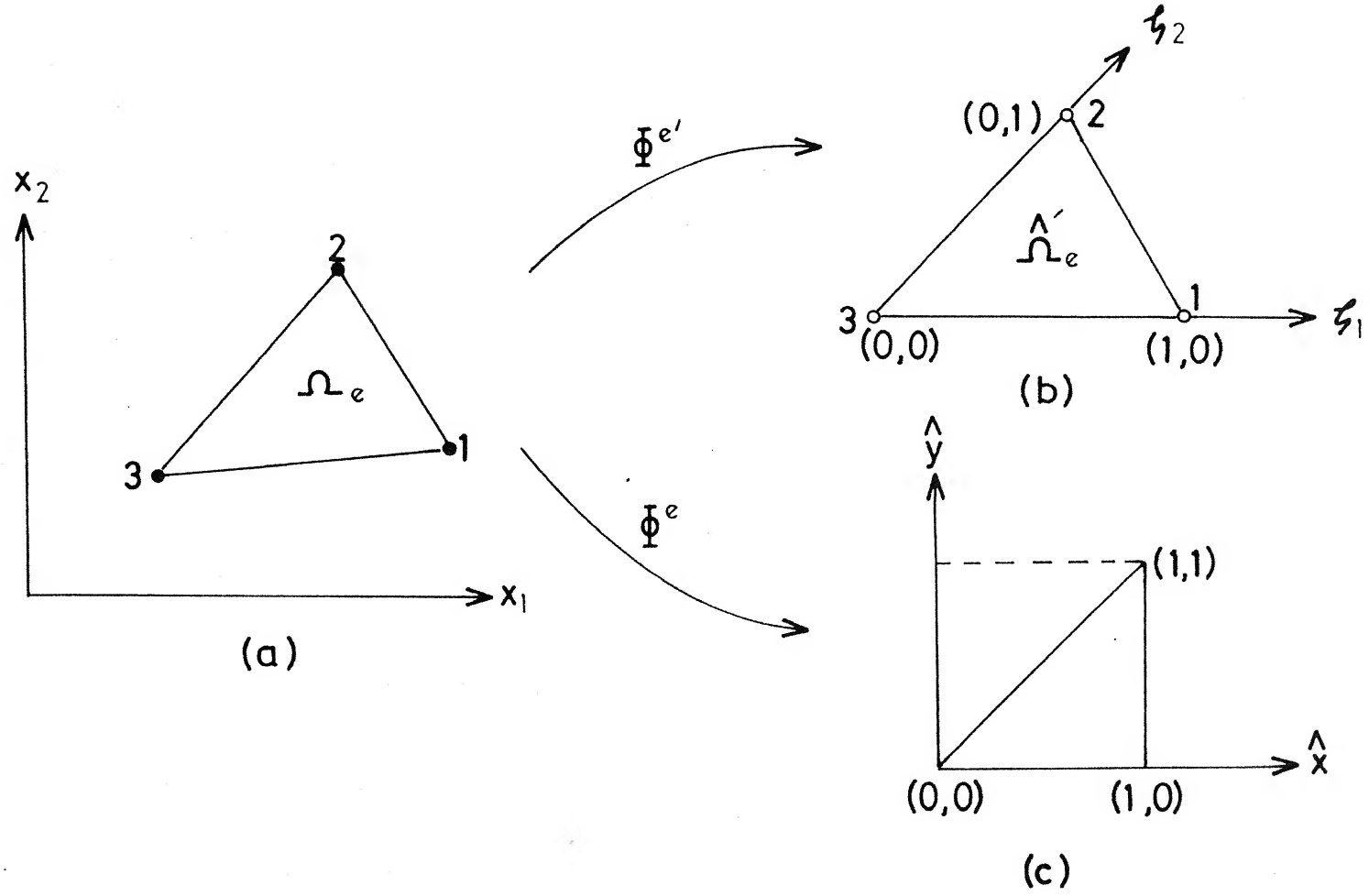

Fig.4.1 (a) Physical domain element.

(b) Isoparametric reference element

(c) Special reference element.

$$I_{es} = \frac{A_e}{4} \int_{-1}^{1}\int_{-1}^{1} (1+\xi_1)\, \frac{1}{2\pi} \ln(1/\hat{r})\chi^k \, d\xi_1 \, d\eta_1$$

$$= \frac{A_e}{4} \sum_{i=1}^{n_1} \sum_{j=1}^{n_2} w_i w_j \, f(\xi_1^i, \eta_1^j) \qquad (4.32)$$

with $f = (1+\xi_1)\, \frac{1}{2\pi} \ln(1/\hat{r})\, \chi^k$ and

$$\hat{r} = \frac{1}{2}(1+\xi_1)\{1 + \frac{1}{4}(1+\eta_1)^2\}^{1/2}$$

Interpolation functions for linear approximation χ^k are defined in the terms of coordinates (ξ_1, η_1) by:

$$\chi^1 = \frac{1}{4}(1+\xi_1)(1-\eta_1)$$

$$\chi^2 = \frac{1}{4}(1+\xi_1)(1+\eta_1) \qquad (4.33)$$

$$\chi^3 = \frac{1}{2}(1-\xi_1)$$

In the procedure discussed above, we assumed that the collocation point is a vertex of the triangular element. However, even when the collocation point is on one of the sides or in the interior of the element, the domain element can be divided in two or three subelements, the integration procedure detailed above can be applied to evaluate integrals over each subelement and we finally add these to obtain the required integral. We employ this procedure of subdivision to evaluate integrals corresponding to the situation of collocation point belonging to one of the sides of the domain element, as will be

the case if a constant or partially continuous linear element forms one of its sides.

A word about sequence of computation of integrals is in order. As we have noted that evaluation of an integral over an element requires computation of coordinates of integration points, its centroid etc., it is advisable that we take an element, and compute integrals over it from each collocation point. This will require lesser number of operations as compared to the sequence of choosing a collocation point, and computing integral over each element. We adopt same sequence of computation for boundary integrals also.

4.3 Consideration of Symmetries

By "symmetry" in this section, we mean planar symmetry with respect to global coordinate planes or sectorial symmetry. Symmetry conditions are used to reduce the number of elements needed to define the problem with consequent reduction in number of equations needed to solve it, and, hence, considerable reduction in computing time and memory requirements.

Two approaches have been suggested and used in literature. The first one corresponds to the employment of knowledge of boundary conditions over the axes (planes) of symmetry, thereby, replacing the initial problem by a smaller one. This approach is quite general and can be applied to any kind of planar a sectorial symmetry.

The second approach consists in introducing symmetry conditions over the coordinates and the boundary conditions. We employ herein a direct condensation process with integration over reflected elements. In this approach, no discretization of symmetry axes is required in direct contrast to the first approach. The number of equations required is, thus, reduced drastically.

The second approach has the advantages of greater accuracy, and lesser number of equations. However, it requires greater number of integrations as compared to the former. Also, for each type of symmetry, a special consideration is required. If in addition, domain terms are also present, the process of discretization of domain and reflections involved are not quite clear. In view of its restricted generality, we have adopted the first approach, which does not require any additional operations in program.

4.4 Solution of System of Equations

Depending on the nature of the diffusion process, and boundary conditions of the problem at hand, system of equations (3.48), (3.51) or (3.66) will be either linear or nonlinear. The system matrix is invariably full. Also that for 2-D problems, the size of system matrix is usually not very large as compared to the comparable system of equations obtained using Finite Element Method. Thus, in most of the cases, a direct solution procedure based on Gauss-elimination or its variants is usually the most suitable.

In our work, we have used a NAG Routine F04ATF based on Crout's factorization method for solution of linear system of equations.

Solution of nonlinear system of equations requires a considerable effort in terms of selection of solution procedure, starting guess (as all of these methods are iterative in nature, and require a initial solution to start with). In general, for weak nonlinear systems, modified Newton Methods are recommended, while for others, full Newton-Raphson Iteration is recommended. All these methods are strongly dependent on closeness of initial guess to the exact solution, and none of these has global convergence properly.

4.4.1 Newton-Raphson Algorithm

Let,

$$f(x) = 0 \tag{4.34}$$

represents the nonlinear system of equations. The equality in above equation holds for exact solution vector x. To solve the above system we use iterative solution procedure. Let x_n be the approximate solution at n^{th} iteration. To obtain an expression for improved solution, let us expand f in Taylor series about x_n.

$$f(x) = f(x_n) + \left[\frac{\partial f}{\partial x}\right]_{x=x_n} (x-x_n) + \left[\frac{\partial^2 f}{\partial x^2}\right]_{x=x_n} (x-x_n)^2 + \ldots. \tag{4.35}$$

Supposing that x is the exact solution, and neglecting terms containing second and higher order derivatives, we get:

$$0 = f(x_n) + \left[\frac{\partial f}{\partial x}\right]_{x=x_n} (x - x_n)$$

or, $$J_n \Delta x_n = -f(x_n) \tag{4.36}$$

with $\Delta x_n = x - x_n$, and $J_n = \left[\frac{\partial f}{\partial x}\right]_{x=x_n}$ is the Jacobian or tangent matrix. Having computed Δx, we can obtain the improved solution at $(n+1)^{th}$ step by

$$x_{n+1} = x_n + \Delta x_n \tag{4.37}$$

We note that at each step, we have to solve a new set of linearized equations (4.36).

The process of iteration is continued until the residual vector defined by $f(x_{n+1})$ is sufficiently small.

To check the convergence of iterative procedure, we make use following vector norms for residual vector f and solution vector x:

$$FNORM_n = \underset{j}{\text{Max}} \, |f_n^j| \quad , \; j = 1, \ldots N \tag{4.38}$$

$$XNORM_n = \frac{1}{N} \sum_{j=1}^{N} \frac{|x_j^n - x_j^{n-1}|}{|x_j^n|} \tag{4.39}$$

where N represents the number of equations. Process of iteration is said to be converging if

$$FNORM_n < FNORM_{n-1}$$
$$\text{and} \quad XNORM_n < XNORM_{n-1} \tag{4.40}$$

If FTOL and XTOL denote the specified tolerances, then process of iteration ceases with message for converged solution if any or both of the following inequalities are satisfied:

$$\text{(i)} \quad FNORM_n < FTOL$$
$$\text{(ii)} \quad (FNORM_n < FNORM_{n-1} \text{ and } XNORM_n < XNORM_{n-1}) \tag{4.41}$$
$$\text{and} \quad XNORM_n < XTOL$$

Process of iteration also terminates with an appropriate message if iteration is not making satisfactory progress.

4.4.2 Initial Solution for Newton-Raphson Iteration

The application of Newton-Raphson Algorithm discussed in above section requires a starting solution. In the present work, we compute a linear solution at each time-step of a linear system obtained by dropping the nonlinear part. We use this linear solution as initial solution for Newton-Raphson Iteration.

For problems with linear conduction and nonlinear boundary conditions, linear system is obtained by neglecting the nonlinear part of boundary conditions. For nonlinear heat diffusion problems, to obtain linear system for computation of initial solution we:

(i) assume $\Delta\tau_j = \Delta t$ for all j,

(ii) assume $u = U$ in flux boundary condition, and drop the nonlinear part of modified expression.

The resulting system is linear in transformed variable U.

4.5 Solution Procedure for Linear Conduction

For physical problems with constant material properties, system of boundary element equations - Eq. (3.48) or Eq. (3.51) remains linear as long as the boundary conditions are linear. We introduce prescribed boundary conditions in system of equations (3.48) or (3.51).

4.5.1 Linear Systems

For linear systems, we rearrange Eq. (3.48) or Eq. (3.51) after introducing the boundary conditions such that left hand side contains the unknowns, and right hand side is known. Resulting system is solved using a linear equation solver based on direct elimination or iterative procedures for fully populated real coefficient matrix system. We use NAG Library Routine F04ATF based on Crout's Method.

4.5.2 Nonlinear Systems

Solution procedure for nonlinear systems involves two steps:

Step 1: Obtain a linear solution, which is used as the initial solution for step 2.

Step 2: Using linear solution from step 1 as initial guess for solution vector, use a routine based on Newton-Raphson Method detailed in Section 4.4.1.

To obtain linearized system for step 1 above we use the procedure given in Section 4.4.2.

4.6 Solution Procedure for Nonlinear Conduction

Nonlinear heat conduction problems may be classified into two distinct categories:

(i) Problems involving constant diffusivity,

(ii) Problems involving temperature dependent diffusivity.

In the first category of problems, although the conductivity is temperature dependent, yet the variations of k and ρc with temperature are such that (these differ at the most by a multiplicative constant) diffusivity is constant. Thus, time variable in transformed equation

$$\frac{\partial U}{\partial \tau} = \nabla^2 U + \dot{q}_g \qquad (3.63)$$

is independent of space coordinates. The system of equations (3.66) is, therefore, same as that obtained for linear conduction problems, and procedure detailed in Section 4.5 for linear problems is applied for solution of problems of this category.

For problems with temperature-dependent diffusivity, we outlined the iterative solution scheme in Section 3.4.2. In the following lines, we briefly discuss the computational details involved in iterative solution scheme.

4.6.1 Iterative Solution Scheme

Step 1: To obtain linear solution which is used as the starting solution for Newton-Raphson Iteration, we put $\Delta\tau_j = \Delta t$ in Eqn . (3.66). Flux boundary conditions in transformed space are linearized by putting u = U, and retaining only the linear part. By introducing this linear part in the appropriate system of equations, solve the resulting linear equation system, to get the linear solution.

Step 2: With linear solution obtained from step 1, employ Newton-Raphson Algorithm to obtain final solution. Expression for residual vector is

$$f(X^{m+1}) = (\bar{C} + \Theta H)\, U^{m+1} - \Theta\, GQ^{m+1} - [\bar{C} - (1-\Theta)H]U^{m}$$

$$-(1-\Theta)\, GQ^{m} - B\,[(1-\Theta)\,\dot{Q}_g^{m} + \Theta\,\dot{Q}_g^{m+1}] \qquad (4.42)$$

where X denotes vector of unknowns. The coefficient of the Jacobian matrix are defined by

$$J_{ij}^{m+1} = \frac{\partial\, f_i\,(X^{m+1})}{\partial\, X_j^{m+1}} \qquad (4.43)$$

From (4.42), we have:

(i) when $X_j^{m+1} = Q_j^{m+1}$: $J_{ij} = -\Theta\, G_{ij}$

(ii) when $X_j^{m+1} = U_j^{m+1}$:

$$J_{ij} = \frac{1}{\Delta\tau_j} C_{ij} + \Theta\, H_{ij} - \Theta\, G_{ij}\, \frac{\partial Q_j^{m+1}}{\partial U_j^{m+1}} + C_{ij}$$

$$(U_j^{m+1} - U_j^{m})\, \frac{\partial}{\partial U_j^{m+1}} (\Delta\tau_j)^{-1} \qquad (4.44)$$

with $$\frac{\partial\,(\Delta\tau_j)^{-1}}{\partial U_j^{m+1}} = -\frac{\rho_j\, C_j}{k_j^3\, \Delta t} \left(\frac{d\, k_j}{d\, u_j^{m+1}} - \frac{k_j}{C_j}\, \frac{d\, C_j}{du_j^{m+1}}\right.$$

$$\left. - \frac{k_j}{\rho_j}\, \frac{d\rho_j}{du_j^{m+1}}\right) \qquad (4.45)$$

and $$\frac{\partial Q_j^{m+1}}{\partial U_j^{m+1}} = \frac{1}{k_j}\, \frac{\partial f_c(u,x,t)}{\partial u_j}$$

4.6.2 Approximation of Property Variations

In the present work,we employ piecewise linear approximation to model the temperature dependence of material properties. Derivatives of k, ρ , and c with respect to u, at any point j, are, thus, given by the slope of segment of curves to which u_j belongs. With reference to Fig. 4.2, the property value at temperature u lying on the segment i can be computed by:

$$A(u) = A_i + a_i (u - u_i) \tag{4.46}$$

where, a_i denotes the slope of segment 'i.

To compute initial conditions and temperature boundary conditions in the Kirchhoff transform space with above variation for thermal conductivity, we first carry out a search to determine to which segment does a given u belong . Thereafter, we can write

$$U = T(u) = \int_{u_r}^{u} k(u)\, du = \int_{u_r}^{u_i} k(\lambda) d\lambda + \int_{u_i}^{u} k(\lambda) d\lambda \tag{4.47}$$

$$\Rightarrow \quad U = U_i + \frac{(k_i + k)}{2} (u - u_i)$$

with $U_i = \int_{u_r}^{u_i} k(\lambda)\, d\lambda$, assumed to be known.

To perform an inverse transform, we again localize the segment i corresponding to given value of U. Using

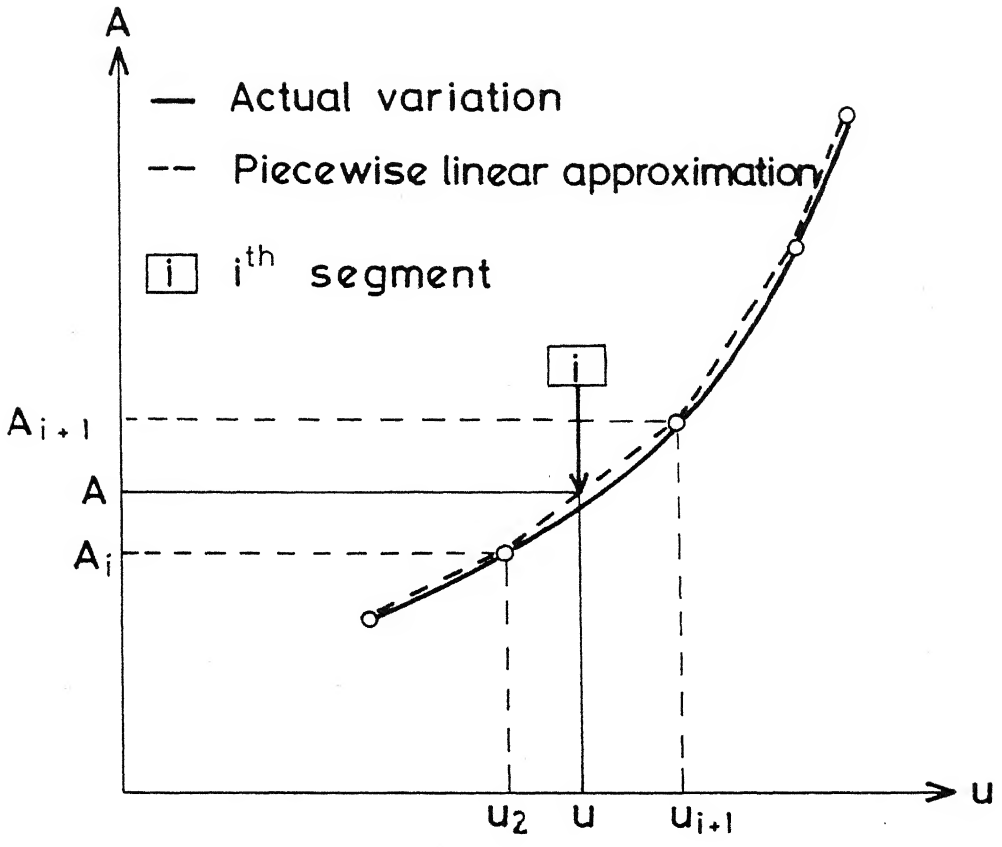

Fig. 4.2 Piecewise-linear approximation of property (A)- temperature (u) curve.

Eq. (4.46) and Eq. (4.47), we obtain following expression for u

$$u = T^{-1}(U) = u_i + \frac{-k_i + \sqrt{k_i^2 + 2a_i (U - U_i)}}{a_i} \qquad (4.48)$$

4.7 Program Structure

In the following, we briefly discuss the macro-structure and organization of the Boundary Element program developed herein. The general scheme of the program is composed of a Main Program, and several Procedure Modules which can be run independently. The Main Program defines the dimensions of arrays and the common areas, and calls the rest of routines during the running of the program. Procedure Modules are usually composed of a general routine, which may control a set of other subroutines either specific for this module or shared with others. Each Procedure Module performs a specific function. Figure 4.3 shows the typical scheme for the program.

In accordance with a scheme in Fig. 4.3, we have written a program which capable of solving a steady state or transient heat conduction problem in two-dimensions. The program can account for time-dependent boundary conditions and heat generation. It is composed of about 50 routines and 3000 lines. General flow chart of the program is shown in Fig. 4.4. Appendix contains FORTRAN listing of the Main Program "DRBEM".

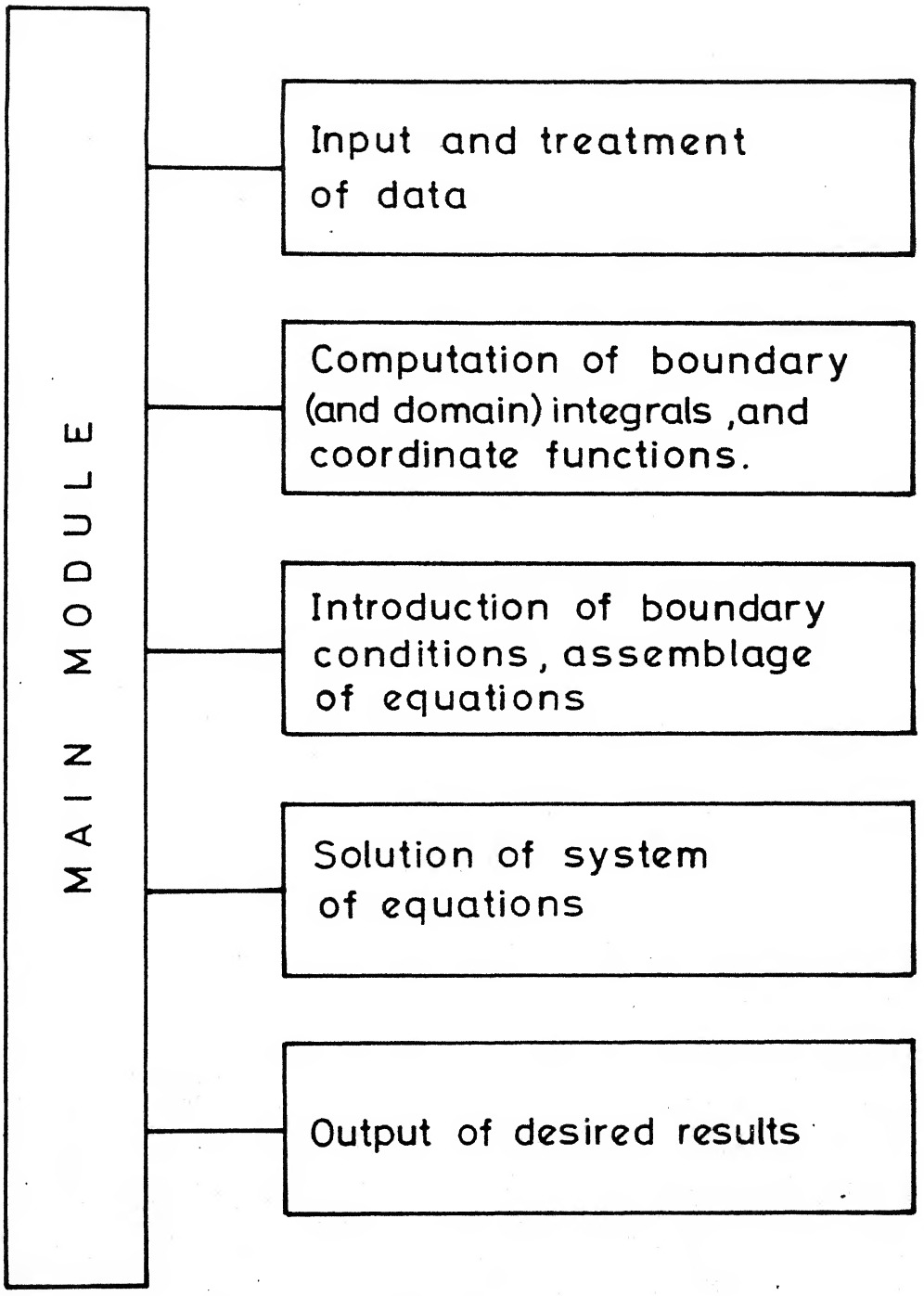

Fig. 4.3 Scheme of the programe.

FIG. 4.4 GENERAL FLOW CHART OF THE PROGRAM

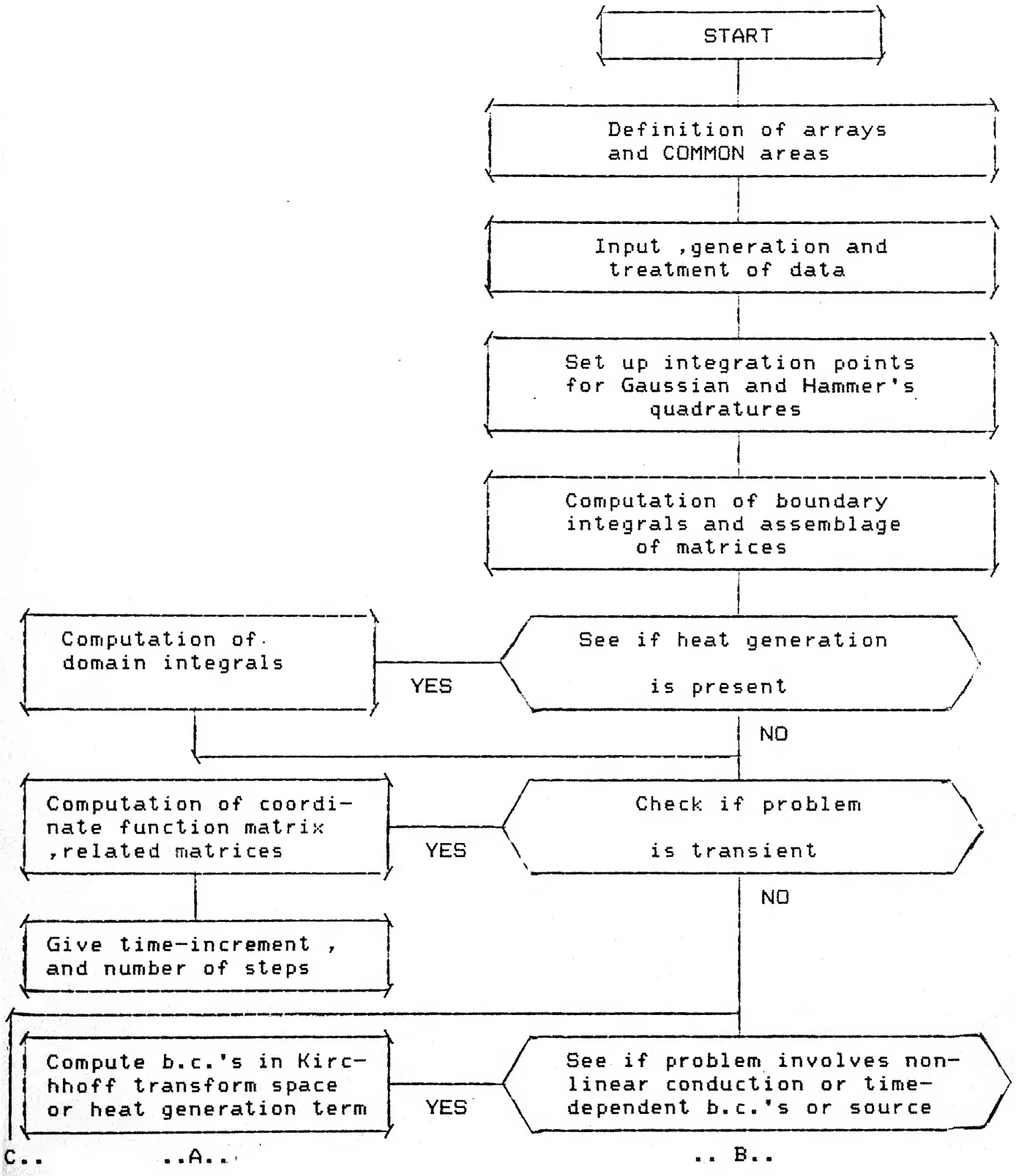

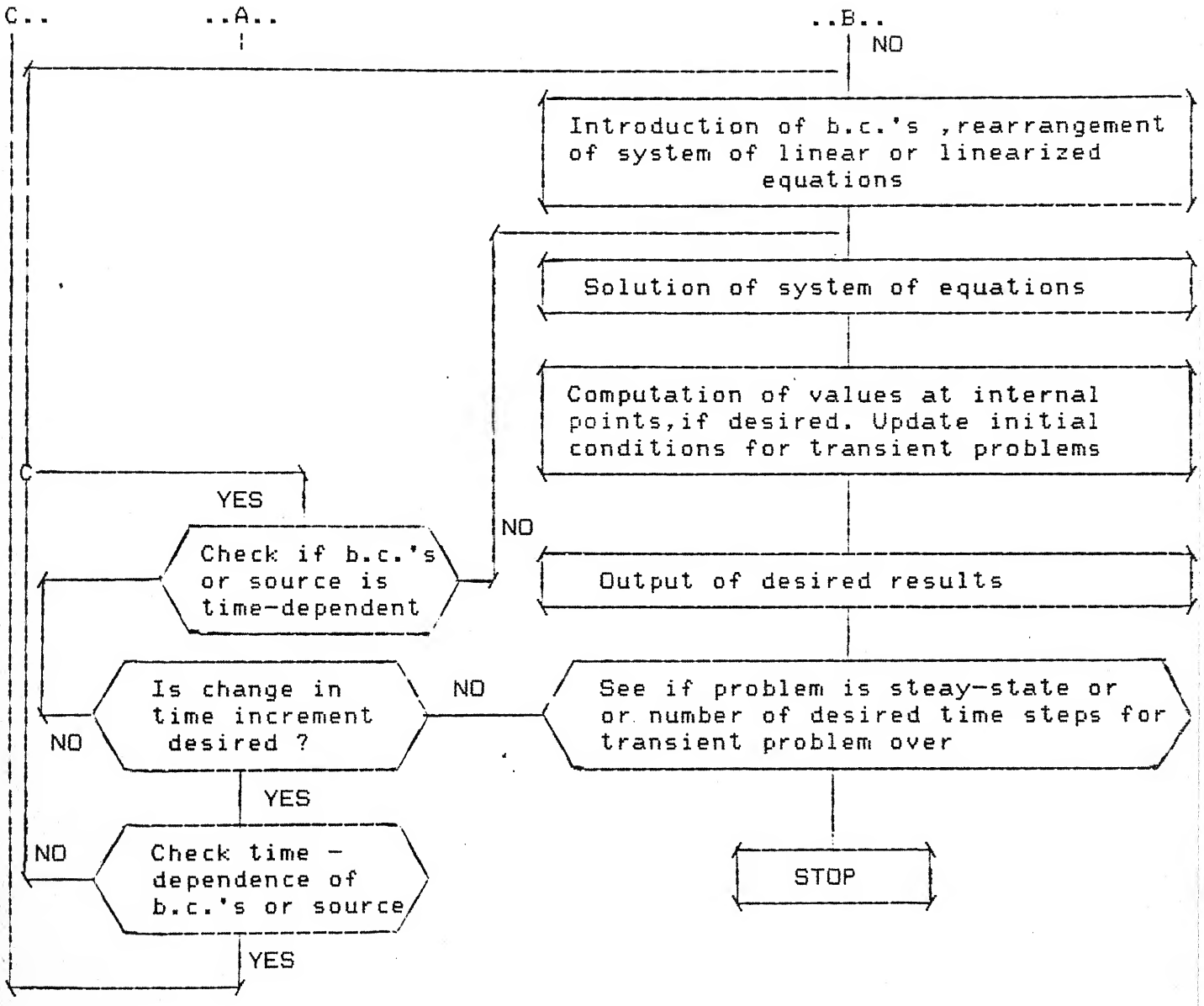

FIG. 4.4 GENERAL FLOW CHART OF THE PROGRAM

CHAPTER 5

RESULTS AND DISCUSSIONS

We present in the following sections results of analyses performed with the program DRBEM (outline of which has been presented in Chapter 4). We have checked this program using three test-problems representing three possible cases of linear conduction, nonlinear conduction with constant diffusivity and nonlinear conduction with variable diffusivity. Section 5.1 contains results of these test runs. Having checked the working of the program, we next present the results of studies on the convergence of the method with refining discretizations (keeping time-step fixed), and with decreasing time-step (keeping spatial discretization fixed) in Section 5.2. Section 5.3 brings results of comparative performance of various time-stepping schemes. Finally, in Section 5.4, we present numerical solutions for nonlinear problems.

5.1 Testing of the Program

Test-Problem 1:

This non-dimensional problem, used in References [40,41], is defined by

$$\frac{\partial u}{\partial t} - \frac{\partial^2 u}{\partial x_1^2} = 0 \quad \text{in} \quad 0 < x_1 < 1 \qquad (5.1)$$

subject to the initial and the boundary conditions:

$$u(x,0) = \sin \pi x_1 \qquad (5.2)$$

$$u(0,t) = u(1,t) = 0 \qquad (5.3)$$

Two-dimensional model of this problem together with appropriate initial and boundary conditions is shown in Fig. 5.1. The model has accounted for symmetry about x = 0.5. The exact solution is given by

$$u(x_1,t) = \exp(-\pi^2 t) \sin x_1 \qquad (5.4)$$

Table 5.1 shows calculated boundary temperatures along x_1-axis at two time instants obtained with time-step $\Delta t = 0.01$, and, 20 equal linear boundary elements. Results are, in general, within 3% of the exact solutions and, thus, attest the correct working of the program for linear conduction problems.

Test Problem 2 : Nonlinear Bar

This one-dimensional problem of a long bar with initial temperature of $0^{o}C$, subject to a unit heat input at the face x = 0 and insulated at x = L has been studied in References [8,42]. The geometrical dimensions and physical properties has been chosen as: L = 3m, $K = (1.0 + 0.5\ T)W\ m^{-1}\ {}^{o}C^{-1}$, $c = (1.0 + 0.5T)J\ kg^{-1}\ {}^{o}C^{-1}$ and $\rho = 1\ kg\ m^{-3}$. The bar was modelled as two-dimensional, with height 0.2m. This problem, representing the case of nonlinear diffusion with constant diffusivity was solved in Reference [8] using linear boundary elements of the size $\Delta\Gamma = 0.2m$. We, instead, have modelled this

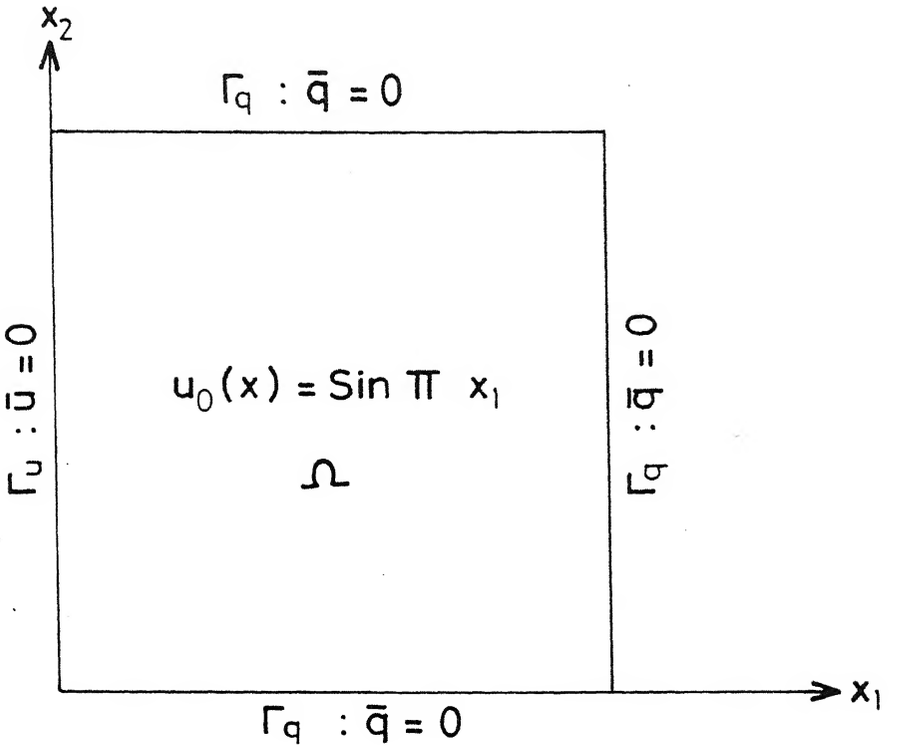

(a)

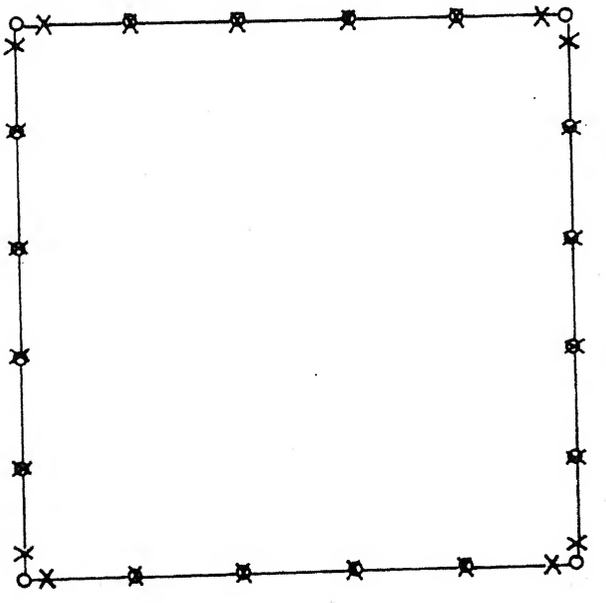

∘ Geometric node

x Freedom node

(b)

Fig.5.1 Test problem - 1
(a) Two-dimensional model
(b) Discretization

Table 5.1. Boundary Temperatures along x_1-axis at Two Time Instants : Test Problem 1

Time Step $\Delta t = 0.01$

x_1	$\Delta t = 0.01$			$\Delta t = 0.05$		
	Exact	Point-Collocation $\theta = 1$	Least-Squares	Exact	Point Collocation $\theta = 1$	Least-Squares
0.025	0.711 E-01	0.714 E-01	0.676 E-01	0.479 E-01	0.491 E-01	0.291 E-01
0.1	0.280	0.281	0.271	0.189	0.194	0.135
0.2	0.532	0.535	0.536	0.359	0.368	0.348
0.3	0.733	0.737	0.741	0.494	0.507	0.514
0.4	0.862	0.866	0.867	0.581	0.596	0.602
0.475	0.903	0.908	0.902	0.609	0.624	0.612

problem using constant elements of the size $\Delta\Gamma = 0.3$ m. Analysis has been performed in non-dimensional form, and, results are presented in Table 5.2 in dimensional variables. The exact solution at $x_1 = 0$ is given by:

$$T = 2 \{ [1 + 2 (t/\pi)^{1/2}]^{1/2} - 1 \} \qquad (5.6)$$

where T is the temperature in ^{o}C and t is the time in seconds.

Results show a large error at first step which decreases to 0.1% at third step, and, then again shows an increasing trend. The initial error is due to the fact in numerical solutions,unit flux is applied linearly over the first time-step. The latter trend can be attributed to the coarseness of the discretization and interpolation employed. We can still observe that errors are well within 15%, which is quite satisfactory in view of the discretization employed. The results of this problem further attest the sound working of the developed program.

Test Problem 3 : Nonlinear Wall

This problem has been taken from References [8,42] to check the performance of the program for general nonlinear conduction problems. The wall is defined by the domain, $\Omega = \{(x_1, x_2) \mid 0 \leq x_1 \leq 20, \; 0 \leq x_2 \leq 1 \}$. Initial and boundary conditions are:

Table 5.2. Temperature Variation (^{o}C) of face $x_1 = 0$ of a Nonlinear Bar : Test Problem -2 .
$\Delta t = 0.05$ s

Time (s)	Exact	BEM-L*	BEM-C (Present Work)	% Error
0.05	0.238	0.200	0.205	13.7
0.10	0.330	0.302	0.316	4.1
0.15	0.397	0.376	0.398	-0.1
0.20	0.453	0.435	0.468	-3.4
0.25	0.501	0.485	0.530	-5.7
0.30	0.544	0.530	0.585	-7.5
0.35	0.583	0.570	0.635	-9.1
0.40	0.618	0.606	0.682	-10.4
0.45	0.651	0.640	0.726	-11.6
0.50	0.682	0.671	0.768	-12.6

* Results from Reference [8], Table 6.

$$T\ (x_1, x_2, 0) = 100 \tag{5.7}$$

$$T\ (0, x_2, t) = 200 \quad \text{for } 0 < t \leq 10$$

$$= 100 \quad \text{for } t > 10 \tag{5.7}$$

$$T\ (20, x_2, t) = 100$$

$$q\ (x_1, 0, t) = q(x_1, 1, t) = 0.0$$

In the above x_1 and x_2 are geometrical dimensions in cm, t is the time in seconds, and T is temperature in ^{o}C. q denotes heat flux in W cm^{-2}. Material properties are conductivity $K = 2+0.01T$ (W cm^{-1} $^{o}C^{-1}$) and heat capacity $\rho c = 9$ (J cm^{-3} $^{o}C^{-1}$). Taking $T = 0^{o}C$ as the reference temperature, and length of the wall as the characteristic length, we have non-dimensionalized the above variables, parameters and specified functions. Analysis has been performed in non-dimensional form.

Results of analysis are presented in dimensional form at time t = 10s and time t = 13s, and, compared with finite element solution obtained with 20 equal linear finite elements [42], and boundary element solution using equal quadratic elements of length $\Delta\Gamma$ = 1 cm [8] in Table 5.3. Present analysis has used equal constant elements of size $\Delta\Gamma$ = 2 cm. We clearly observe that despite the crude discretization employed, results are fairly close to the reference solutions. This observation shows the correct working of the program for general nonlinear conduction problems also.

Table 5.3. Temperature Variation along Length of Nonlinear Wall at t = 10s and t = 13s.

Time-step: Δt = 1s

Boundary element size: $\Delta\Gamma$ = 2 cm in present work (DRBEM)

= 1 cm in BEM - Q^{++}

x_1 cm	t = 10s			t = 13s		
	FEM+	BEM-Q^{++}	DRBEM	FEM+	BEM-Q^{++}	DRBEM
0	200.00	200.00	200.00	100.00	100.00	100.00
2	153.21	151.03	150.88	138.70	138.95	166.12
4	118.60	117.32	114.13	121.29	121.27	130.36
6	103.72	104.14	101.11	106.56	106.71	106.98
8	100.37	100.87	99.52	101.56	101.62	101.42
10	100.01	100.14	99.98	100.33	100.36	100.18

+ Results from Reference [42], Table 5.

++ Results from Reference [8], Tables 7-8.

5.2 Numerical Convergence of Boundary Solutions

Having tested the program DRBEM, we have next performed numerical experiments to study the numerical convergence of boundary solutions with refining discretization and decreasing time-increment. In following lines, we discuss the results obtained with fully-implicit ($\theta = 1$) and least-squares time integration schemes. The following linear problem has been considered:

$$\frac{\partial u}{\partial t} - \nabla^2 u = 0 \text{ in } \Omega = \{x : |x_1| < 1 , |x_2| < 1\}, \; x = (x_1, x_2) \tag{5.10}$$

with initial and boundary conditions:

$$u(x, 0) = 1 \quad \text{on} \quad \Omega \tag{5.11}$$

$$u(x,t) = 0 \quad \text{on} \quad \Gamma_u \times (0,t) \tag{5.12}$$

Owing to the symmetry of the problem, we have solved Eq. (5.10) on a quadrant $\Omega_{1/4} = \{x \mid 0 \leq x_1 \leq 1, \; 0 \leq x_2 \leq 1$ with appropriate initial and boundary conditions shown in Figure 5.2(a). The exact solution from Carslaw and Jaeger [43] is given by

$$u = \frac{4}{\pi} \sum_{n=0}^{\infty} \frac{(-1)^n}{2n+1} \cos\left(\frac{2n+1}{2}\pi x_1\right) \exp\left[-(2n+1)^2 \frac{\pi^2 t}{4}\right]$$

$$x \frac{4}{\pi} \sum_{n=0}^{\infty} \frac{(-1)^n}{2n+1} \cos\left(\frac{2n+1}{2}\pi x_2\right) \exp\left[-(2n+1)^2 \frac{\pi^2 t}{4}\right] \tag{5.13}$$

For small t, rapidly converging solution is given by [43]

$$u = \left[1 - \sum_{n=0}^{\infty} (-1)^n \left\{ \operatorname{erfc} \frac{(2n+1)-x_1}{2\sqrt{t}} + \operatorname{erfc} \frac{(2n+1)+x_1}{2\sqrt{t}} \right\}\right] \tag{5.14}$$

$$x \left[1 - \sum_{n=0}^{\infty} (-1)^n \left\{ \operatorname{erfc} \frac{(2n+1)-x_2}{2\sqrt{t}} + \operatorname{erfc} \frac{(2n+1)+x_2}{2\sqrt{t}} \right\}\right] \tag{5.15}$$

where erfc (v) is the complimentary error function.

5.2.1 Convergence with Mesh-Refinement

For boundary element solution, we first employed a crude grid of 8 boundary elements with element size $\Delta\Gamma = 0.5$. To observe the convergence of boundary solutions with mesh refinement, we further subdivided the original mesh much more such as : $\Delta\Gamma = 0.25$ (16 element) and $\Delta\Gamma = 0.125$ (32 elements) for subsequent computations. Figs.5.2(b)-(d) show these meshes.

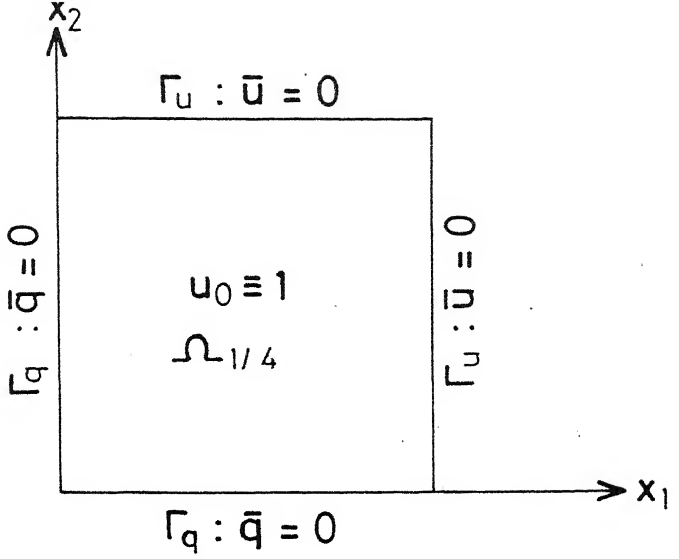

(a)

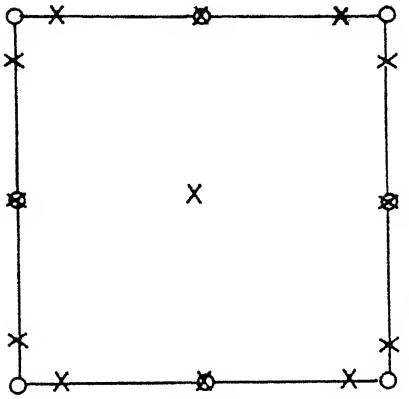

o Geometric node

x Freedom node

(b)

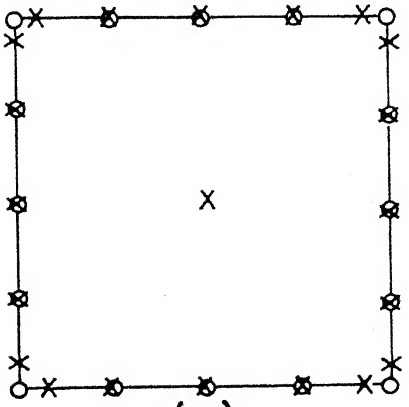

(c)

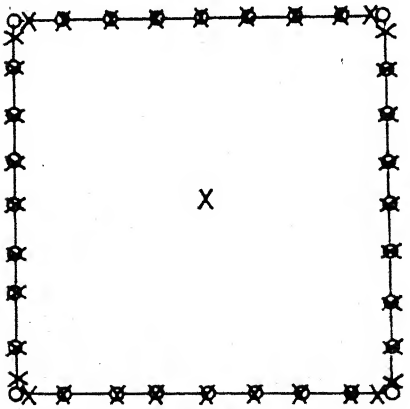

(d)

Fig.5.2(a) Initial and boundary conditions

With fully-implicit ($\theta = 1$) point-collocation scheme, we kept fixed time increment $\Delta t = 1/128$ for all computations. Boundary temperatures along x_1-axis at the constant time $t = 1.0$ are plotted for the first two subdivisions in Fig.5.3. We can numerically observe uniform convergence of computed solutions to the exact solutions. Figure 5.4 shows the plot of relative error vs. boundary element size for the chosen subdivisions. Relative errors have been calculated at the point (0.1, 0.1). Slope of the regression line is 1:2, suggesting the second order of convergence with respect to mesh-refinement.

With the least-squares scheme, we have chosen $\Delta t = 1/64$. Figure 5.5 shows the boundary temperatures along x_1 - axis for various subdivisions at time $t = 1.0$. We observe that the approximate solutions converge to the exact values, but the convergence is not uniform.

To assess the convergence property of the approximate heat-fluxes, computed heat fluxes along the boundary $x_1 = 1.0$, $0 < x_2 < 1.0$, at time $t = 1.0$ are plotted for various discretizations in Fig. 5.6 for the fully-implicit scheme,and in Fig. 5.7,for the least squares scheme. Time increments were $\Delta t = 1/128$ for the fully-implicit scheme, and $\Delta t = 1/64$ for the least-squares scheme. From Fig. 5.6, we observe uniform convergence of boundary fluxes to the exact value with the fully implicit time integration scheme. With

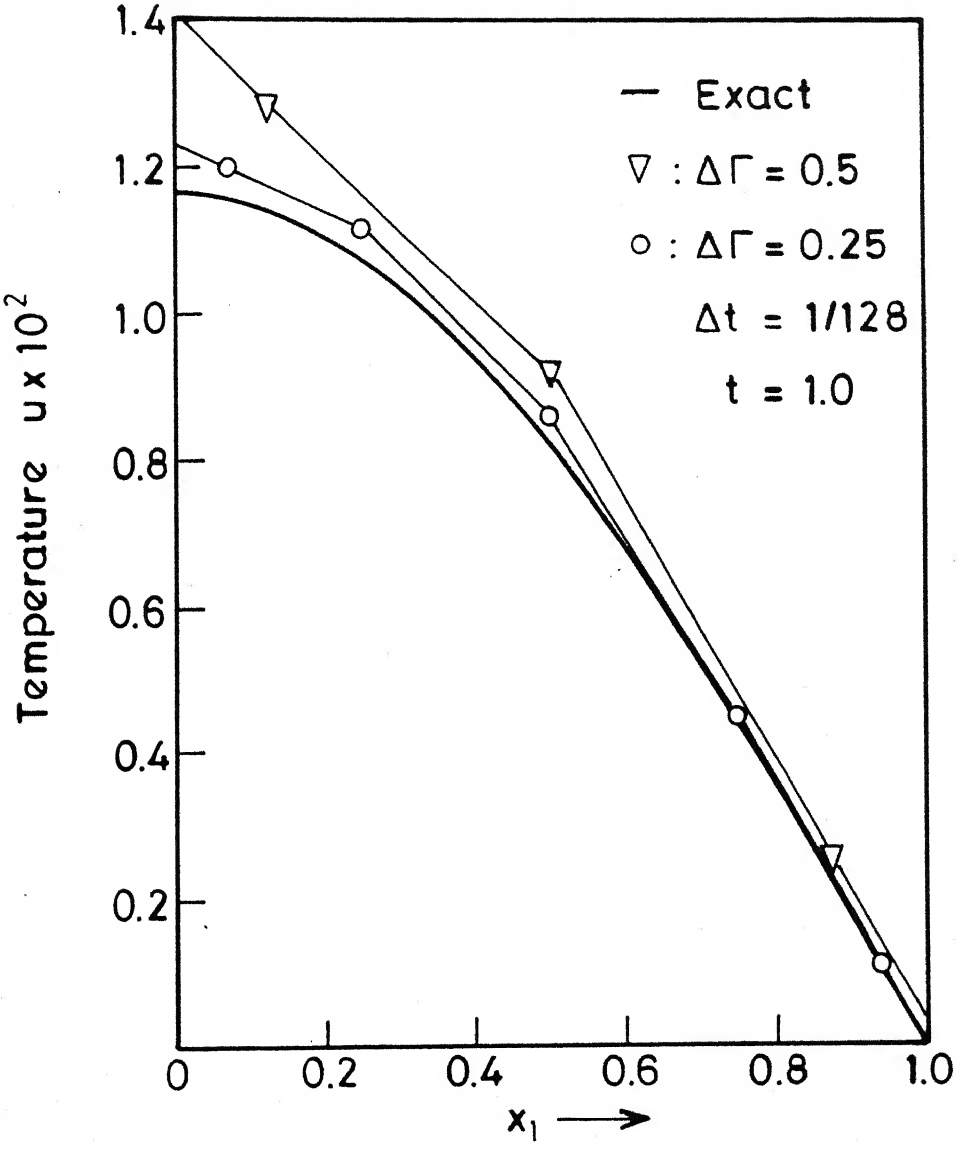

Fig. 5.3 Boundary temperatures along x_1 - axis for two element sizes (Point collocation: $\theta = 1$)

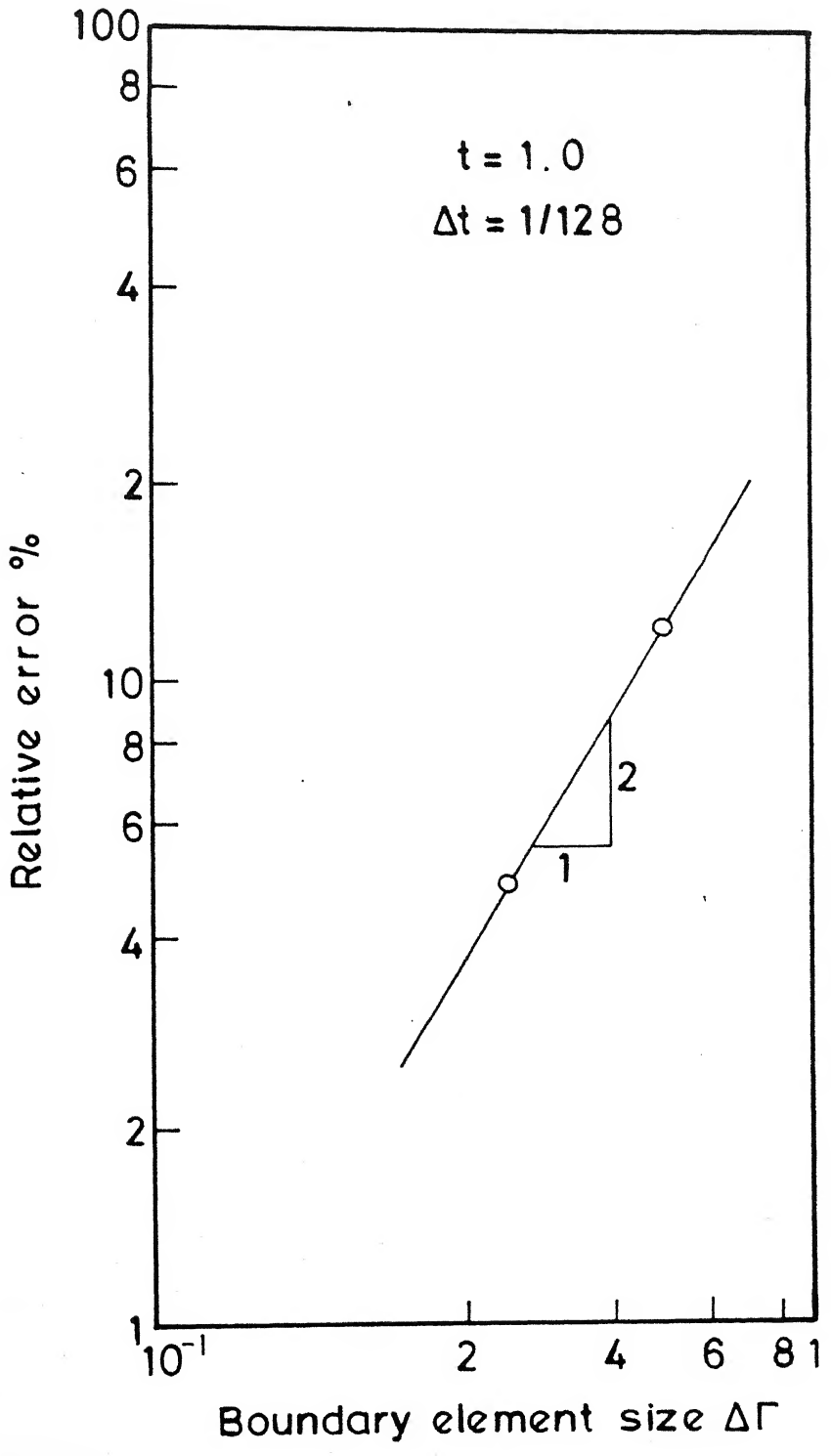

Fig.5.4 Rate of convergence of the temperature.($x_1 = x_2 = 0.1$)

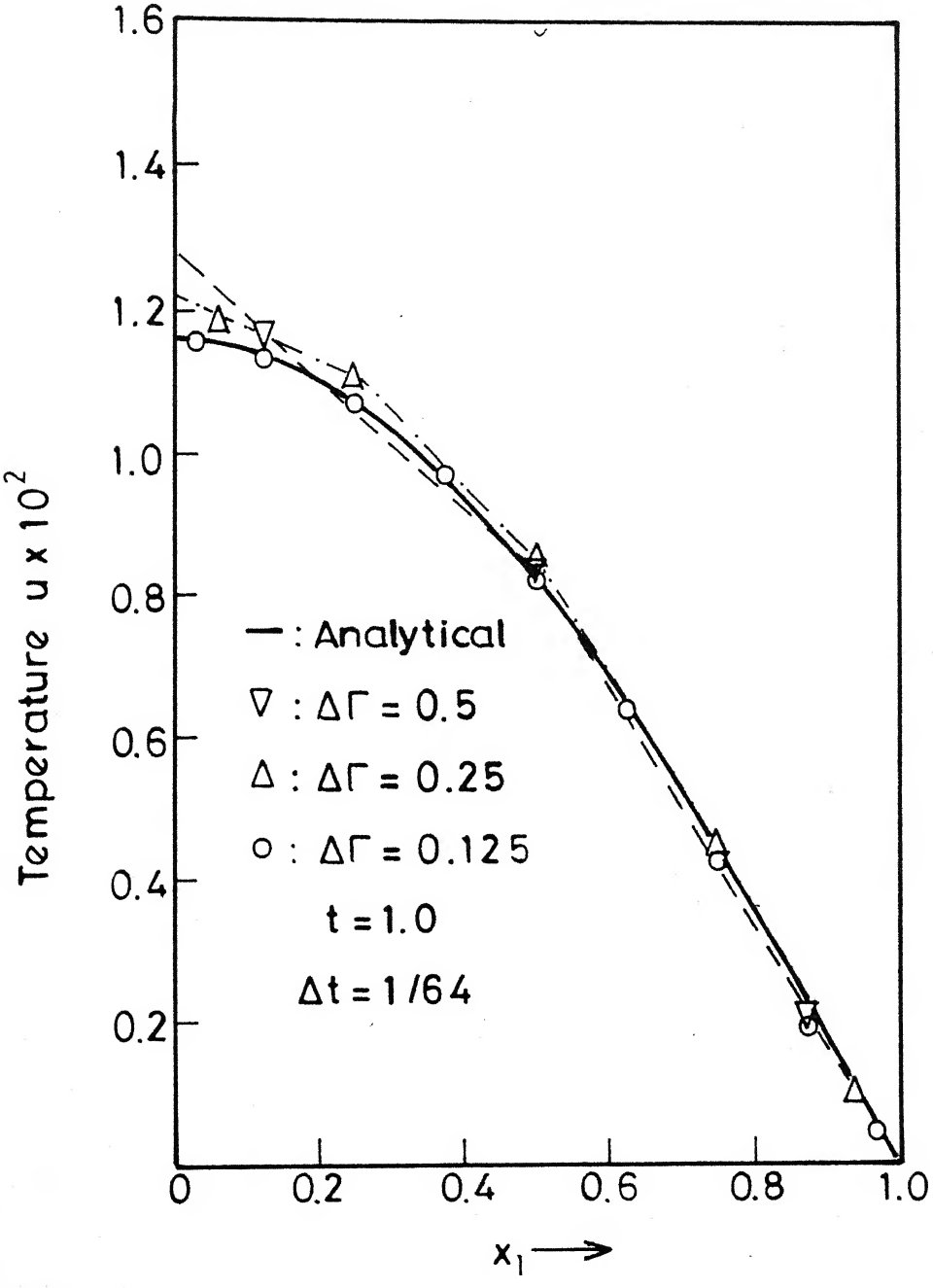

Fig. 5.5 Boundary temperatures along x_1 - axis for various spatial grid sizes (Least-squares scheme)

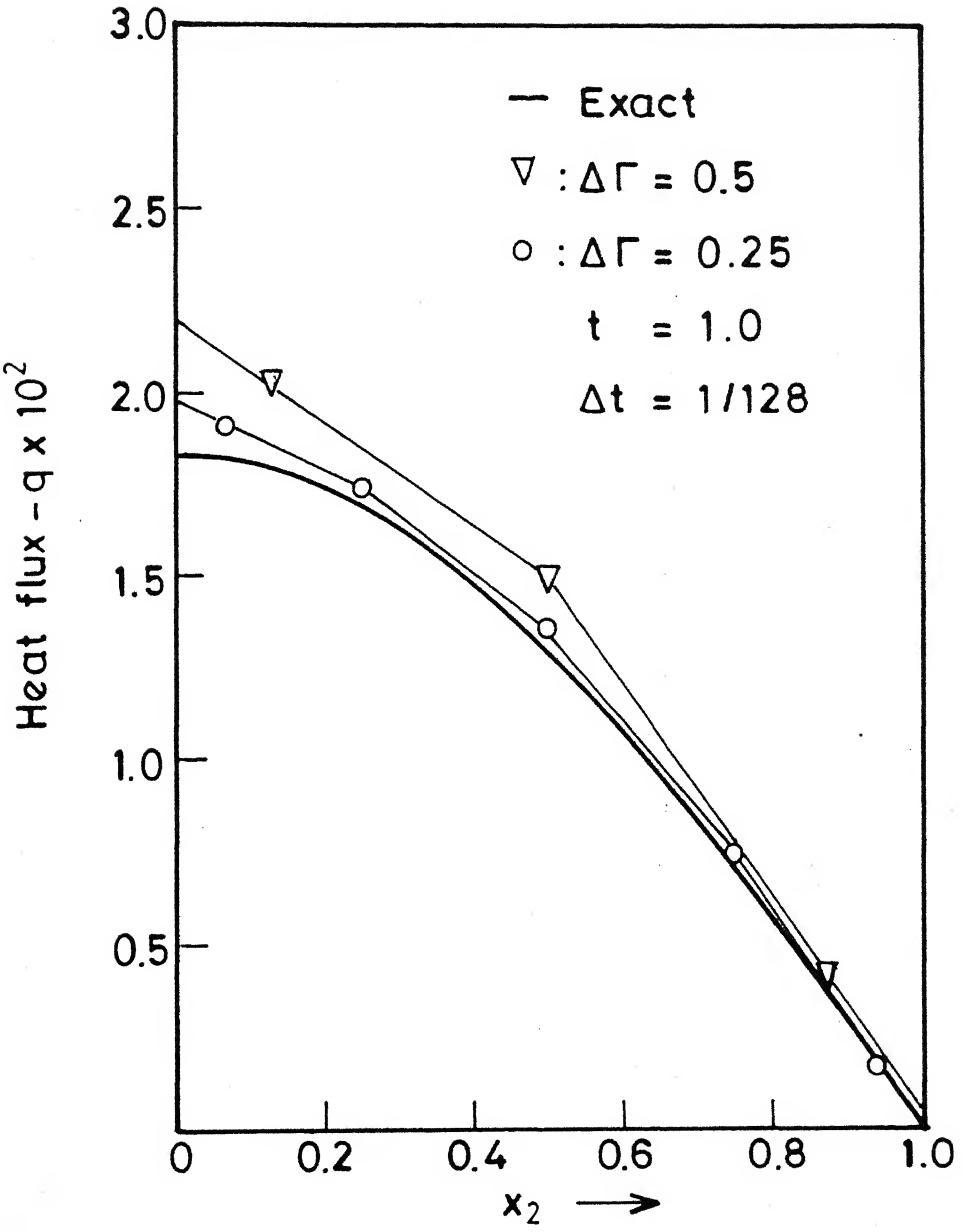

Fig.5.6 Heat fluxes along the boundary : $x_1 = 1, 0 \leqslant x_2 \leqslant 1$ for two-element sizes (Point collocation: $\theta = 1$)

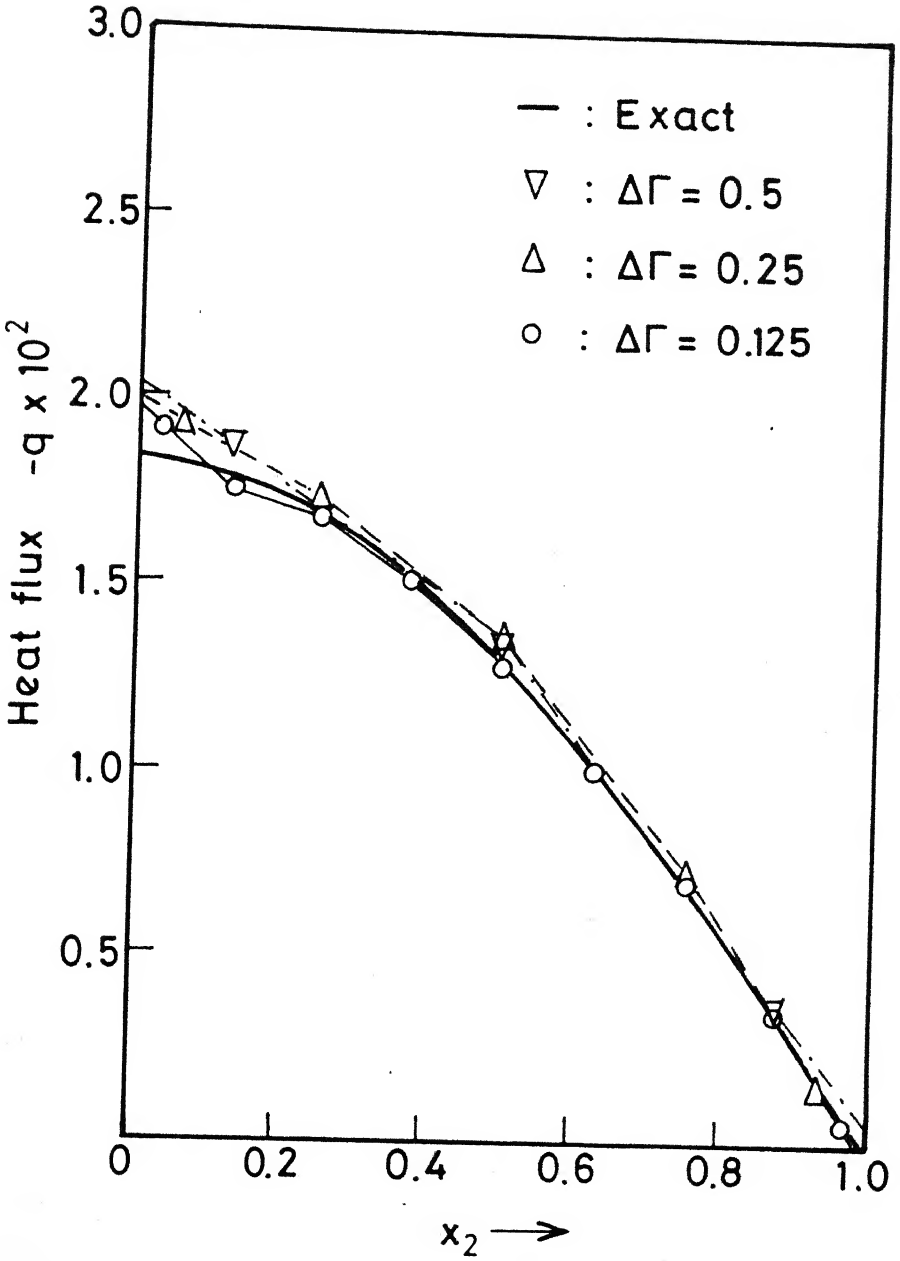

Fig. 5.7 Heat fluxes along boundary $x_1 = 1.0, 0 \leq x_2 \leq 1$ for various element sizes. (Least-squares scheme)

the least-squares scheme (Fig. 5.7), we once again see that the calculated fluxes converge to the exact values, but the convergence is not uniform.

5.2.2 Convergence with Decreasing Time-increment

To investigate the convergence of the approximate solution to the exact solution for the temperature and heat flux, we varied the time-increment while keeping the spatial mesh fixed. We chose the finest mesh shown in Fig. 5.2(d). Calculated temperatures along x_1-axis are plotted in Fig.5.8 and Fig. 5.9 for the fully implicit and the least-squares schemes respectively, for various time-increments. Fig.5.8 shows uniform convergence of calculated boundary solutions to the exact values with the fully implicit time-integration scheme. From Fig. 5.9 we can observe that the solutions obtained using the least-squares scheme show oscillatory behaviour with a large time-step of $\Delta t = 1/8$. With the smaller time increments, however, we observe the uniform convergence of the boundary solutions to the exact ones with this scheme also.

To assess the order of convergence with decreasing time-increment for the two schemes, we calculated relative errors at point (0.03, 0.0) for various time-increments. The slope of regression line in Fig. 5.10, for the fully implicit scheme, is 1:0.8, which suggests the first order of convergence. From the same figure, we observe that,

with the least-squares time-integration scheme, the regression line is a curve with non-constant slope. For range of time increments $\Delta t = 1/16$ to $1/32$, the slope of regression line is approximately 1:2, suggesting the second order of convergence. Slope of the second segment of the regression line corresponding to the time-increment range of $1/32$ to $1/64$ is approximately 1:4. This suggests the fourth order of convergence with respect to time-increments. These observations clearly indicate increasing order of convergence for the least-squares scheme with decreasing time-increment.

Figures 5.11 - 5.12 show the plots of the computed heat fluxes along the boundary $x_1 = 0$, $0 \leq x_2 \leq 1.0$ for various time increments with the fully implicit and the least-squares schemes respectively. The results in Fig. 5.11 corresponding to the fully-implicit scheme indicate uniform convergence of the boundary fluxes to the exact solution. On the other hand, results obtained with the least-squares scheme (Fig. 5.12) are oscillatory for large time step, and converge to the exact solution with decreasing time step, but uniform convergence is not indicated.

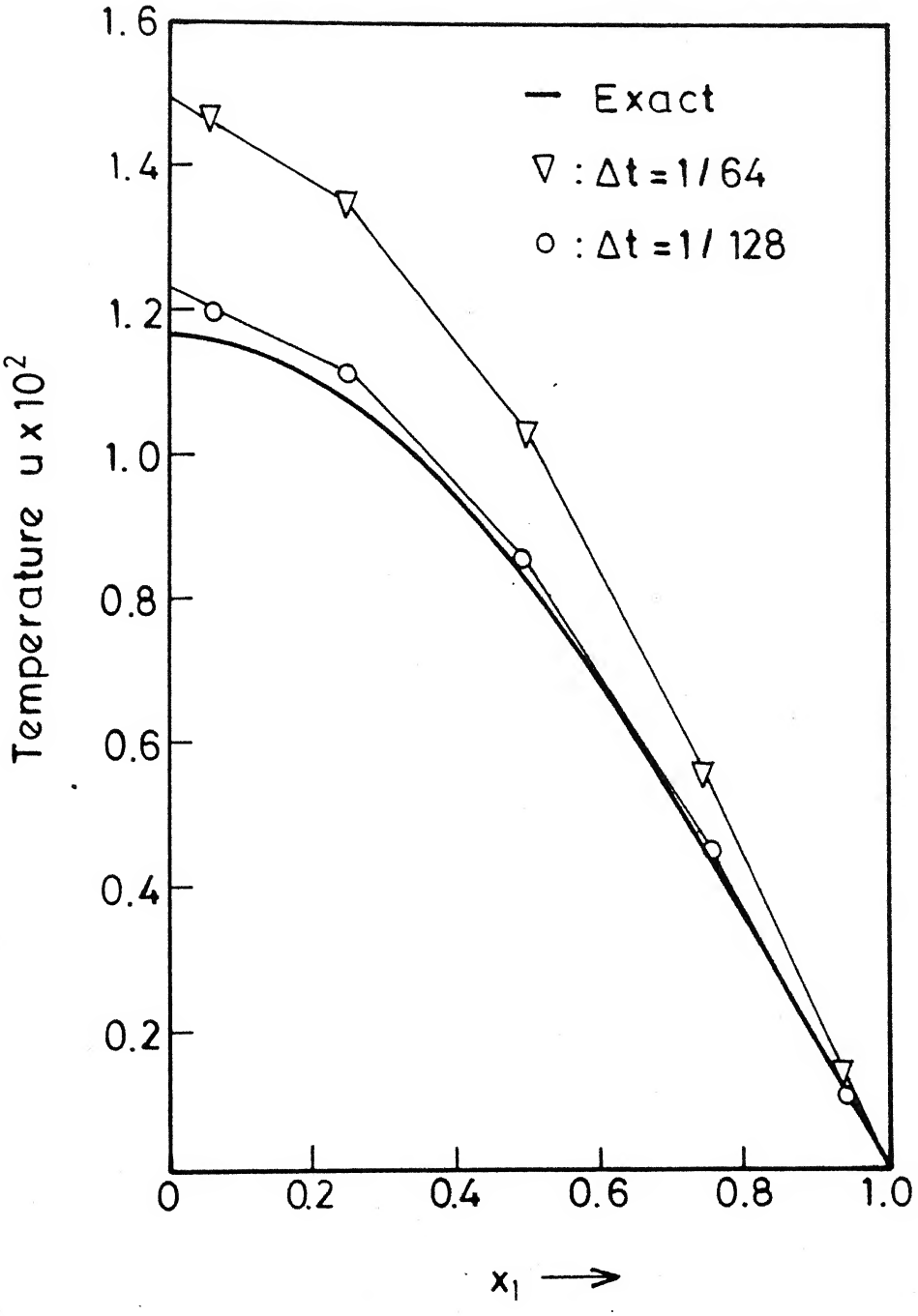

Fig. 5.8 Boundary temperatures along x_1 - axis for various time increments (Point collocation: $\theta = 1$)

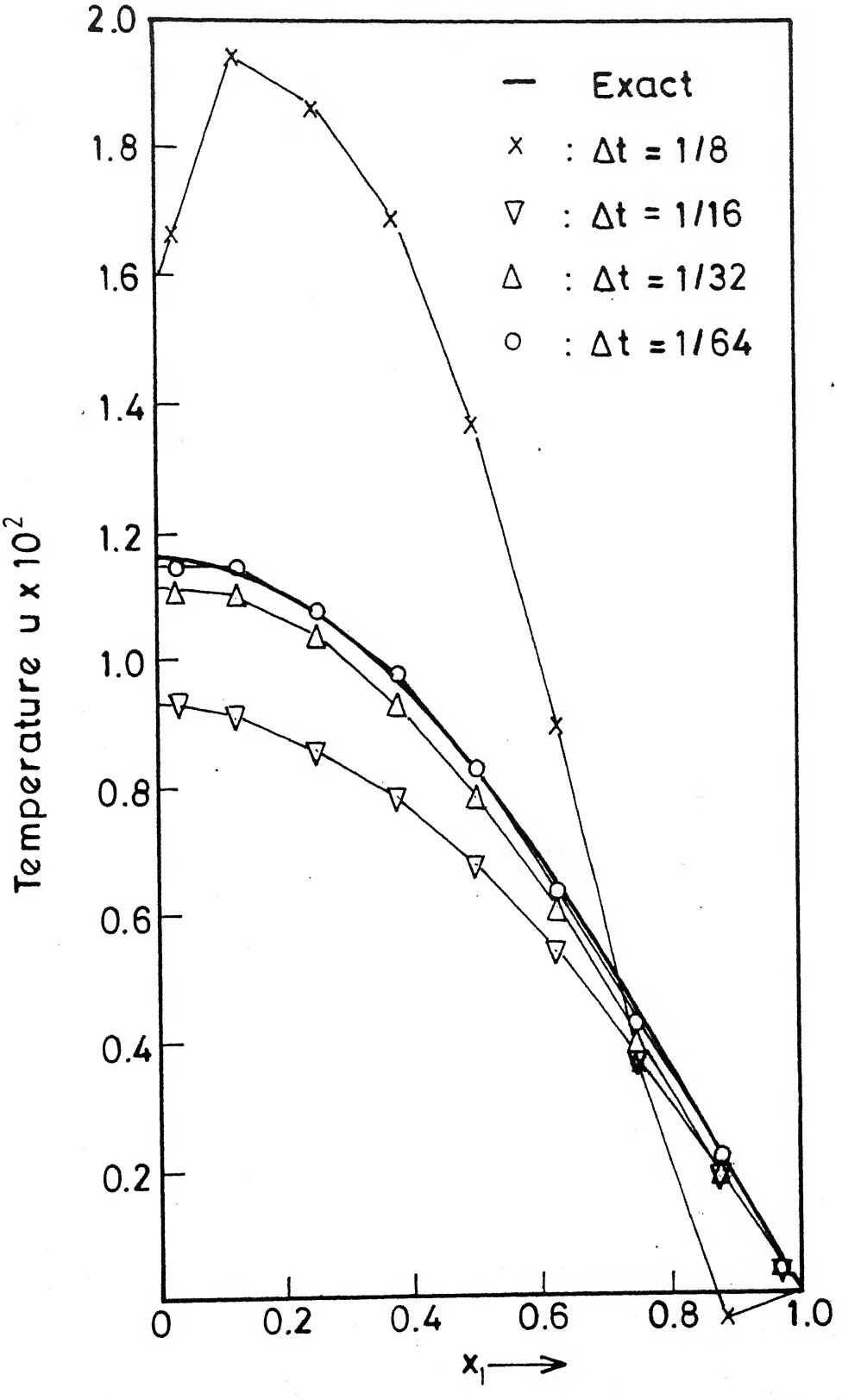

Fig. 5.9 Boundary temperatures along x_1 -axis for various time-increments (Least-squares scheme)

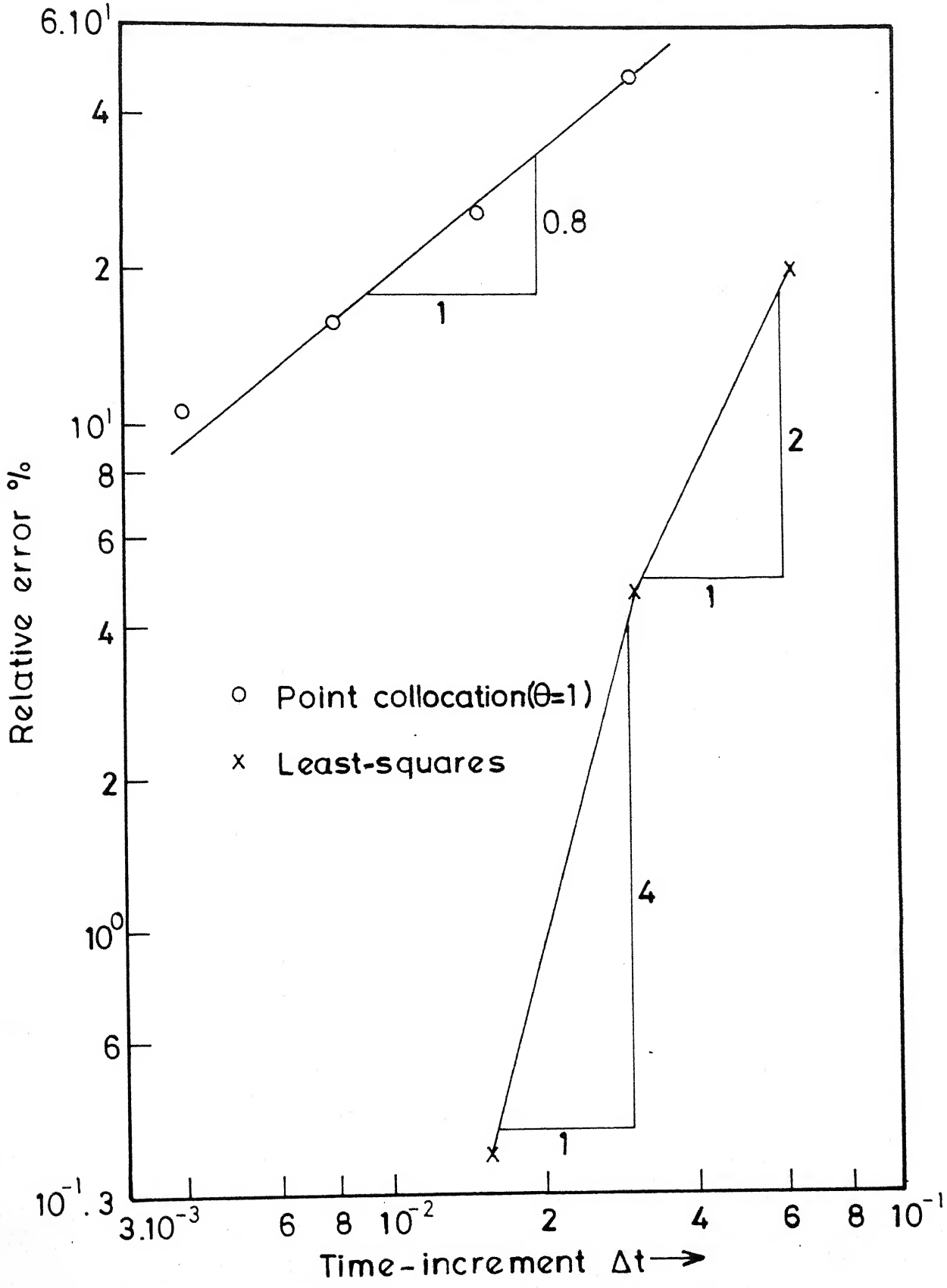

Fig.5.10 Rate of convergence of the temperature ($x_1=0.03, x_2=0$)

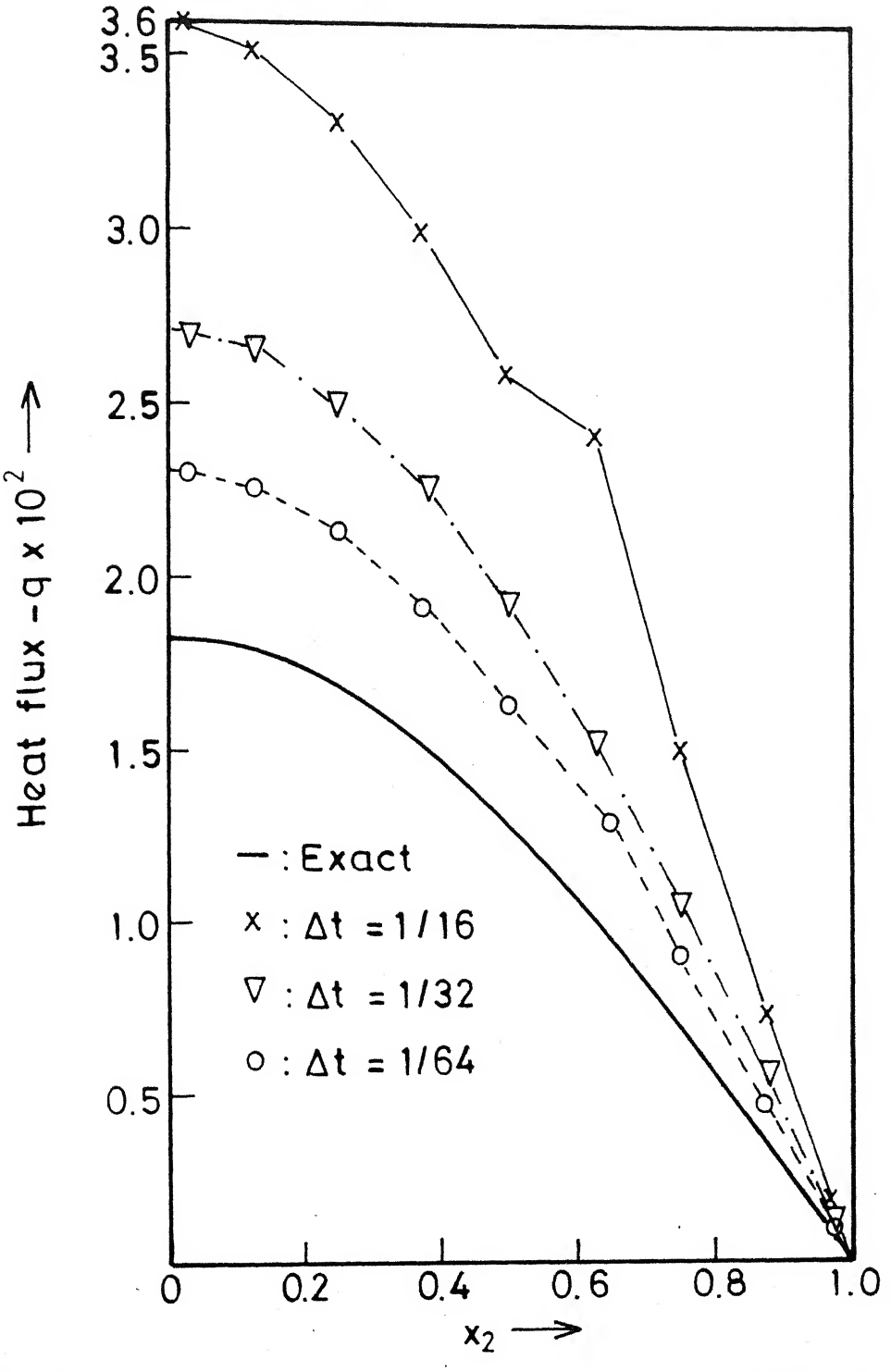

Fig. 5.11 Heat fluxes at the boundary: $x_1 = 1.0, 0 \leq x_2 \leq 1$ for various time - increments (Weighted residual scheme: $\theta = 1$)

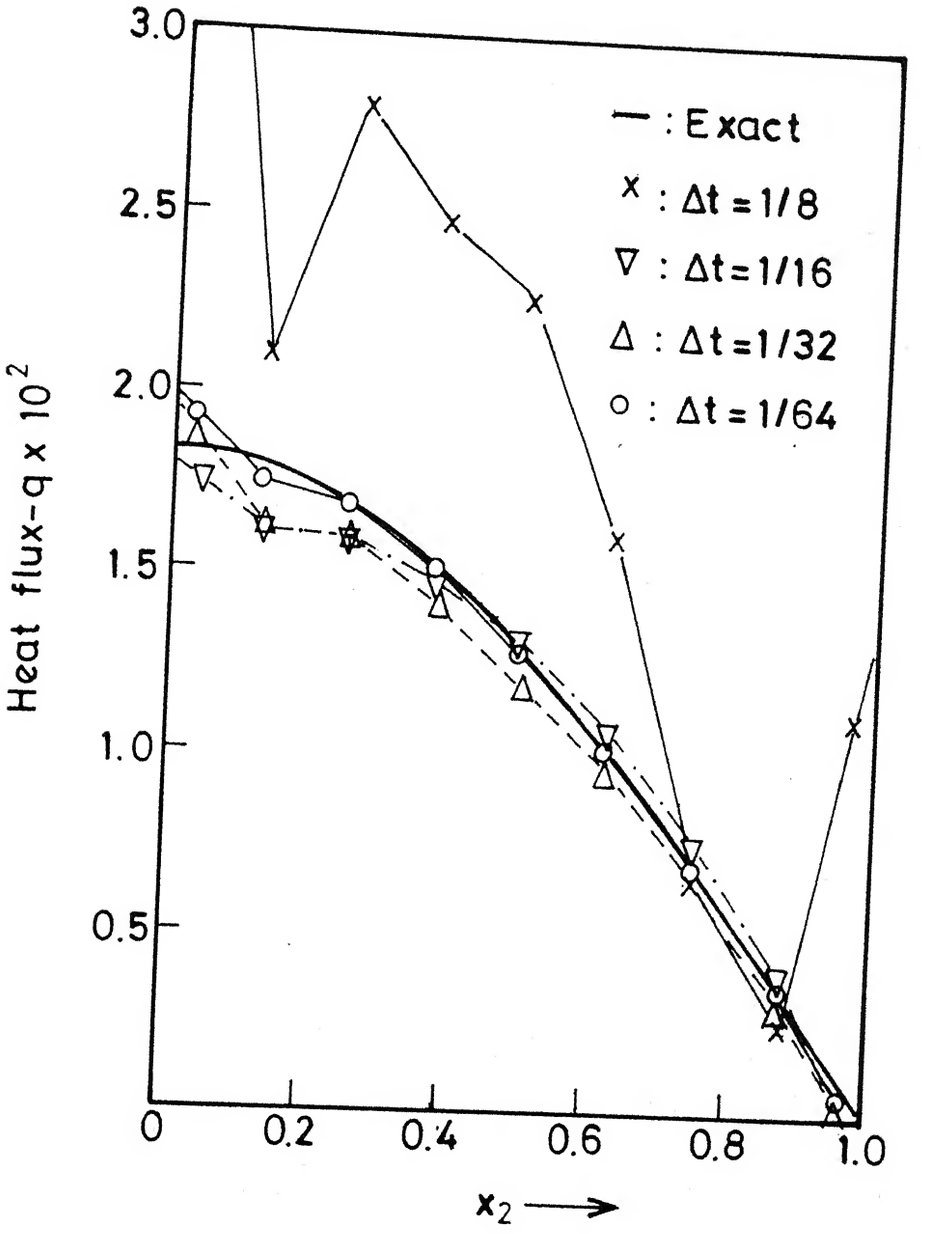

Fig. 5.12 Heat fluxes along the boundary : $x_1 = 1.0, 0 \leq x_2 \leq 1.0$ for various time increments (Least-squares scheme

5.3 Comparison of the Least-Squares Scheme with other Weighted-Residual Schemes

To compare the performance of the proposed least-squares scheme with the point collocation and the Galerkin schemes, the problem in Section 5.2 has been considered. The finest-grid in Fig. 5.2(d) has been employed. Calculated temperatures along x_1-axis, at time t = 1.0 with a time increment $\Delta t = 1/64$, are plotted in Fig. 5.13 for the fully-implicit ($\theta = 1$), the Galerkin ($\theta = 2/3$), the Crank-Nicholson ($\theta = 1/2$), and the least-squares schemes. The least-squares scheme shows the greatest accuracy, but with associated larger-computational cost (computation time required with the least-squares scheme has been $\sim$51 s as compared to $\sim$46 s with other schemes for 64 time steps). The Crank-Nicholson, the Galerkin and the fully-implicit schemes follow in order of decreasing solution accuracy

To compare the computational cost associated with various schemes (which is directly proportional to the computation time), we have presented computation time required for various number of time-steps with the least-squares and the fully-implicit schemes in Table 5.4 (Computation time with the Crank-Nicholson or the Galerkin scheme is almost same as that with the fully implicit scheme). We can observe that the least-squares scheme requires larger computation time. However, the relative difference in

required time decreases with increasing number of time-steps. (It is just 6% for 200 steps as compared to 35% for 10 steps). Thus, in view of its higher accuracy, the least-squares scheme promises higher computational efficiency for large number of time steps. When number of time-steps is small, the difference in computation cost is marginal, and, a scheme offering higher accuracy is preferred. So, in this case too, least-squares scheme seems to be a better choice.

Further, a comparison of Fig. 5.8 and Fig. 5.9 reveals that the least-squares scheme obtains more accurate solutions with a time increment twice as large as that used with the fully implicit scheme. This observation further indicates the desirability of the least-squares scheme over the fully implicit scheme.

Further, from Fig. 5.10, we observe that the rate of convergence for the fully-implicit scheme is of the first order. In comparison, the rate of convergence for the least-squares scheme is quadratic or higher.

However, we note from Fig. 5.9 that least-squares scheme has produced oscillatory solution with large time-increment. Further investigation is called for understanding this behaviour fully. At present, we add that with the least-squares scheme, caution must be exercised in selection of time-increment.

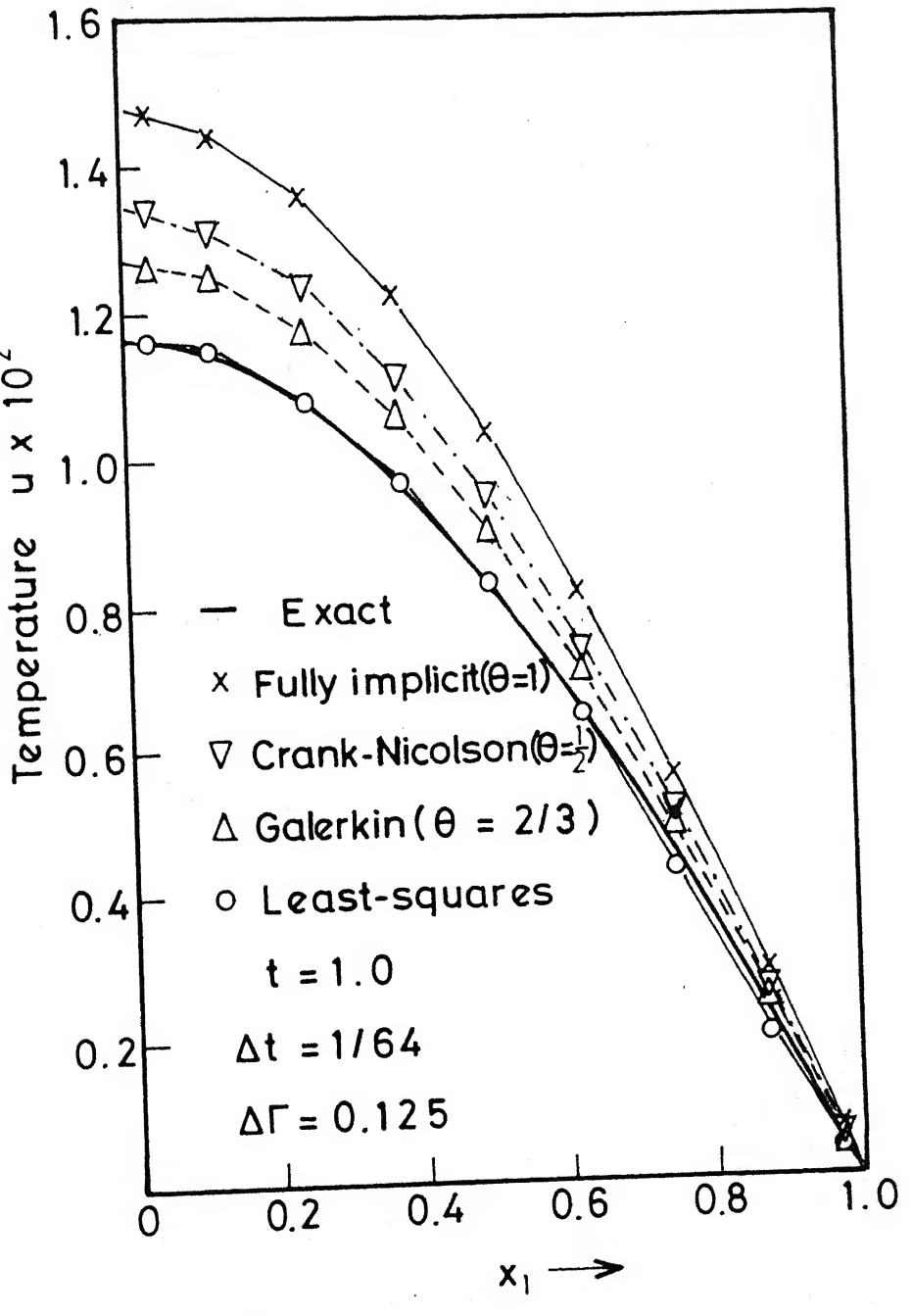

Fig. 5.13 Boundary temperatures along x_1-axis for various time-integration schemes.

Table 5.4. Comparison of Computation Time for Various Number of Time-steps

Sl.No.	Number of Time Steps	Central Processing Unit (CPU) Time (Seconds)*		Difference $(CPU)_{LS} - (CPU)_{PC}$ (Seconds)	% Difference
		Point-Collocation $(CPU)_{PC}$	Least-Squares $(CPU)_{LS}$		
1	10	10.95	13.74	3.79	34.61
2	20	17.72	21.70	3.98	22.46
3	40	31.27	35.72	4.48	14.33
4	100	71.80	77.72	5.92	8.24
5	200	139.36	147.64	8.28	5.94

* Central Processing Unit Time on DEC-1090.

5.4 Application to Problems with Nonlinear Boundary Conditions

We consider an infinite slab of width 2L subjected to simultaneous convection and radiation at its surfaces. Dimensionless boundary condition has the form:

$$q = k \frac{\partial u}{\partial n} = - Bi(u + a_c) - Gr \{ (u+a)^4 - a_r^4 \} \qquad (5.16)$$
$$= f_c(u)$$

with
$$Bi = \frac{hL}{K} \quad , \quad a = \frac{T_a}{T_b - T_a}$$
$$Gr = \frac{\varepsilon \sigma (T_b - T_a)^3 L}{K_o} \quad , \quad a_c = \frac{T_a - T_c}{T_b - T_a} \qquad (5.17)$$
$$a_r = \frac{T_r}{T_b - T_a} \quad , \quad u = \frac{T-T_a}{T_b-T_a}, \quad k = \frac{K(T)}{K_o}$$

where h is the convective heat transfer coefficient, K_o the thermal conductivity at chosen temperature $\bar{T}_o$, ε the relative emissivity, σ the Stefan-Boltzmann constant, T_c the temperature of convecting fluid, T_r the temperature of the radiation source, and T_a and T_b are suitably chosen reference temperatures for non-dimensionalization. Bi denotes the Biot number, and Gr is referred to as the radiation parameter. We have taken Bi = 4.0, and Gr = 4.0. Initial temperature of the slab has been taken to be $T_o = 1000$. T_c and T_r have been assumed to be zero. We have chosen $T_b = 1000$ and $T_a = 0$. Thus, we have $a = a_c = a_r = 0$, and the initial condition

$$u_o(x) = 1.0. \tag{5.18}$$

Owing to the symmetry with respect to the mid-plane of the slab, only half portion of width L needs to be analyzed. Figure 5.14(a) shows the geometric parameters, initial and boundary conditions, and two-dimensional rectangular region chosen for analysis. This two dimensional model has a length of 1.0 and height of 0.2. The boundary has been discretized using 24 linear boundary elements. For computation of energy residual using finite element type approximation, the problem domain has been discretized using 40 linear triangular cells. 8 internal nodes in addition to the one corresponding to constant function have been chosen. Figure 5.14(b) shows the discretization employed.

For both of following problems, the fully implicit time-integration scheme ($\theta = 1$) with time-increment $\Delta t = 1/128$ has been employed.

5.4.1 Linear Slab

For linear slab, material properties are independent of temperature. In this case, dimensionalless properties are all equal to unity. Table 5.5 summarizes the results of the analysis in which temperature values at two extreme nodes - node A (1.0, 0.1) and node B (0.0, 0.1) - are presented. The calculated temperatures (denoted as DRBEM) are compared with the boundary element solutions using time-dependent

fundamental solution (denoted as BEM) by Onishi and Kuroki [25] in Fig. 5.15. The comparison shows quite good agreement between the two solutions.

Furthermore, from last column of Table 5.5, we can see that the energy residuals are very small (less than 0.7%). This clearly shows the satisfactory maintenance of input-output energy balance, which, in turn, suggests that the computed solutions are accurate.

In the above analysis, the Newton-Raphson algorithm detailed in Chapter 4 has been utilized. With a tolerance of 10^{-4} for relative norm of increments of unknown vector, number of Newton-Raphson iterations was 2.

5.4.2 Nonlinear Slab

For nonlinear slab, following variation of properties has been assumed:

$$\begin{aligned} k(u) &= 1.0 - 0.3\,u \\ \rho(u) &= 1.0 \\ c(u) &= 1.0 \end{aligned} \qquad (5.19)$$

Results of the analysis are presented in Table 5.6. Figure 5.16 shows variation of temperatures at two extreme nodes - node A (1.0, 0.1) and node B (0.0, 0.1) with time. A tolerance of 10^{-4} for the relative norm of the increments has been specified. Average number of Newton-Raphson iterations has been 4.

From the last column of Table 5.6, we can observe that relative energy residual is less than 1%. The input-output energy balance is, thus, maintained satisfactorily. This, in turn, suggests high accuracy and physical acceptability of the approximate solution obtained.

From Fig. 5.16, we observe the same tendency as in Fig. 5.15 for linear slab with respect to the transient behaviour of boundary solutions. This observation further reinforces the physical acceptability of computed solutions.

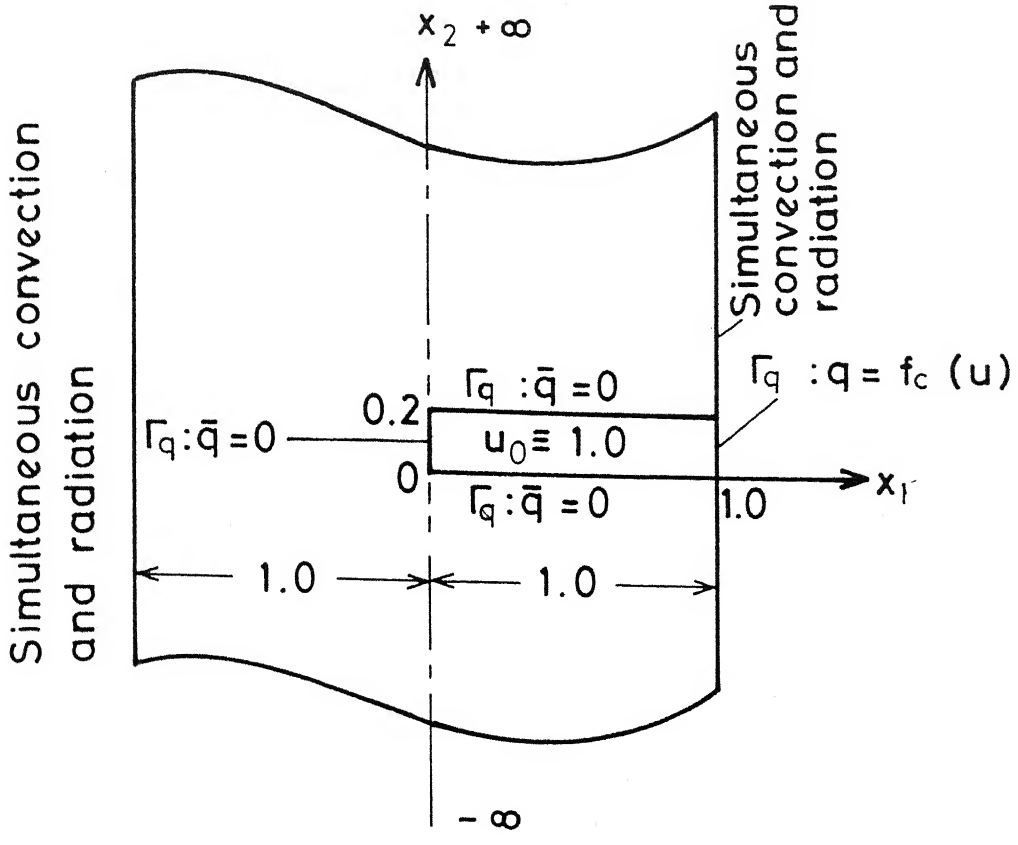

(a)

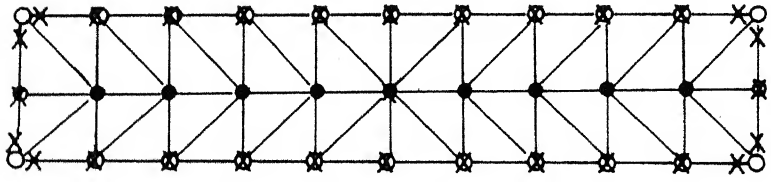

- ○ Geometric nodes (Boundary)
- × Freedom nodes
- • Internal points

Fig.5.14 (a) Geometry, initial and boundary conditions.

(b) Discretization.

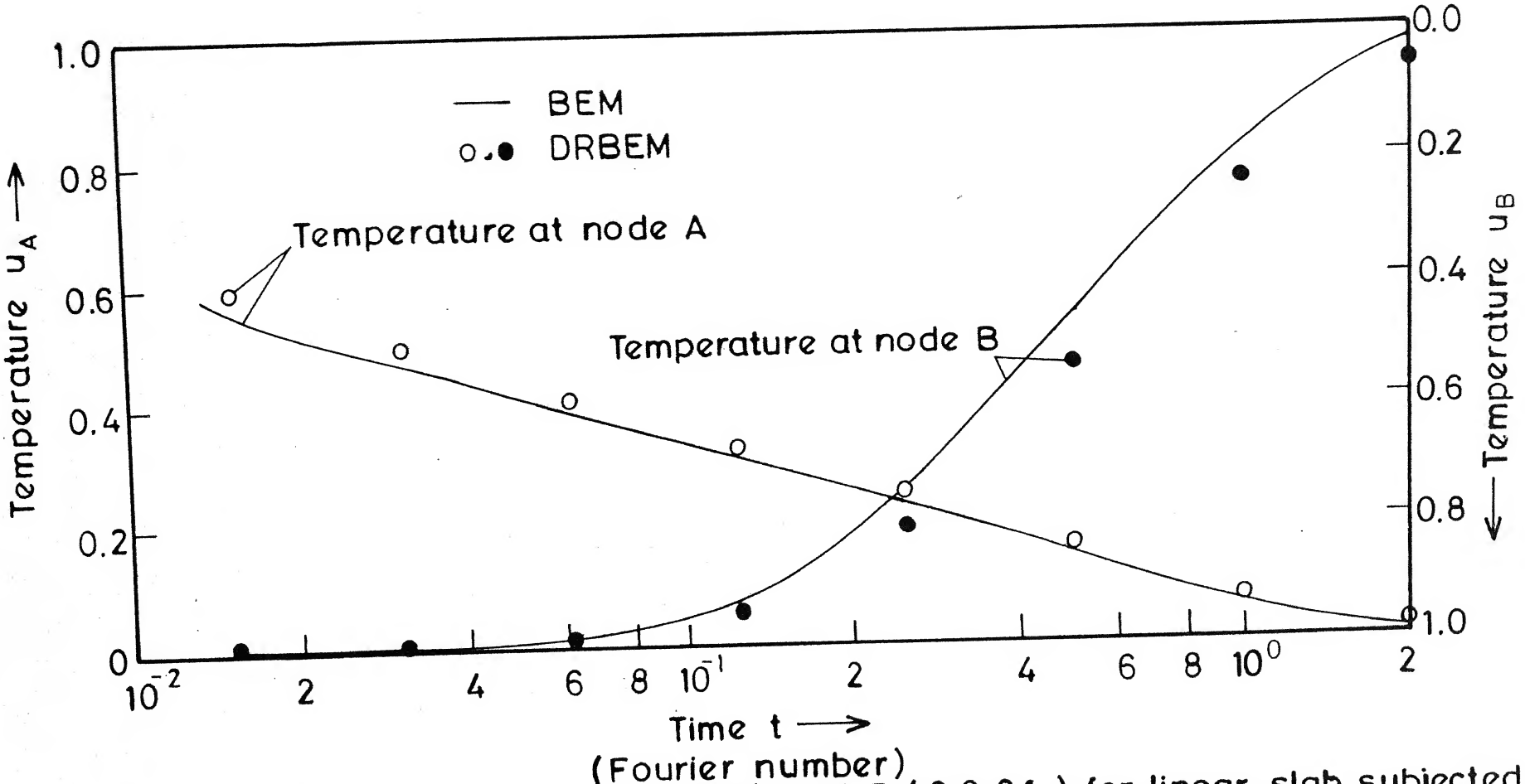

Fig. 5.15 Temperatures at nodes A (1.0, 0.1) and B (0.0, 0.1) for linear slab subjected simultaneous convection and radiation.

Table 5.5. Calculated Temperatures for Linear Slab subjected to Simultaneous Boundary Convection and Radiation*

Bi = 4.0 Node A : (1.0, 0.1)

Gr = 4.0 Node B : (0.0, 0.1)

Time Increment $\Delta t = 1/128$

Step No.	Time	Temperature at Node A	Temperature at Node B	Total Thermal Energy	Energy Residual	% Energy Residual
1	0.0078125	0.6999	1.0062	0.1954	0.1296 E-02	0.663 E+00
2	0.015625	0.5960	1.0035	0.1904	-0.4561 E-03	-0.240 W+00
4	0.03125	0.5010	1.0029	0.1830	-0.2168 E-03	-0.118 E+00
8	0.0625	0.4106	0.9959	0.1708	-0.6008 E-04	-0.351 E-01
16	0.125	0.3262	0.9543	0.1519	-0.2033 E-04	-0.134 E-01
32	0.25	0.2477	0.8103	0.1230	-0.1067 E-04	-0.867 E-02
64	0.5	0.1640	0.5467	0.0823	-0.6385 E-05	-0.776 E-02
128	1.0	0.0739	0.2457	0.0370	-0.2850 E-05	-0.771 E-02
256	2.0	0.0149	0.0497	0.0075	-0.5766 E-06	-0.771 E-01

* Central Processing Unit Time for 256 Steps on DEC-1090 : 11 minutes 6.61 seconds.

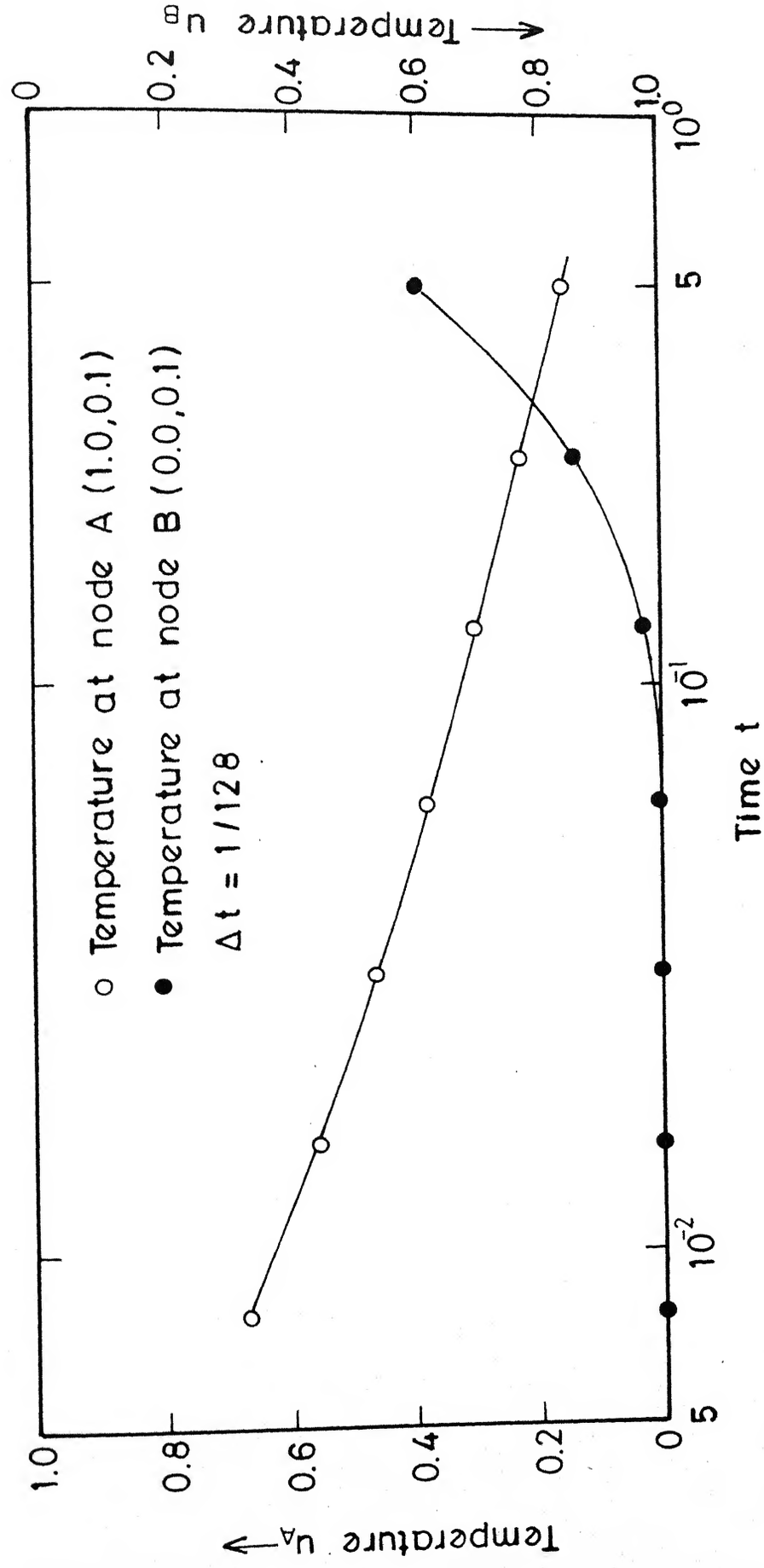

Fig.5.16 Temperatures for nonlinear slab subjected to simultaneous convection and radiation.

Table 5.6. Calculated Temperatures for Nonlinear Slab Subjected to Simultaneous Boundary Convection and Radiation*

Bi = 4.0 Node A : (1.0, 0.1)

Gr = 4.0 Node B : (0.0, 0.1)

Time-increment $\Delta t = 1/128$

Step No.	Time	Temperature at Node A	Temperature at Node B	Total Thermal Energy	Energy Residual	% Energy Residual
1	0.0078125	0.6750	1.0092	0.1961	0.1594 E-02	0.813 E+00
2	0.015625	0.5651	1.0009	0.1904	-0.1470 E-02	0.772 E+00
4	0.03125	0.4709	1.0004	0.1833	-0.1484 E-02	0.810 E+00
8	0.0625	0.3836	0.9968	0.1719	-0.1212 E-02	0.705 E+00
16	0.125	0.3049	0.9763	0.1544	-0.4949 E-03	0.320 E+00
32	0.25	0.2340	0.8640	0.1276	-0.2960 E-04	0.224 E-01
64	0.5	0.1629	0.6024	0.0882	-0.7282 E-05	0.826 E-02

* Central Processing Unit Time for 64 Steps on DEC-1090 : 3 minutes 44.75 seconds.

CHAPTER 6

CONCLUSIONS AND RECOMMENDATIONS

6.1 Conclusions

The results of the present study have shown that our attempt to develop a computer program based on the dual reciprocity boundary element method for general transient heat conduction problems in two dimensional isotropic medium has been successful. We have extended the method to deal with problems involving nonlinear boundary conditions. We have successfully incorporated the least-squares time integration scheme for linear problems. A systematic numerical study of convergence behaviour of the numerical solutions has been made. The following are the specific conclusions of the present work:

(i) The program developed herein has successfully implemented the dual reciprocity boundary element method to solve transient nonlinear heat conduction problems - involving nonlinear material as well nonlinear boundary conditions. The program provides the choice of constant and linear boundary elements for spatial discretization. It provides for the weighted-residual as well as the least squares time integration schemes (the latter for linear problems only). The program has successfully accounted for time-varying boundary conditions.

Performance of the program with respect to the problems involving heat generation cannot be commented on, as no tests with such problems have been performed. The program, thus, provides many features of a comprehensive program.

(ii) As mentioned above, a least-squares scheme has been successfully incorporated for linear problems. This has been done in the context of two point time integration schemes.

(iii) From numerical experiments, with the fully-implicit time integration scheme, the second order uniform convergence of boundary solutions with respect to mesh-refinement is obtained. With respect to time-increment, the above scheme shows first order convergence of the boundary solutions.

With least-squares scheme, the convergence of the boundary solutions with refining spatial grid is not uniform. With respect to time-increment, this scheme shows atleast quadratic rate of convergence. With very large time-increment, this scheme has resulted in oscillatory solutions.

(iv) As compared to the fully-implicit, the Galerkin and the Crank-Nicholson schemes, the least-squares scheme has been shown to be a computationally more efficient alternative in the context of linear problems.

(v) Problems involving nonlinear boundary conditions have been successfully solved. Accuracy of the computed solutions has been suggested by satisfactory maintenance of the input-output energy balance.

6.2 Scope and Limitations

The program developed herein can be used to analyze the thermal transients in the practical problems involving 2-D single homogeneous isotropic region. With nominal additions and modifications, this program can be used to analyze three-dimensional axisymmetric problems as well.

The program, however, cannot be applied to multi-region problems in its present form. Also, the limitations imposed by fixed-storage assignation will make it difficult to run this program for large number of boundary nodes on a medium size machine.

With its modular nature, the program offers immense flexibility in terms of modifications and enlargements.

6.3 Recommendations for Further Study

The computer program developed herein requires specific attention with respect to the storage and management of the data. To handle problem-discretizations with large number of boundary nodes, the optimum use of in-core storage and use of auxiliary storage area by means

of variable number of buffer areas are called for. Incorporation of higher order interpolations in space and time are desirable. Theoretical and numerical investigations of convergence and stability of the method are needed. Extensive modifications are required for analyzing the coupled problems and the multi-region problems. Based on our experiences from the present work, we enlist in the following lines few suggestions towards the development of a comprehensive program based on the dual reciprocity boundary element method, and the development of the method itself.

A. Programming Aspects : Storage and Management of Data

We suggest incorporation of the following data structure [33] to take into account the restrictions on the in-core storage, easy checking and access to each of the arrays involved and use of auxiliary memory:

- Dynamic assignation of the in-core storage area during the running of the program.
- Use of auxiliary memory by means of a variable number of buffer areas.
- Use of a set of routines for initialization of the global control area, creation of a specific array, its location in the working area and location of a particular element of an array and its replacement, if necessary.

B. Numerical Integration

Incorporation of adaptive numerical integration schemes is suggested. In the present work, a heuristic criterion for selection of the number of integration points has been employed. Instead, use of a criterion based on limitation of the truncation error of integration or ratio of the distance of the collocation point from the integration element to the length of the element is recommended. For quadratic and higher order elements incorporation of a finite-part integration scheme for evaluation of Cauchy principal value integrals is required.

C. Interpolation and Shape Functions

To better model the geometry of the problem domain and variation of field variables, incorporation of quadratic and cubic elements, and interpolation and shape functions is suggested.

D. Axisymmetric Problems

The present 2-D program can be easily modified to account for three-dimensional axisymmetric problems as well. To affect this extension, incorporation of routines to compute integral coefficients and coordinate functions for axisymmetric problems is recommended.

E. Time-Integration Schemes

In the context of two-point time integration schemes, the least-squares scheme has shown considerable promise for linear problems. Further extensions for linear conduction with nonlinear boundary conditions and nonlinear conduction problems are recommended. We recommend theoretical investigations of stability and convergence of this scheme. Computational viability of the scheme for nonlinear problems also needs to be investigated.

Use of three-point time integration schemes comes as the next choice. Also recommended is the theoretical as well as numerical experimental stability analysis of these schemes. To account for the abrupt discontinuity at the start of time-integrations introduced by rapid change of boundary conditions, incorporation of a procedure for smoothing the discontinuity is recommended. Such a procedure in the context of the finite element methods is detailed in Reference [32], and we suggest for adoption of a similar procedure in our context.

F. Theoretical and Experimental Analysis of Convergence of Boundary Solutions

Theoretical analysis of approximation errors, stability and convergence of boundary solutions in the context of the dual reciprocity boundary element methods remains an open area. Estimation of approximation errors forms the first pre-requisite for the

development of the adaptive grid techniques based on this method.

Numerical experiments are recommended to investigate the convergence behaviour of the solutions with spatial and time grid refinements for each choice of spatial and time-interpolation.

G. Adaptive Grid Techniques

As a next step in the development of the method, attempts towards the development of adaptive schemes for the time-dependent problems are called for.

H. Extensions to Multi-region and Anisotropic Problems

For analysis of temperature field in composite bodies using the dual reciprocity boundary element method, the following step by step procedure is recommended:

Step-1: Set up equations of the form of Eq.(3.48) or Eq. (3.66) for each region assuming it to be a separate one. To affect this process, compute the integral coefficient matrices and coordinate function matrices for each region.

Step-2: Apply the compatibility of physical temperatures and equilibrium of heat fluxes at each interface. Imperfect contact can be modelled as a convective resistance.

Step-3: Assemble the coupled system of equation.

Step-4: Apply the boundary conditions, and follow the same set of solution procedure as for the single region problems.

The above solution procedure will require a careful ordering of the coupled system of equations. A systematic assemblage process is called for at the Step-3 above. The solution of system of equations requires further considerations.

Extensions to anisotropic problems should also be considered.

I. Analysis of Coupled Problems

For analysis of the practical problems involving coupling with temperature field in a conducting region, the program developed herein can be suitably augmented with the one(s) dealing with the other field variable(s). For problems involving weak coupling such as thermo-mechanical problems in analysis of thermal stresses, the results of analysis obtained with our program can be used as the temperature history for computation of stresses.

REFERENCES

1. Rizzo, F.J. and Shippy, D.J., "A method of solution for certain problems of transient heat conduction", AIAA J., 8(11), 2004-9 (1970).

2. Curran, D.A.S., Cross M. and Lewis, B.A., "Solution of parabolic differential equations by the boundary element method using discretization in time", Appl. Math. Modelling 4, 398-400 (1980).

3. Chang, Y.P., Kang, C.S. and Chen, D.J., "The use of fundamental Green's functions for the solution of problems of heat conduction in anisotropic media", Int. J. Heat Mass Transfer 16, 1905-1918 (1973).

4. Brebbia, C.A. and Wrobel, L.C., "The boundary element method for steady-state and transient heat conduction", in: Numerical Methods in Thermal Problems (R.W. Lewis and K. Morgan, Eds.), Pineridge Press, Swansea, U.K., 1979.

5. Wrobel, L.C., Brebbia, C.A. and Nardini, D., "The dual reciprocity boundary element formulation for transient heat conduction", in: Finite Elements in Water Resources VI (A. Sa da Costa, A. Melo Baptiste, W.G. Gray, C.A. Brebbia and G.F. Pinder, Eds.), Springer, Berlin, 1986.

6. Wrobel, L.C., Brebbia, C.A. and Nardini, D., "Analysis of transient thermal problems in the BEASY System", in: BETECH 86 (J.J. Connor and C.A. Brebbia, Eds.), Computational Mechanics Publication, Southampton, U.K., 1986.

7. Wrobel, L.C., Telles, J.C.F., and Brebbia, C.A., "A dual reciprocity boundary element formulation for axisymmetric diffusion problems", in : Boundary Elements VIII (C.A. Brebbia and M.Tanaka, Eds.), Springer, Berlin, 1986.

8. Wrobel, L.C. and Brebbia, C.A., "The dual reciprocity boundary element formulation for nonlinear diffusion problems", Comp. Methods Appl. Mech. Engg., 65, 147-164 (1987).

9. Jawson, M.A., "A review of the theory", Chapter 1 in : Topics in Boundary Element Research, Vol. 1 (C.A.Brebbia, Ed.), Springer, Berlin, 1984.

10. Brebbia, C.A., Telles, J.C.F. , Wrobel, L.C., "Boundary Element Techniques - Theory and Applications in Engineering", Springer-Verlag, Berlin, 1984.

11. Ligget, J.A. and Liu, P.L.-F., "Applications of Boundary Element Methods to Fluid Mechanics", Chapter 4 in : Topics in Boundary Element Research Vol. 1 (C.A. Brebbia, Ed.), Springer-Verlag, Berlin, 1984.

12. Brebbia, C.A. and Walker, S., "Boundary Element Techniques in Engineering", Newnes-Butterworths, London, 1980.

13. Shaw, R.P., "An Integral Approach to Diffusion", Int. J. Heat Mass Transfer, 17, 693-699 (1974).

14. Wrobel, L.C. and Brebbia, C.A., "Time-dependent Potential Problems" in: Progress in Boundary Element Methods 1 (C.A. Brebbia, Ed.), Pentech Press, London, 1981.

15. Nardini, D. and Brebbia, C.A., "Boundary Integral Formulation of Mass Matrices for Dynamic Analysis", in: Topics in Boundary Element Research, Vol. 2, (C.A. Brebbia, Ed.), Springer-Verlag, Berlin, 1985.

16. Wrobel, L.C. and Brebbia, C.A., "A Formulation of the Boundary Element Method for Axisymmetric Transient Heat Conduction", Int. J. Heat Mass Transfer, 24, 943-950 (1981).

17. Banerjee, P.K. and Shaw, R.P., "Boundary Element Formulation for Melting and Solidification Problems", Chapter 1 in: Developments in Boundary Element Methods 2 (P.K. Banerjee and R.P. Shaw, Eds.), Elsevier Applied Science Publishers, London, 1982.

18. Hong, C.P., Umeda, T. and Kimura, Y., "Application of the Boundary Element Method in Two and Three Dimensional Unsteady Heat Transfer Problems involving Phase Change", in: Boundary Elements V (C.A. Brebbia, T. Futagami and M. Tanaka, Eds.), Springer-Verlag, Berlin, 1983.

19. Wrobel, L.C., "A Boundary Element Solution to Stefan's Problems", in: Boundary Elements V (C.A. Brebbia, T. Futagami and M. Tanaka, Eds.), Springer-Verlag, Berlin, 1983.

20. Pina, H.L.G. and Fernandes, J.L.M., "Three Dimensional Heat Conduction by the Boundary Element Method", in: Boundary Elements V (C.A. Brebbia, T. Futagami, and M. Tanaka, Eds.), Springer-Verlag, Berlin, 1983.

21. Kihara, J., Umeda, T. and Taneda, K., "Accuracy of Boundary Element Method in Non-stationary Heat Transfer Problems", in: Boundary Elements VIII (M. Tanaka and C.A. Brebbia, Eds.), Springer-Verlag, Berlin, 1986.

22. Iso, Y., "Uniform Convergence Theorem for Boundary Element Solutions of Heat Equation with the Second Initial - Boundary Value Problems", in Boundary Elements VIII (M. Tanaka and C.A. Brebbia, Eds.), Springer-Verlag, Berlin, 1986.

23. Iso, Y. Takahashi, M. and Onishi, K., "Numerical Convergence of Boundary Solutions in Transient Heat Conduction Problems", Chapter 1: in Topics in Boundary Element Research, Vol. 3 (C.A. Brebbia,Ed.), Springer-Verlag, Berlin, 1987.

24. Koizumi, M., Utamura, M. and Kotani, K., "Application of BEM to Unsteady 3-dimensional Heat Conduction Problems with Nonlinear Boundary Conditions", in:Boundary Elements V (C.A. Brebbia, T. Futagami, and M. Tanaka, Eds.), Springer-Verlag, Berlin, 1983.

25. Onishi, K. and Kuroki, T., "On Nonlinear Heat Transfer Problems", Chapter 6 in: Developments in Boundary Element Methods-4 (P.K. Banerjee and J.O. Watson, Eds.), Elsevier Applied Science Publishers, London, 1986.

26. Brebbia, C.A. and Skerget, P., "Nonlinear Time Dependent Potential Problems Using BEM", in: Boundary Elements VI (C.A. Brebbia, Ed.), Springer-Verlag, Berlin, 1984.

27. Kikuta, M., Togoh, H. and Tanaka, M., "Boundary Element Analysis of Nonlinear Transient Heat Conduction Problems", Comp. Methods Appl. Mech. Engg., 62, 321-329 (1987).

28. Kikuta, M., Togoh, H. and Tanaka, M., "A Boundary Element Method for Nonlinear Transient Heat Conduction Problems", in: Boundary Elements VIII (M. Tanaka and C.A. Brebbia, Eds., Springer-Verlag, Berlin, 1986.

29. Kellog, O.D., "Foundations of Potential Theory", Springer-Verlag, Berlin, 1929.

30. Patterson, C. and Sheikh, M.A., "Interelement Continuity in the Boundary Element Method", Chapter 6 in: Topics in Boundary Element Research, Vol. 1 (C.A. Brebbia, Ed.), Springer-Verlag, Berlin, 1984.

31. Nardini, D. and Brebbia, C.A., "The Solution of Parabolic and Hyperbolic Problems using an Alternative Boundary Element Formulation", in: Boundary Elements VII (C.A. Brebbia, Ed.), Springer-Verlag, Berlin, 1985.

32. Zienkiewicz, O.C., "The Finite Element Method", Tata McGraw Hill, New Delhi, 1979.

33. Doblare', M., "Computational Aspects of the Boundary Element Method", Chapter 4 in: Topics in Boundary Element Research, Vol. 3 (C.A. Brebbia,Ed.), Springer-Verlag, Berlin, 1987.

34. Wrobel, L.C., "Potential Problems", Chapter 8 in: Topics in Boundary Element Research, Vol. 3 (C.A. Brebbia, Ed.), Springer-Verlag, Berlin, 1987.

35. Telles, J.C.F., "Elastostatic Problems", Chapter 9 in: Topics in Boundary Element Research, Vol. 3 (C.A. Brebbia, Ed.), Springer-Verlag, Berlin, 1987

36. Stroud, A.H., and Secrest, D., "Gaussian Quadrature Formulas", Prentice-Hall, New York, 1966.

37. Pina, H., "Numerical Integration", Chapter 3 in: Topics in Boundary Element Research, Vol. 3, (C.A. Brebbia, Ed.), Springer-Verlag, Berlin, 1987.

38. Kutt, H.R., "The Numerical Evaluation of Principal Value Integrals by Finite Part Integration", Numer. Math., 24, 205-210 (1975).

39. Duffy, M.G., "Quadrature over a Pyramid or Cube of Integrals with a Singularity at a Vertex", SIAM J. Numer. Anal., 19(6), 1260-1262 (1982).

40. Pina, H.L.G. and Fernandes, J.L.M., "Applications in Transient Heat Conduction", Chapter 2 in: Topics in Boundary Element Research, Vol. 1 (C.A. Brebbia, Ed.), Springer-Verlag, Berlin, 1984.

41. Curran, D., Cross, M. and Lewis, B.A., "A Preliminary Analysis of Boundary Element Methods Applied to Parabolic Partial Differential Equations", Proceedings of the 2nd Int. Seminar on Recent Advances in Boundary Element Methods, Southampton, 1980.

42. Orivuori, S., "Efficient Method for Solution of Nonlinear Heat Conduction Problems", Int. J. Numer. Methods Eng., 14, 1461-1476 (1979).

43. Carslaw, H.S. and Jaeger, J.C., "Conduction of Heat in Solids", 2nd ed., Clarendon Press, Oxford, 1959.

APPENDIX

FORTRAN LISTING OF MAIN PROGRAM "DRBEM"

```
C**********************************************************************
C
C     ******************************
C     *       PROGRAM DRBEM        *
C     ******************************
C
C
C     DUAL RECIPROCITY BOUNDARY ELEMENT ANALYSIS OF NONLINEAR
C     TRANSIENT HEAT CONDUCTION PROBLEM IN 2-D ISOTROPIC
C     HOMOGENEOUS CONDUCTING REGIONS.
C
C**********************************************************************
C
      PROGRAM DRBEM
      IMPLICIT REAL(A-H,O-Z)
      REAL X(50),Y(50),C(50),XL(50),U0(50),UT0(50),Q0(50)
      REAL UB(50),UTB(50),QB(50),BI(50),GR(50),EATAG(6,3),WG(6,3)
      REAL G(50,50),H(50,50),FC(50,50),PSI(50,50),EATAM(50,50)
      REAL FCINV(50,50),CB(50,50),AREA(80),ED(50),BN(50)
      REAL U(50),UT(50),Q(50),TAU(50),A(50,50),B(50),BX(50)
      REAL PROPR(10,3),QS0(50),QS(50),BD(50,50)
      REAL RK(50),ARK(50),RHO(50),ARHO(50),SPH(50),ASPH(50)
      REAL EATA1(7,2),EATA2(7,2),EATA3(7,2),WH(7,2),HTG(50,50)
      REAL CTC(50,50),CTG(50,50),CTH(50,50),HTH(50,50),GTG(50,50)
      INTEGER KODE(50),ICB(50,3),ICI(80,4)
      INTEGER N,NE,NP,NT,NG,NBS
      COMMON /CONST/LEC,IMP,N,NE,NP,NT,NCI,NBS,PI,FCONST,DT,TH,TA
      COMMON /COOR/X,Y,C,XL/ARTNT/U0,UT0,Q0,EN0
      COMMON /BOCO/KODE,UB,UTB,QB,BI,GR/CONECT/ICB,ICI
      COMMON /PINTG/EATAG,WG/ARGH/G,H/ARCFN/FC,PSI,EATAM
      COMMON /ARFCNI/FCINV,CB/ARSOL/U,UT,Q,EN,RES
      COMMON /ARTIME/IT0,IT,TIME,TAU/ARNOTM/AT,AC,AR
      COMMON /ARSYS/A,B/ARRHS/BX/ARKOD/KODES,KODEI,KODEP,KODESC
      COMMON /REFER/PROPR,NSEG/ARIOL/LWA,TOL
      COMMON /ARPROP/RK,ARK,RHO,ARHO,SPH,ASPH
      COMMON /ARAREA/AREA,ED,BN/ARSORC/QS0,QS,BD
      COMMON /PINTH/EATA1,EATA2,EATA3,WH
      COMMON /ARLST/CTC,CTG,CTH,GTG,HTH,HTG
      LEC=20
      IMP=22
      NA=50
      LWA=3000
```

```
      TOL=1.E-4
C***(A =>ROW DIMENSION OF MATRICES A
      OPEN(UNIT=LEC,DEVICE='DSKC',FILE='ORBMC.INP')
      OPEN(UNIT=IWP,DEVICE='DSKC',FILE='ORBMC.OUT')
      OPEN(UNIT=24,DEVICE='DSKC',FILE='ORBMCM.OUT')

      INPUT REQUIRED DATA.

      CALL INPUT(NR,NTOP)

      SETUP INTEGRATION POINTS FOR GAUSSIAN AND HAMMER QUADRATURES

      CALL GAUSS
      CALL HAMMER

      COMPUTE BOUNDARY INTEGRALS.

      CALL BINT
      IF(NTOP .GE. 2)GO TO 2

      FOR TRANSIENT PROBLEMS,COMPUTE COORDINATE FUNCTION MATRIX
      AND RELATED MATRICES .

      CALL CDFUN
      CALL CFINV

            START COMPUTATIONS  AT EACH TIME STEP.

      IT=0
      TIME=0
      TYPE 12
12    FORMAT(/5X,'TYPE IN ITMAX,DT,TH IN THIS ORDER')
      ACCEPT *,ITMAX,DT,TH
      TYPE 22,ITMAX,DT,TH
22    FORMAT(5X,'ITMAX = ',I5,3X,'DT = ',E12.5,3X,'TH = ',E12.5)
1     IT = IT + 1
      TIME = TIME + DT

      COMPUTE BOUNDARY CONDITONS IN KIRCHHOFF TRANSFORM SPACE IF
      PROBLEM INVOLVES NONLINEAR CONDUCTION . IF B.C.'S OR HEAT
      GENERATION IS TIME-DEPENDENT ,COMPUTE CURRENT VALUES.

2     CALL BCOND(IFBC,NTOP)
      IF(NTOP .GE. 2)GO TO 4
      IF(IFBC .EQ. 0)GO TO 3

      SETUP LINEAR OR LINEARIZED SYSTEM MATRIX.

4     CALL FMAT(NTOP)
```

```
C       SOLUTION OF BOUNDARY ELEMENT EQUATIONS .
C
    3   CALL BDSOLV(NTOP)
C
C       COMPUTE VALUES AT INTERNAL POINTS IF DESIRED. UPDATE INITIAL
C       CONDITION FOR NEXT STEP COMPUTATIONS.
C
        CALL INTERN(NTOP)
C
C       PRINT DESIRED OUTPUTS.
C
        CALL OUTPUT(NTOP)
C
C       DETERMINE WHETHER TO STOP
C
        IF(NTOP .GE. 0)GO TO 11
        TYPE 23,IT,TIME
   23   FORMAT(/5X,'IT =',I5,'TIME =',E12.5)
   10   IF(IT.GT.ITMAX)GO TO 1
   11   CONTINUE
        CLOSE(UNIT=LREC,DEVICE='DSKC',FILE='DRBMCL.INP')
        CLOSE(UNIT=IMP,DEVICE='DSKC',FILE='DRBMCL.OUT')
        CLOSE(UNIT=24,DEVICE='DSKC',FILE='DRBMC1.OUT')
        STOP' JOB DONE !'
        END
C ***************************************************************************
```